Spatial and Temporal Controls on Saturated Overland Flow
in a Regularly Flooded Salt Marsh

Steven Joseph Turaski
Maryville, Tennessee

B.S., University of Georgia, 1997

A Thesis presented to the Graduate Faculty
of the University of Virginia in Candidacy for the Degree of
Master of Science

Department of Environmental Sciences

University of Virginia
January, 2002

Patricia Wiberg, Thesis Advisor ________________________________

John Albertson ________________________________

Linda Blum ________________________________

Aaron Mills ________________________________

ABSTRACT

Turaski, S. J. 2002. Spatial and temporal controls on saturated overland flow in a regularly flooded salt marsh. Master's thesis. University of Virginia, Charlottesville, VA.

Field measurements of soil properties and water table dynamics were used to characterize the hydrology of a study area in a regularly-flooded portion of a salt marsh interior, with particular interest in identifying the processes that control rainfall-runoff. Tidal inundation, evapotranspiration, and precipitation dominated the sediment water balance and were incorporated into a numerical model. Model results were validated by comparison to field measurements and then used to characterize the spatial and temporal controls on modeled runoff events. This thesis describes physical mechanisms for erosion and shows rainfall-runoff occurs with sufficient frequency and spatial extent to be a potentially significant process with respect to long-term marsh development.

Tidal inundation regularly saturated the sediment in the study area. Between inundation events, evapotranspiration removed water from the sediment. Because of frequent tidal inundation, the amount of rainfall necessary to saturate the sediment at any given time was typically small. Rainfall in excess of the modeled saturation deficit was assumed to collect on the surface and generate overland flow. This process was observed in the field, but was not quantified with field measurements.

Model results showed the marsh surface at 80 cm elevation (MSL) was saturated by rainfall for 75% of the rainfall events in 1999 and 2000. Temporal controls included the timing of rainfall with respect to the tides and the timing of the tides with respect to potential evapotranspiration. Modeled saturation events usually included the entire study area. Surface elevation was the only significant spatial control, through its influence on tidal inundation. Inundation frequency affected the antecedent saturation deficit, while inundation during rainfall events limited the extent of the area exposed to rainfall.

Table of Contents

List of figures

List of Tables

Introduction

1.1 Background

In temperate latitudes, salt marshes and mudflats occupy the intertidal zone between subtidal lagoons and terrestrial uplands (Pethick, 1984; Hayden et al, 1995; Brinson et al, 1995). As changes in relative sea level change the extent of inundation, mudflats initially develop from sediment deposited during inundation (Pethick, 1984). Salt-tolerant vegetation colonizes the upper part of the mudflats and marshes develop there, while the lower part remains as mudflats (Pethick, 1984). As sea level rises, the mudflats become subtidal, the lower marsh converts to mudflats, and the upper marsh encroaches on the upland (Brinson et al, 1995).

Allen and Pye (1992) described four physical factors that largely control salt marsh development: sediment supply, tidal regime, relative sea level, and wind-wave climate. The amount and size distribution of mineral and organic sediment affect soil formation and the hydraulic properties of the sediment. Mineral sediment is deposited by tides and organic material accumulates from plant growth and decay. The relative mineral and organic content of marsh soils is a highly variable property among locations, and, to an extent, within locations. Sediment entrainment and deposition are influenced by tidal regime. Sediment is entrained from the lagoon or tidal creek channels when bottom boundary shear stress is greater than the critical stress needed to dislodge sediment. Deposition occurs when shear stress is less than the critical shear stress of suspended sediment or flocs. Relative sea level determines the frequency and duration of tidal flooding at a given elevation. Tidal flooding, particle settling and tidal flow velocities, and the concentration of suspended sediment determine the rate of mineral sediment deposition. Waves, which are directly related to wind speed and direction, can erode marsh edges, increase tidal elevations, and increase bottom boundary shear stresses.

In addition to mineral sediment deposition, the organic debris of plant shoots and roots accumulates and contributes to soil formation (Pethick, 1984). Blum (1993) suggested that organic matter accumulation might be primarily derived from root production and decay, without significant input from above-ground plant shoots. Organic matter accumulation was determined by total inputs, minus decomposition. Blum (1993) showed that root turnover was slower in the interior than at the creekbank. Annual root production at the creekbank decomposed (did not accumulate), but root production exceeded decay in the interior (did accumulate). The rates of decomposition at the creekbank and in the interior were similar, and the difference was attributed to greater root production in the interior. Blum (1993) suggested that high and fluctuating porewater salinity in the interior stressed the plants, inducing greater root production than at the creekbank. Net vertical accretion by organic matter accumulation is modified by compaction (Pethick, 1984). In a marsh with low organic content, compressibility of the sediment is low (Knott et al, 1987).

Hayden et al (1995) described the relative vertical positions of the land, sea and fresh-water table surfaces as controls on ecological and geomorphological processes on

Virginia barrier islands, including vegetation zonation and changes in ecosystem state. The land surface position is changed by organic matter accumulation and deposition of marine and terrestrial sediment. Both of these processes are related to sea-level. Sea-level can change based on gradual long-term changes in relative sea-level, short-term periodic changes in daily and spring/neap tidal cycles, and episodic large changes of short duration. In the marsh the groundwater is saline. The fresh-water table exists above Mean High Water in the upland , and its position is a function of precipitation, evapotranspiration, and surface elevation.

The surface sediments of salt marshes are typically fine-grained silts and clays (Pethick, 1984). Larger grains (sands) are typically deposited on the lower part of mudflats (Pethick, 1984). The lower settling velocity of finer grains keeps them in suspension and enables transport to the salt marshes (Pethick, 1984). Sediment deposition is greater in the low marsh than the less frequently inundated high marsh, and is greater at creekbanks than in the marsh interior (Pethick, 1984).

Marsh surface sediments are cohesive (Pethick, 1984). Sediment is deposited as individual grains or flocs, but on the surface sticks together and resists resuspension by tidal flows. Once deposited, sediment can be held on the surface by algae mats (Pethick, 1984).

Previous work on sediment deposition provided evidence for the possible occurrence of surface erosion at Phillips Creek Marsh (the location of field measurements for this thesis). Christiansen (1998) showed the long-term vertical accretion rate at Phillips Creek Marsh was less than the sum of annual mineral sediment deposition rates.

This indicated the potential for sediment removal from the marsh surface after initial deposition. Although tidal flows delivered sediment to the marsh on flood tides, the dense canopy of marsh grasses dampened ebb flow so that the shear stress was inadequate to entrain sediment (Christiansen et al, 2000).

Rain events, then, are the next possible means of erosion to be investigated and are the subject of this thesis. The energy of raindrops is a function of drop size and terminal velocity (Smith and Wischmeier, 1962). The impact of individual raindrops can dislodge sediment particles. For erosion by rainfall to occur on a salt marsh, the surface must be exposed (ie, not inundated by tidal flooding). Some minimum depth of inundation would be sufficient to absorb the energy of the falling rain drops and effectively buffer the surface from the impact. Disturbed sediment must also be transported in rainfall-runoff for erosion to occur. Runoff occurs when the soil is saturated (saturation excess overland flow) or, less frequently, when rain intensity exceeds the infiltration capacity of the soil (infiltration excess overland flow). This thesis shows soil saturation is a critical parameter for sediment transport, and that saturation excess overland flow occurs with sufficient frequency to be a viable and potentially significant process with respect to the geomorphology of salt marshes.

1.2 Previous work

Marshes are highly productive ecosystems both above ground (Nixon, 1980) and below (Good et al, 1982). Research was conducted to determine possible mechanisms and significance of solute flushing from the marsh sediment into tidal creeks and, thus, to adjacent estuaries and coastal waters. Jordan and Correll (1985) and Yelverton and Hackney (1986) showed that drainage at creekbanks can be significant, but other workers showed that drainage is not significant in the marsh interior (Hemond and Fifield, 1982; Harvey et al, 1987; Nuttle and Hemond, 1988; and Nuttle, 1988). The combined effects of low topographic slope and low hydraulic conductivity limited drainage of soil pore-water to within 5-15 m from creekbanks. Harvey et al (1987) showed that surface elevation had a greater effect on drainage in the creekbank zone than did hydraulic conductivity.

Water loss in interior areas beyond the creekbank zone is dominated by evapotranspiration (Hemond and Fifield, 1982; Dacey and Howes, 1984; Nuttle and Hemond, 1988; Nuttle, 1988). Removal of water at the surface by evapotranspiration creates a negative pressure gradient in the soil that pulls porewater upward (Hemond and Fifield, 1982). Tidal infiltration is the main source of water to balance evapotranspiration, along with intermittent rainfall (Nuttle and Hemond, 1988). Regional groundwater can be a significant source of water to a marsh (Nuttle and Harvey, 1995), but is not a ubiquitous feature of salt marshes (see, for example, Nuttle and Hemond, 1988; Nuttle, 1988).

Hemond et al (1984) showed exfiltration (surface seepage) did not occur during periods of tidal infiltration. Harvey and Nuttle (1995) showed porewater circulates within the sediment, even in the absence of drainage and seepage. Water infiltrates primarily through macropores (crab burrows) to a maximum depth of 10-15 cm, the extent of the burrows. Infiltrated water is then pulled into the soil matrix and to the surface by evapotranspiration. This circulation allows import of solutes by infiltration and simultaneous export of evapoconcentrated solutes at the surface by diffusion down a concentration gradient into the overlying tidal water.

The surface soil layers typically have a low hydraulic conductivity. If there is a higher conductivity sediment below the surface layer, rising water level in the tidal creek can force lateral transport into the adjacent marsh via the high conductivity layer (Hemond and Fifield, 1982). Hemond and Fifield (1982) showed that this lateral transport can be transmitted into the overlying surface layer if vertical hydraulic conductivity is sufficient; however, this was modeled only for hydraulic conductivity greater than what was measured for marsh sediment and did not represent actual conditions. Carr and Blackley (1986) provided field evidence of lateral transport by tidal forcing in the creek and subsequent vertical transport into the surface layer. Nuttle (1988) and Nuttle and Hemond (1988) showed the effect of tidally varying head quickly dampens with distance from the creekbank and is mostly limited to a few meters adjacent to the creek.

One of the noticeable features of some marshes is a taller growth form of *Spartina alterniflora* along creeks than in the interior. When it was seen the difference was not genetic (Shea et al, 1975; Valiela et al, 1978), research for the underlying cause revealed some basic hydrologic functions of salt marshes. The importance of porewater movement was implied in hypotheses involving the delivery or availability of nutrients, sediment oxidation, and removal of sulphur and sodium (Wiegert et al, 1983). Wiegert et al (1983) used plastic pipe to artificially increase drainage, leading to increased height and biomass of *S. alterniflora* along a creek on Sapelo Island, GA.

Drainage was correlated with increased growth, but sediment oxidation was the underlying cause (Howes et al, 1986). Drainage increases oxidation directly by air entry and indirectly by flushing reduced sulphur and sodium (Howes et al, 1986). Sulphur binds oxygen, and sodium causes roots to consume oxygen more quickly. In the interior, where subsurface transport by drainage usually does not occur, the sediment is oxidized as the water table is drawn down by evapotranspiration (Dacey and Howes, 1984). This creates a positive feedback where water uptake by plants oxidizes the sediment, facilitating plant production and further water uptake (Dacey and Howes, 1984). By day, water in the roots is transported to the plant shoot in exchange for air (Dacey and Howes, 1984). The rate of water usage by the plant exceeds the rate of water uptake by the roots. Plant roots continue to take up water overnight, when there is no evapotranspiration, to restore the water deficit of the day (Dacey and Howes, 1984).

Although there has been much work on sediment deposition at various locations and time scales (for example, Delaune et al, 1978; Letzsch and Frey, 1980a; Pethick, 1981; Stevenson et al, 1985; Oertel et al, 1989; French and Spencer, 1993; Christiansen, 1998) and some work on lateral erosion of marsh edges (Letzsch and Frey, 1980b; Allen, 1989; Wray et al, 1995; Kastler and Wiberg, 1996), there have been few studies of vertical erosion of the marsh surface. Pethick (1992) found the marsh surface was eroded by wave action in a series of winter storms in a river-mouth estuary. This is an environment more prone to waves than a closed, or sheltered, marsh. Seasonal measurements of sediment deposition by Letzsch and Frey (1980a) showed some surface erosion on the interior-side of creekbank levees (spring only) and in ponded water areas (winter and spring). These zones and the entire marsh were depositional overall. Rainfall was suggested as a possible means of erosion, but no systematic effort was made to determine the process of erosion.

There have also been a few studies that referred to saturated overland flow by rainfall. Chalmers et al (1985) investigated the carbon balance for a coastal river and adjacent marshes. Particulate organic carbon (POC) circulated between the marsh surface and the river. POC was transported to the river in runoff during rain events when the marsh surface was exposed and was deposited by tides on the marshes.

In a modeling study by Nuttle and Portnoy (1992), an increase in mean water table elevation (caused by an increase in mean sea level) would lead to greater surface runoff by saturated overland flow. Their work was conducted for elevations beyond tidal input and with a shallow water table.

Hughes et al (1998) used field measurements to calibrate a two-dimensional model for soil- and ground-water transport in a salt marsh. Model results indicated saturation and/ or infiltration excess by rainfall, but runoff was not investigated.

1.3 Objectives

In this thesis, sediment transport by overland flow is hypothesized to be an important mechanism of sediment removal from a marsh. The following questions regarding overland flow as a means of erosion in a regularly flooded salt marsh interior have been investigated. *What conditions are conducive to overland flow? How often do these conditions occur? What are the potential mechanisms for erosion? What is the spatial and temporal extent of saturated overland flow that could lead to sediment erosion?* These questions were investigated with field measurements, observations, and numerical modeling. The occurrence of runoff and sediment mobilization was observed in the field; however, direct measurements of runoff and sediment concentration in runoff were outside the scope of this thesis. In the absence of runoff measurements, a water balance model was tested against field measurements of water table position.

The main objective of this thesis was to determine the spatial and temporal controls on saturated overland flow on a tidal salt marsh. The specific objectives were to characterize water table dynamics on an hourly time-scale over a period of two years, identify and characterize the physical and biological controls on the water table, and to relate this understanding of water table fluctuations to the saturation deficit and identify potential occurrences of saturated overland flow from tidal and meteorological data. In this thesis, saturation deficit refers to the amount of water required to saturate the sediment and is expressed as a length (volume per area).

Field measurements of the water table elevation across a topographic transect were used to characterize water table dynamics in a small area of marsh interior. Controls on the water table position (evapotranspiration, precipitation, tidal inundation, and soil hydraulic properties) were incorporated into a numerical model to estimate the saturation deficit. Surface elevation data were used with the model to assess spatial variability in soil saturation. Temporal variability was assessed by correlating modeled saturation events with tidal and meteorological variables to determine what types of precipitation events were most effective at producing runoff and how often these conditions occurred.

1.4 Conceptual model

In general, runoff occurs when water input exceeds the storage capacity of the soil (saturated overland flow), or when the rate of input is greater than the infiltration rate (infiltration excess overland flow). The depth to the water table and water content above the water table determine the saturation deficit.

In terrestrial catchments, saturation is controlled by drainage, precipitation, and evapotranspiration. Convergent topography and riparian areas are the most likely to become saturated. The saturated area varies during and after storms, and not all of the catchment contributes surface runoff to the stormflow hydrograph. (As reviewed in Chorley, 1978).

An area of salt marsh can be considered as a hillslope defined by the tidal creek at lower elevations and the forested upland at higher elevations. The marsh interior differs from terrestrial hillslopes in the absence of drainage and the presence of the tides. In marsh areas that receive frequent tidal inundation, the depth to the water table is typically small, with an extensive capillary fringe, so that the saturation deficit is also small (Harvey et al, 1987; Hughes et al, 1998). Within the marsh interior, the sediment water balance is controlled by tidal flooding, precipitation, and evapotranspiration (Nuttle and Hemond, 1988) (**figure 1**). During tidal inundation, the water table rises to the surface, saturating the sediment. Precipitation affects the sediment water balance only when the marsh is exposed (Carr and Blackley, 1986). Inundation frequency and duration decrease as elevation and/ or distance from the tidal creek increases (Hmieleski, 1994). Regularly flooded portions of a salt marsh experience frequent periods of soil saturation by the tides, with brief intervals (hours to days) for the development of a saturation deficit by evapotranspiration. This contrasts strongly with terrestrial catchments, where there are extended periods (days to months) of evapotranspiration and drainage, with episodic water input by precipitation or snowmelt.

The critical amount of rainfall for saturated overland flow is determined by the saturation deficit at the onset of rain. Because the saturation deficit of regularly flooded areas is typically small, saturated overland flow is possible during any period of rainfall onto an exposed marsh. Infiltration excess overland flow is also a possible occurrence. When the marsh surface is inundated, overland flow does not occur; any rainfall at such times is absorbed by the tidal waters and does not affect the surface.

1.5 Site Description

Field measurements were conducted at Phillips Creek Marsh in the Virginia Coast Reserve on the Atlantic coast of Virginia (**figure 2**). The Nature Conservancy owns and manages the Reserve. Research for this thesis was conducted as part of the National Science Foundation Long-Term Ecological Research site (LTER) that includes the Reserve (Hayden et al, 1991).

Phillips Creek Marsh is a mainland marsh in the Hog Island Bay barrier island-lagoon system. Much previous work has been conducted there (**figure 3**). It is a closed marsh, sheltered from the open lagoon and therefore not exposed to significant wave action. Water and suspended sediment from the lagoon are transported via tidal creek channels into the salt marsh and are advected onto the surface wherever water level in the creek exceeds its banks. Vegetation in Phillips Creek Marsh is primarily *Spartina alterniflora, Spartina patens, Juncus roemarianus,* and *Distichlis spicata*. The marsh formed in a stream floodplain during sea level transgression and is migrating landward along the former channel longitudinal axis, but is constrained laterally by steeper slopes (Brinson et al, 1995).

The current study was focused in a small area of the marsh interior adjacent to an upland (**figures 3-5**), on one of the lateral slopes mentioned by Brinson et al (1995). Vegetation in the study area was delineated into low marsh, mid marsh, upland, and marsh-upland transition zones. The low marsh was defined by intermediate height *Spartina alterniflora* (~1.0 m). The mid marsh was defined by short form *S. alterniflora* (~0.4 m). The transition into the forested upland was defined by shrubs (*Iva fructescens, Myrica cerifera, Baccharis halimifolia*) and standing dead trees, along with grasses (*Panicum virgatum, S. alterniflora, S. patens*, and *Distichlis spicata*). The upland forest was a mix of pine and hardwoods (*Pinus taeda, Juniperus virginiana, Liquidambar styraciflua, Prunus serotina*, and other species).

High marsh species, not found in the study area, were defined as *Juncus roemarianus, S. patens*, and *Distichlis spicata* (eg, Bertness, 1991; Tolley and Christian, 1999). The absence of high marsh species in the study area provided evidence that the site was regularly inundated, because *S. patens* competitively excludes *S. alterniflora* above Mean High Water (Bertness, 1991). *Spartina alterniflora* therefore roughly indicates the area of regular inundation, and the study area was within the *S. alterniflora* zone of Phillips Creek Marsh (**figure 6**). Hmieleski (1994) included a high marsh zone on his "Steep-Near Transect" at the same location as the current study area, but the grasses he used to make this classification were not present in the current study.

The surface sloped gradually from the tidal creek toward the upland, with a noticeable increase in local slope 25-30 m from the tidal creek (**figure 4**). The distance from the tidal creek to the transition zone was approximately 50 m. Much of the results and discussion in this thesis focus on the mid marsh, an approximately 25 m wide zone with approximate surface elevation of 80 cm (referenced to Mean Sea Level). The 70-80 cm elevation contour (**figure 4A**) was 22% of the study area, with 73% of the study area at or below 80 cm elevation (**figure 7**).

Tides of 80 cm would flood the entire low and mid marsh portions of the study area (**figure 4B**). Christiansen (1998) reported that 30% of maximum measured tidal elevations at high tide exceeded 80 cm in Phillips Creek Marsh during the period 1990-1997 **(figure 8**). This was based on water level data that were recorded at Wachapreague, VA (~20 km north of the study area on the Atlantic Coast of Virginia) and converted to water level in Phillips Creek Marsh (details in Methods section). Hourly tidal elevations for 1999 and 2000 (also converted from Wachapreague measurements) indicated the study area at 80 cm elevation was flooded for 31 and 30% of total time, respectively.

Observed water levels are affected by meteorological forcing, primarily barometric pressure and wind (Christiansen, 1998). Because of this, the measured water levels differ from predicted astronomical tides (**figure 8**). Tidal characteristics based on converted Wachapreague water levels for 1999 and 2000 were similar (**figure 9**). The tidal range at the LTER tide gauge at Redbank (~1.6 km from the study area) was 2.25 m (Christiansen, 1998).

Monthly temperature and precipitation recorded in 1999 and 2000 by the National Weather Service at Painter, VA (~15 km from the site, on the center of the Delmarva peninsula) were compared to 30-year averages for that station (**figure 10**). Average annual precipitation for the 30-year period was 106.5 cm. The annual precipitation totals for 1999 and 2000 were higher than average, 122.0 and 114.2 cm, respectively, but within the 30-year range (**figure 10A**). Monthly precipitation totals for 1999 and 2000 were also consistent with the 30-year averages (**figure 10B**). However, Hurricanes Dennis and Floyd caused exceptionally high rainfall in September 1999, and a prolonged lack of precipitation occurred in October 2000. Monthly average temperatures were also consistent with the 30-year averages (**figure 10C**). Solar radiation recorded at the LTER meteorological station in Phillips Creek Marsh was similar in both 1999 and 2000 to the ten-year average at that station (**figure 11**).

The following review of the sedimentary and hydrologic environment at Phillips Creek marsh is based on results of previous work conducted there. Refer to figure 3 for specific location of research sites within the marsh.

Groundwater discharges into parts of Phillips Creek Marsh from the adjacent upland and the regional aquifer. Flow paths from the upland to the marsh include near-surface transport in the root zone (Harvey, 1990; Hmieleski, 1994), surface seepage at the base of the upland (Harvey, 1990), and lateral flow in the shallow sandy unconfined aquifer (~2-8 m depth) (Fetsko, 1990). Input from the regional aquifer was required to close the water balance of the upland (Fetsko, 1990) and a location in the marsh (Nuttle and Harvey, 1995). Regional groundwater input was also indicated by a nocturnal rise in the water table when there were no tidal or precipitation inputs (Nuttle and Harvey, 1995).

Surface sediments for marshes within the Hog Island Bay system are primarily clay minerals from the nearshore marine environment (Robinson, 1994). The marine sediments are delivered through inlets into the lagoon and by tidal creeks onto the marshes. Sediment in the top 10 cm of the marsh is fine silt (mean diameter 7.1 ϕ or approximately 8 μm; Kastler, 1993) with low organic content (9.4% by weight; Kastler, 1993). The sand content is low for the surface sediments of Phillips Creek Marsh because of distance from the barrier islands (**figure 2**), the local source of sand (Robinson, 1994). Sand content is high at depth, however, because Phillips Creek Marsh developed over sandy upland areas (Robinson, 1994). Sediment of mainland origin was not found in the marsh surface sediments, suggesting that input from mainland sources is absent or sufficiently small that weathering alters it upon deposition (Robinson, 1994).

Landscape evolution of marshes in the Hog Island Bay system was correlated to sedimentary processes using monthly sediment samples and analysis of land cover changes over approximately 50 years (Kastler, 1993; Kastler and Wiberg, 1996). Different sedimentary processes dominated in different parts of the system. In the mainland fringing marsh around Phillips Creek, marsh area increased as it encroached onto the upland at a rate of 10-20 m in 50 years. The net sediment flux at Phillips Creek Marsh is depositional, and the surface is vertically accreting (Kastler, 1993; Christiansen, 1998). Kastler (1993) concluded the marsh was receiving adequate sediment input to maintain its elevation against sea-level rise. Christiansen (1998) showed sediment suspended in tidal creeks was advected onto the marsh primarily by non-storm tides. Deposition during tidal storm surges accounted for approximately 25% of annual sediment mass deposited at creekbanks, but was not significant in the interior.

Surface slope and distance from the tidal source determine the hydroperiod (depth and duration of flooding) and drainage at Phillips Creek Marsh (Hmieleski, 1994). Hydroperiod and drainage determine physical and chemical variables of the soil (saturation, oxidation, and salinity). The location of the marsh-forest transition zone corresponds to areas where salinity is reduced by drainage and fresh groundwater input. Hmieleski (1994) found that the transition zone occurred at the base of the upland for a “steep” transect (1.4 % slope) and was narrow with a distinct edge. For a “flat” transect (0.029 % slope), the transition zone was wider and the change in vegetation more gradual. The “flat” transition zone occurred at a lower elevation but was further from the tidal creek, illustrating the trade-off of these two characteristics and their combined effect on tidal inundation.

Based on water table dynamics and the relative contributions of tidal, groundwater, and precipitation inputs at Phillips Creek Marsh, functional differences were found between marsh zones that appeared hydrologically equivalent if based only on hydroperiod (Stasavich, 1998). Water table measurements were used to determine ecologically significant wetland parameters, such as depressional storage, tidal sediment and nutrient exchanges, and anaerobic conditions. These parameters affect biogeochemical cycling and habitat for plants and animals.

In a study conducted concurrently with this thesis and on the same transect, Dusterhoff (2002) assessed near surface soil moisture dynamics in the upland and transition zones. Topographic gradients were low, and elevation and textural characteristics were found to control surface-layer saturation. Based on modeling, the different root distributions associated with different vegetation types were also shown to affect surface saturation.

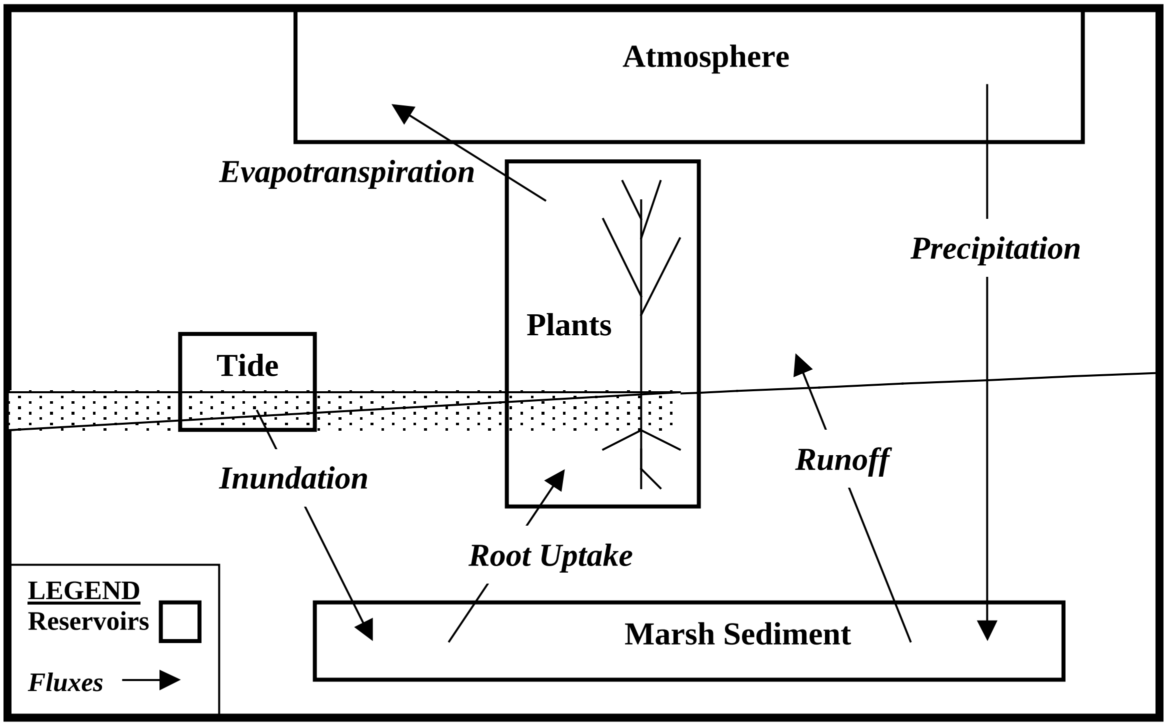

Figure 1. Conceptual diagram of the water balance for salt marsh sediment.

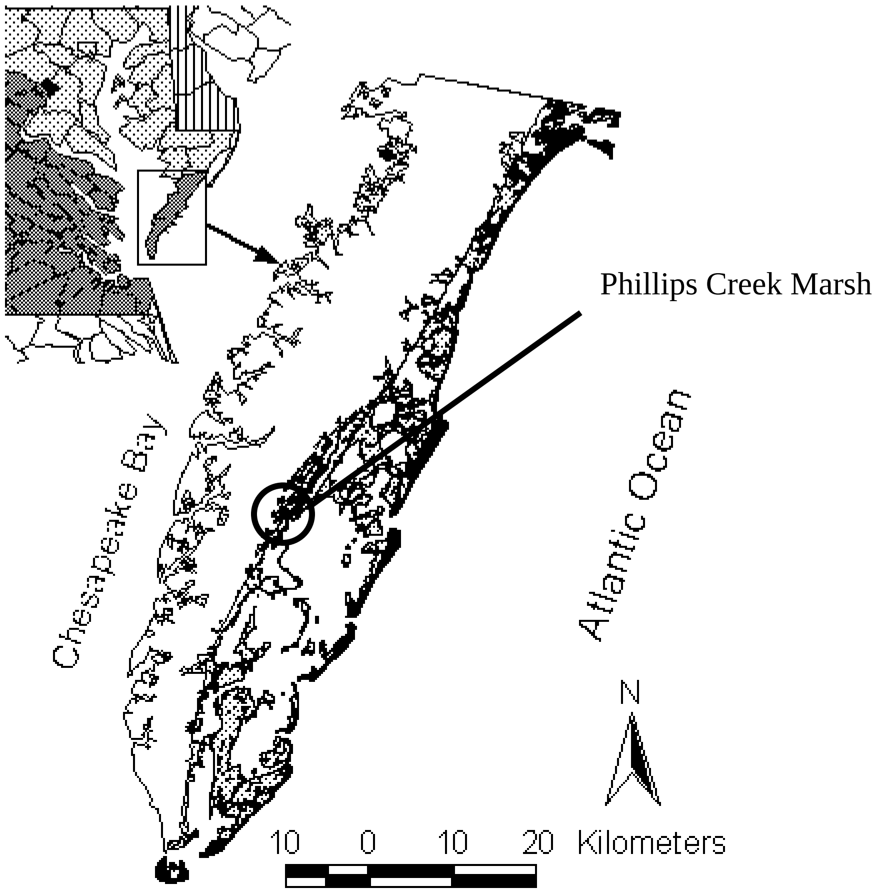

Figure 2. Regional map of the Virginia Coast.

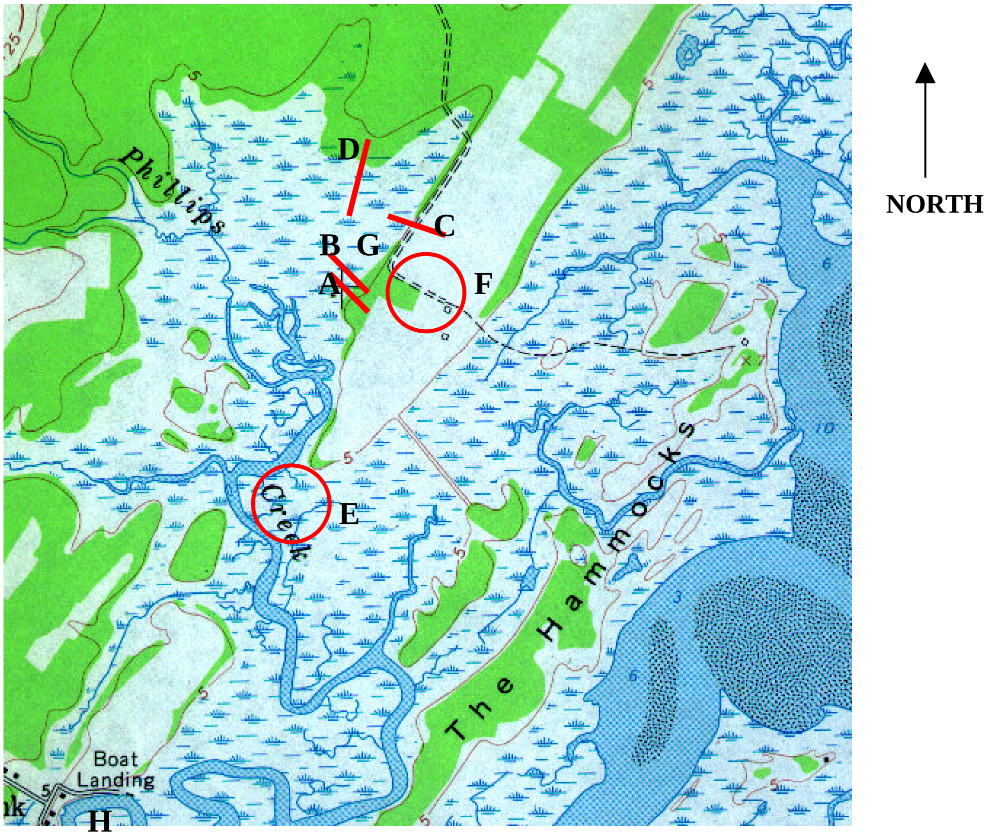

Figure 3. Phillips Creek Area, with locations of research sites.

A. This thesis

A. Hmieleski, 1994; Dusterhoff, 2002 (same location as this thesis)
B. Barr, 1989; Blum, 1993
C. Hmieleski, 1994
D. Hmieleski, 1994; Stasavich, 1998
E. Harvey, 1990; Kastler, 1993; Robinson, 1994; Nuttle and Harvey, 1995; Christiansen, 1998
F. Fetsko, 1990; Robinson, 1994
G. LTER meteorological station
H. LTER tide gauge at Red Bank

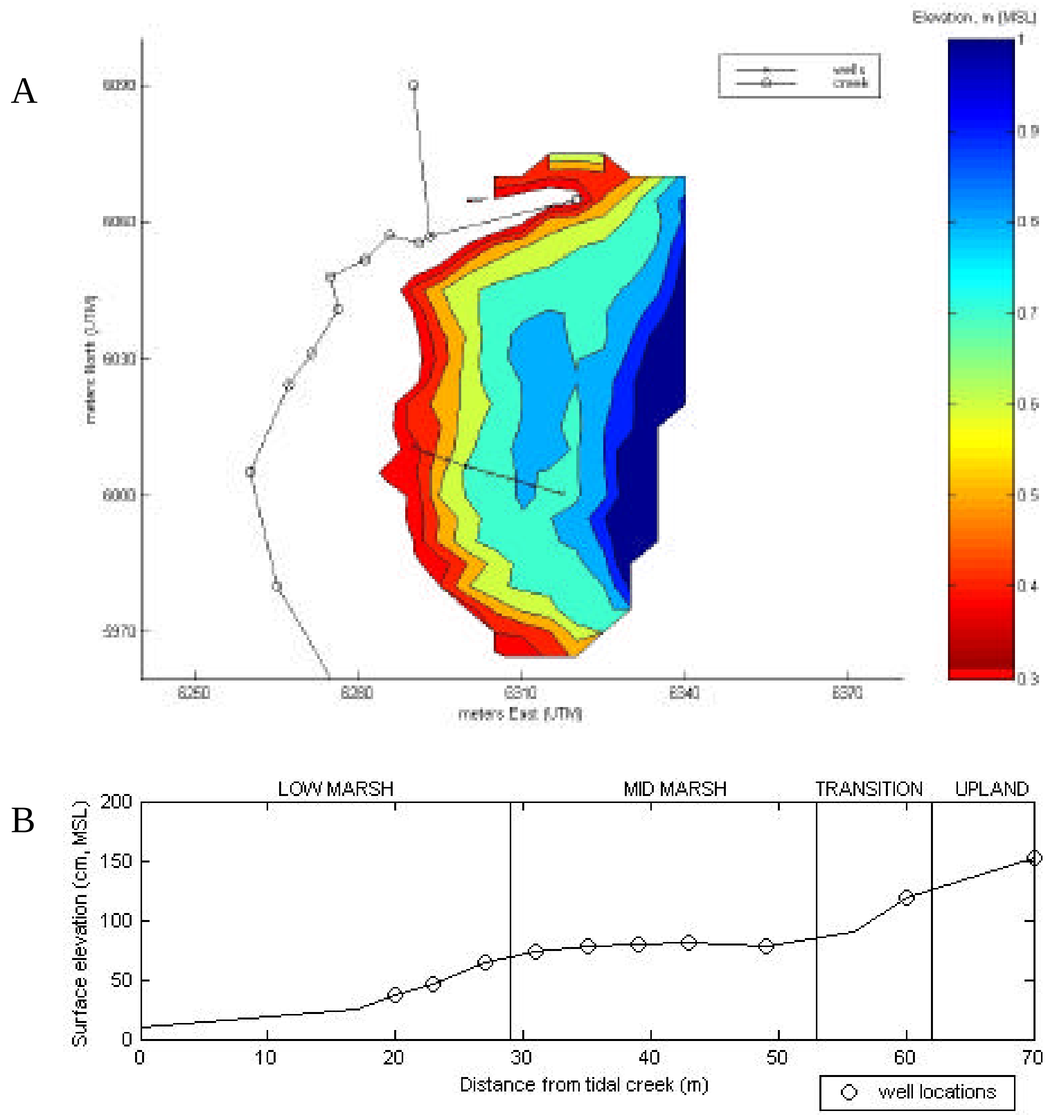

Figure 4. Topography of the study area, with locations of wells.

A. Plan view topographic map. Coordinates (East, North) are for UTM Zone 18 and are abbreviated values; the southeast corner of the map is (426250, 4145970). Contour interval is 10 cm. The upper elevation on the eastern side of the study area is the western side of the upland area adjacent to the site in figure 3.

B. Topographic transect with position and elevation of wells. Surface elevation data for the wells are given in Appendix 2. Designation of low marsh, mid marsh, transition, and upland zones was based on vegetation.

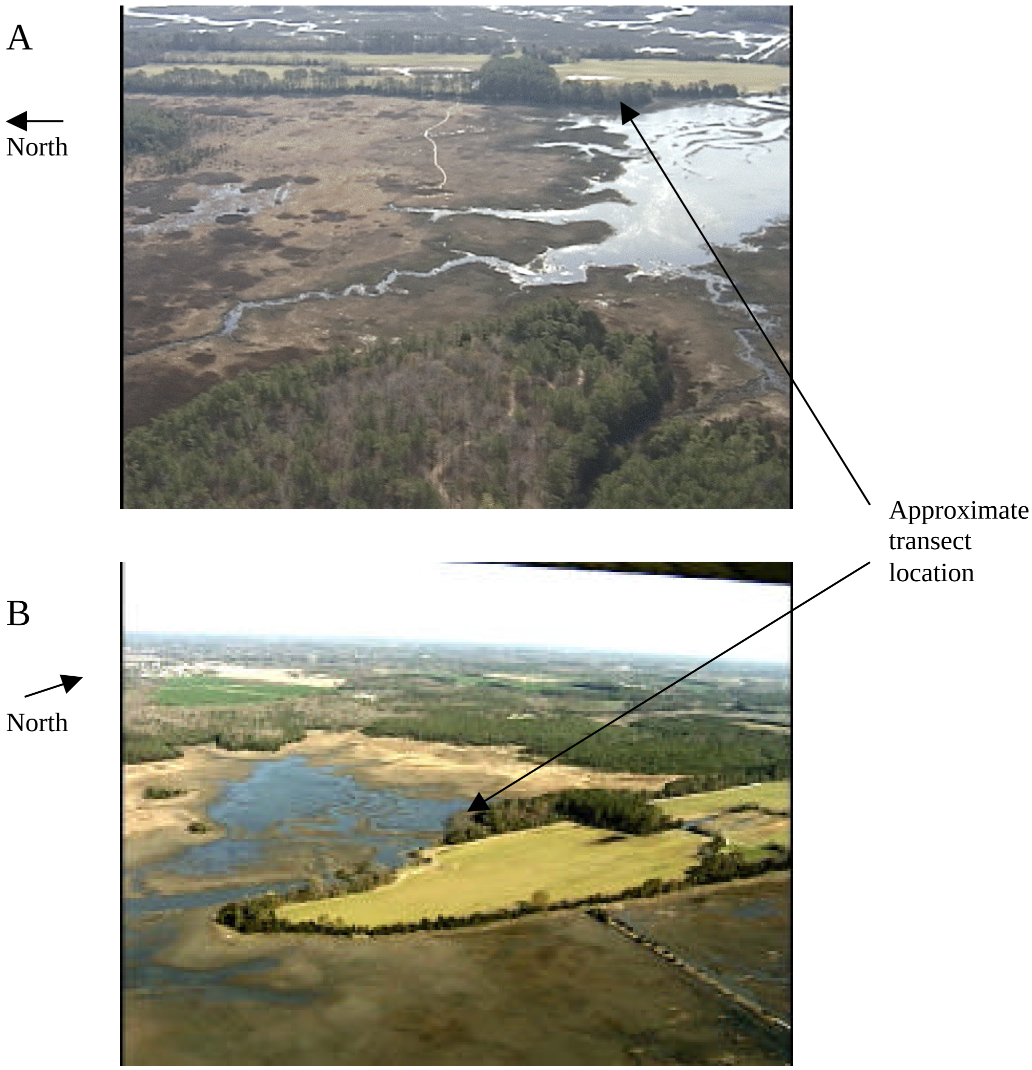

Figure 5. Aerial photographs of Phillips Creek Marsh.

A. View of the study site from the west. The tide comes into the marsh from the south. Tree line marks the transition from the marsh to the upland.

B. View of Phillips Creek Marsh from the east. The elevation of the upland area east of the study area is approximately 5 feet above MSL and is used for agriculture.

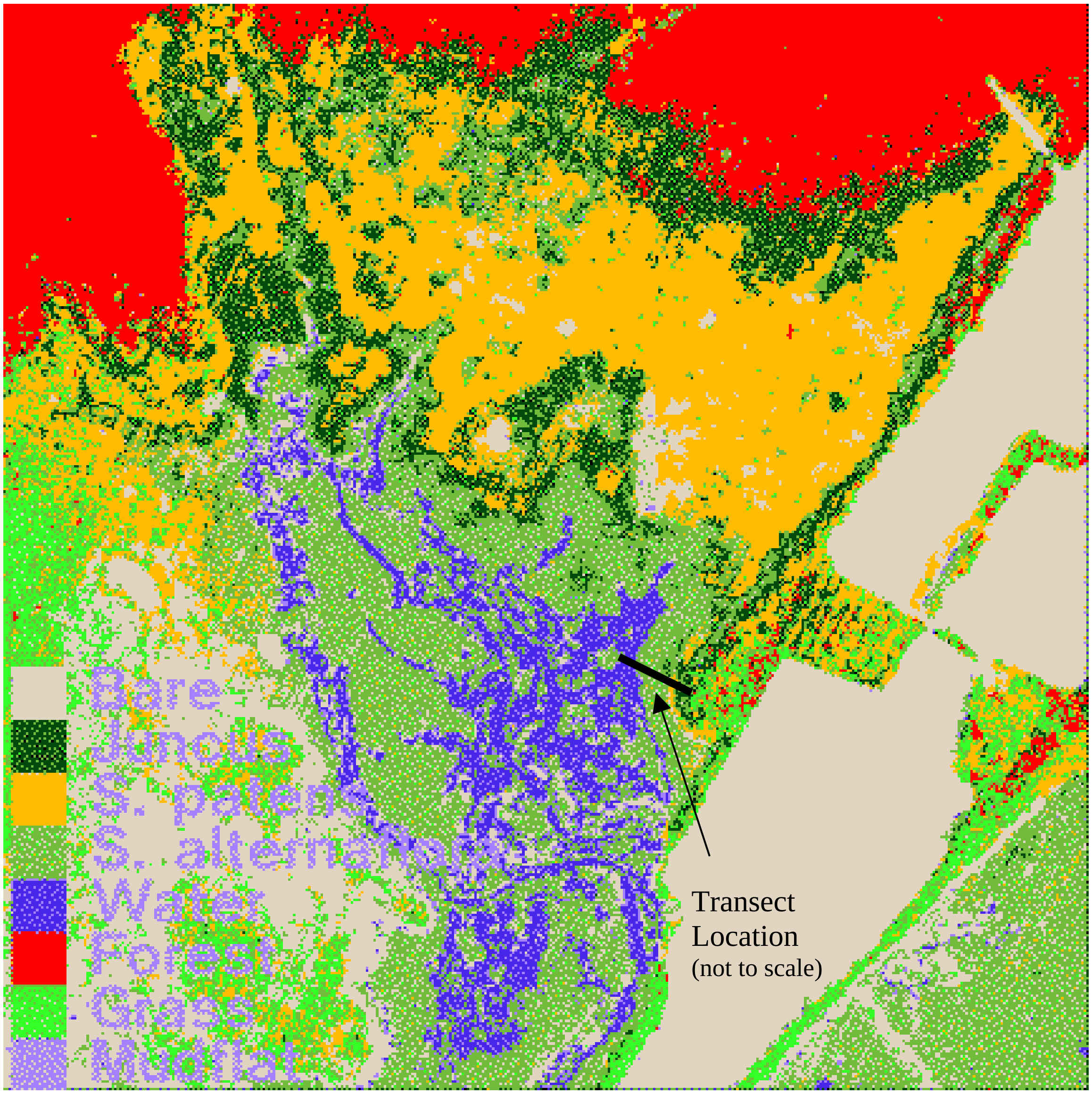

Figure 6. Unverified vegetation classification for Phillips Creek Marsh.

This image was made available through the Virginia Coast Reserve Long-Term Ecological Research station by L. Blum and J. Porter. Data for the image were collected in 1990.

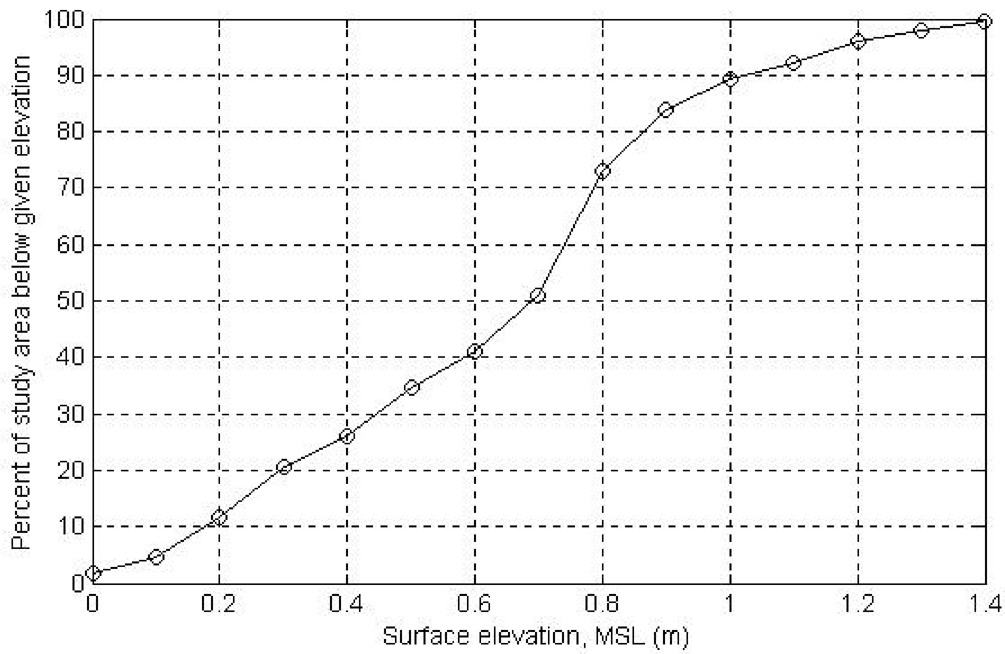

Figure 7. Hypsometric curve for study area (from interpolated survey data).

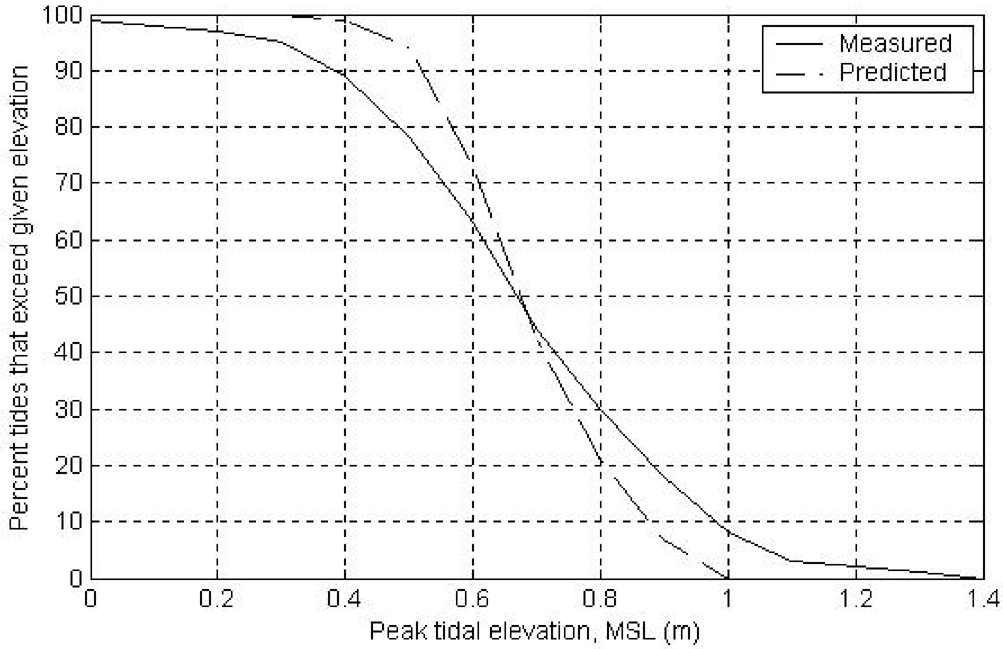

Figure 8. Measured and predicted tides for Phillips Creek Marsh, 1990-1997. (Values were from Christiansen (1998) and were based on tide data from Wachapreague converted to water levels at Phillips Creek Marsh).

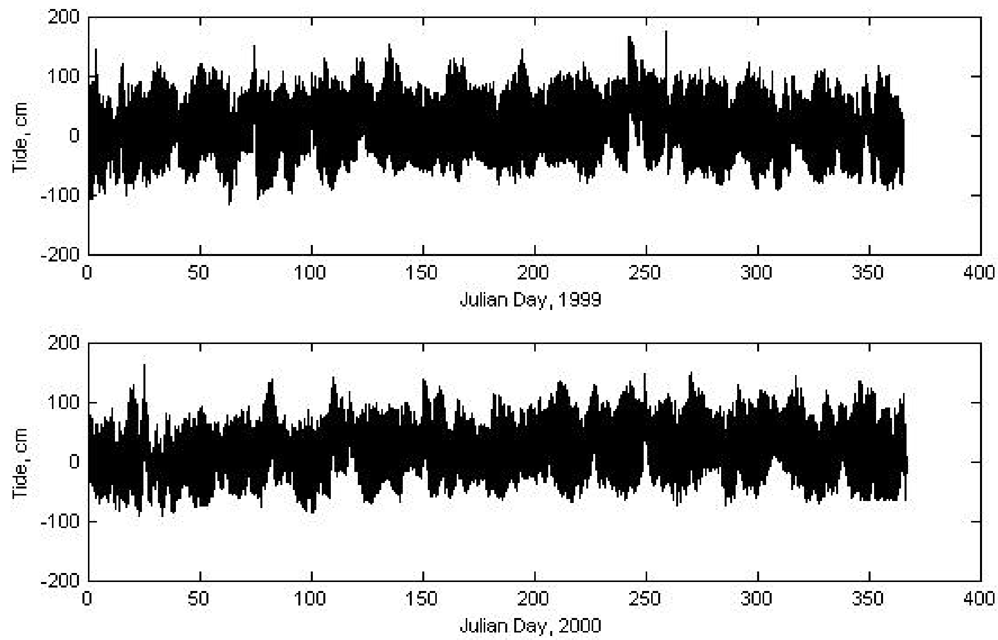

Figure 9. Tidal water levels at the study site (referenced to Mean Sea Level), 1999 and 2000 (from converted Wachapreague tide data).

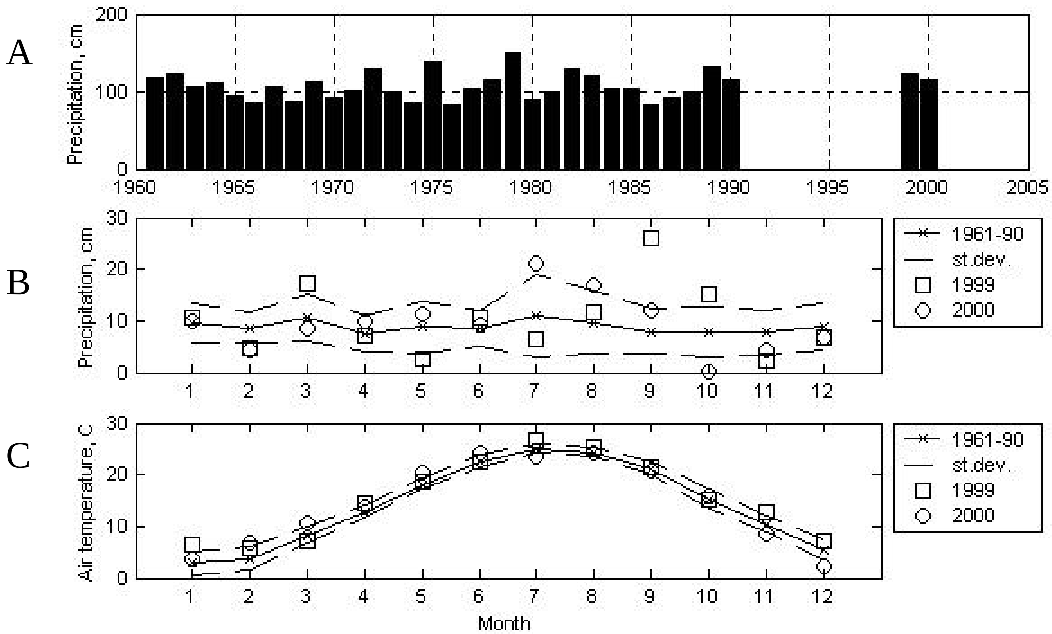

Figure 10. Climate data from the National Weather Service station at Painter, VA, 1961-1990, with data for 1999 and 2000.

A. Annual precipitation, cm.
B. Monthly total precipitation, cm. Average and standard deviation for 1961-1990, with data for 1999 and 2000.
C. Monthly average temperature, C. Average and standard deviation for 1961-1990, with data for 1999 and 2000.

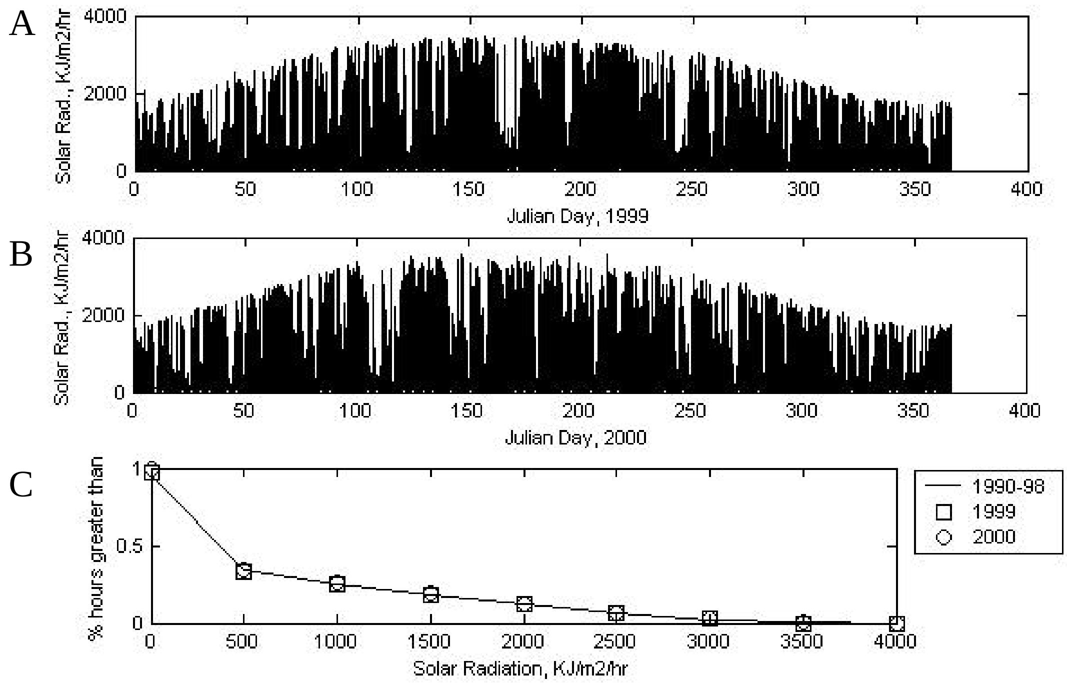

Figure 11. Solar radiation characteristics, 1990-2000, Phillips Creek meteorological station.

A. Hourly data, 1999 (kJ m^{-2} hr^{-1})
B. Hourly data, 2000 (kJ m^{-2} hr^{-1})
C. Probability distributions, 1990-1998, 1999, and 2000

Materials and Methods

2.1 Tidal and meteorological data acquisition

Tidal and meteorological data were necessary as inputs to an hourly model of the sediment water content. Model results were used to achieve the objective of determining spatial and temporal controls on overland flow. Tidal data were acquired from the National Oceanic and Atmospheric Administration (NOAA) station 8631044 at Wachapreague, VA (on the sea-side of the Delmarva Peninsula, ~20 km north of the site). The record extends from 1978 to the present. Deviations from predicted astronomical tides were determined as the difference between measured and predicted tides. Tidal elevation at Wachapreague was converted to tidal elevation at the study area by accounting for the difference in reference datums (1.85 m) and using a formula determined by Christiansen (1998):

$$Tide,_{\text{Phillips Creek}}\ (cm, MSL) = [\ Tide,_{\text{Wachapreague}}\ (m) + 1.85\ (m)\ ] * 108\ (cm\ m^{-1}) - B\ (cm).$$

The value for *B* was chosen to minimize the mean water level difference between the two locations (using water table measurements for the site during periods of inundation). For 1995, Christiansen (1998) used B = 199 cm, which gave a mean difference of 4 cm. For 1999 and 2000 tide data, B = 199 and 189 cm, respectively, giving mean differences of 3.7 and 4.1 cm, respectively. One hour was added to the Wachapreague tides to make up for a time lag.

Tide data from the LTER tide gauge on Redbank Creek (~1.6 km from the study area, **figure 3**) were used to fill gaps in the Wachapreague data. Water levels at the two locations were highly correlated (**figure 12**). Redbank was not used as the primary source because gaps in those data were more extensive.

An hourly record of air temperature, solar radiation, precipitation, and wind speed and direction was obtained in the marsh, ~100 m from the transect (**figure 3**), near the Hayden Benchmark (Porter et al, 2001). Average, minimum, and maximum air temperature (^{o}C) were measured with a "Campbell Scientific Temperature/ Relative Humidity probe HMP35C". Hourly averages were derived from 60 readings at one-minute intervals. Solar radiation (kJ m^{-2} hr^{-1}) was measured with a "Li-Cor 200S total radiation sensor". The hourly value is the sum of measurements taken at one second intervals. Precipitation (mm hr^{-1}) was measured in a "Leopold tipping bucket". Wind speed and direction were measured with a "R.M. Young Wind Monitor". All data were stored with a "Campbell Scientific 21x datalogger".

The Phillips Creek meteorological data set extended from 1991 to 2000, though there were significant gaps. To determine if data from meteorological stations at Hog Island and Oyster within the Virginia Coast Reserve were suitable for substitution at Phillips Creek, data from 1997 and 1999 were compared. The meteorological record was nearly complete from Hog Island and Phillips Creek in 1997, and from Oyster and Phillips Creek in 1999. Comparison to each station used both years; therefore, each comparison included one complete year plus one additional year. Values of –9 indicated missing data.

Temperature data from Hog Island and Oyster were similar to the Phillips Creek record (**figure 13A,D**). The range of variability was $\pm$ 10^{o}C. The scattering of data in figure 13A illustrated the need to quality-check the data in addition to identifying gaps. Analysis of the time series of temperature data from Oyster indicated these values were unrealistic. For this comparison, these unrealistic values were not removed. In compiling data for Phillips Creek, unrealistic data were replaced. Solar radiation from Hog Island was also similar to Phillips Creek (**figure 13B**). The range of variability was $\pm$ 200 kJ m^{-2} hr^{-1}. Solar radiation data were not recorded at Oyster. Temperature and solar radiation data from the Hog Island and Oyster meteorological stations were used to substitute for missing data at Phillips Creek, when available (**table 1**).

Precipitation data were not transferable between stations (**figure 13C, F**). A value of zero on one axis, but not the other, indicated that one station received an input that did not occur at the other station. The Phillips Creek record is missing precipitation data for Days 353-365, 1999, and Days 272-274, 2000.

A record of barometric pressure measured at Wachapreague was acquired from NOAA. Gaps were filled with data from NOAA station 8635750 at Lewisetta, VA (on the mainland, near the mouth of the Chesapeake Bay). The two records were well-correlated (**figure 14**).

2.2 Surface elevation survey

Within the study area, tidal inundation was assumed to be dependent only on surface elevation. Surveyed elevation data were used to determine tidal inputs. The study area (~0.5 ha) was surveyed using laser theodelite equipment ("Topcon Electronic Total Station GTS-303D"). Surface elevations were related to Mean Sea Level (MSL) by surveying the Hayden benchmark located near the meteorological station in the marsh. All elevations in this thesis (tides, water table, and surface elevation) are referenced to MSL. A second survey was conducted to extend the original coverage. Duplicate measurements of the elevation at well locations showed survey precision was 0.5-2.0 cm (**table 2**). Survey data were interpolated to a 5-m by 5-m grid (245 points, based on 338 survey points).

2.3 Measurement of microtopography and marsh surface characteristics

The objectives of this thesis were not only to determine if the spatial extent and frequency of occurrence for overland flow were sufficient to consider rainfall-runoff an important geomorphological agent, but to determine if a means of erosion during rainfall exists. Measurements of the marsh surface were used to develop a conceptual model for erosion. Also, the effect of rain was visually observed and liquid dye was used to trace the flow of water on the marsh during actual rainfall-runoff events.

Microtopography was measured using a 1-m^2 PVC frame with slots cut at 5 cm intervals on 2 opposing sides. A meter stick was held across the frame in the slots. The 4 corners of the frame were held in notches made in PVC stakes. The frame was oriented with 2 sides perpendicular to the tidal creek and two sides parallel to the elevation contours. The frame was leveled on all sides by adjusting the stakes and using a standard level. From this level datum, the distance to the surface was measured to the nearest 0.2

cm at 5 cm intervals along the meter stick, and repeated for each set of slots, such that the vertical distance was measured on a 5 cm by 5 cm grid. Plant stems within the frame were cut at the surface to facilitate ease of measurement, and this also made it much easier to qualitatively observe the features of the microtopography. It became apparent that measurements across the entire frame were not necessary, and usually an area of 0.5 to 0.75 m^2 was measured. The density of plant stems and crab burrows within the frame was recorded. The locations of burrows and mounds of sediment excavated from the burrows were recorded. Replicate measurements were made in both the low marsh and mid marsh.

2.4 Soil Measurements

Soil cores 10 cm (4 in.) in diameter were taken to a depth of 1.5-2 m at 7-10 m intervals from the low marsh into the forest. Textural analysis was by the hydrometer method and was completed as part of a separate study of soil moisture dynamics in the upland and transition zone (Dusterhoff, 2002). Soil cores 2.5 cm (1 in.) in diameter were taken in the marsh to a depth of 5-10 cm and used to determine organic content, porosity, bulk density, and volumetric soil moisture content. Soil properties were used to describe the area and enable cross-comparison with other marshes. Moisture content from soil cores was used to compare to water content from water table measurements and model results. Soil cores were the most direct measurement of water content, but also the most limited in time and space.

A copper pipe and wooden dowel were used to remove 1-inch soil cores from the marsh (see **Appendix 1** for details on soil core removal). The following method was used to quantify soil core compaction. The depth of the pipe in the ground was calculated as the total pipe length minus the length above ground. With the pipe in the ground, the dowel was inserted until it touched the soil surface. The length of the dowel inside the pipe was equal to the length of pipe above ground when the soil core was not compacted. If the soil core in the pipe below ground was compacted when the pipe was pushed down into the ground, the length of the dowel in the pipe was greater than the length of pipe above ground. The maximum allowable difference between dowel length and above-ground pipe length was 10% of the below-ground length of the soil core. Thus, cores used for analysis were compacted 10% or less.

Determination of soil properties depended on changes in weight as samples were processed from wet to dry to ashed. Mass measurements were precise to 0.001 g. Samples were dried at 100-105^{o}C for 24 hours, cooled in a dessicator for 15 minutes to prevent weight gain by condensation, and weighed. Samples were dried for an additional 12 hours and re-weighed until a constant weight was reached. Samples were then ashed at 500^{o}C for 5 hours to burn off the organic content. Ashed samples were cooled first in the 100^{o}C oven, then in the dessicator, before weighing. Samples were ashed for another 2 hours and re-weighed until a constant weight was reached.

The following calculations were used to gain information from the soil core data:

Soil mass, g (wet/dry/ashed)	= (sample and pouch, wet/dry/ashed) - (pouch)
Core volume, cm^3	= (core length) * (area of pipe cross-section)

Mass water, g = (sample and pouch, wet) - (sample and pouch, dry)

Bulk density, g cm^{-3} = (mass, dry) / (core volume)

Mass organic matter, g = (mass, dry) - (mass, ashed)

Mass mineral matter, g = (mass, ashed) - (pouch)

Volume organic matter, cm^3 = (mass, organic matter) * (organic matter density)

(organic matter density assumed 1.0 g cm^{-3}; Harvey, 1986)

Volume mineral matter, cm^3 = (mass, mineral matter) * (mineral density)

(mineral density assumed 2.65 g cm^{-3})

Volume "voids", cm^3 = (core volume) - (mineral volume) - (organic volume)

Porosity, dimensionless = (volume voids) / (core volume)

Volumetric water content, dimensionless =

[(mass water)/ (dry weight)] * [(dry bulk density) / (density of water)]

(water density assumed 1.0 g cm^{-3})

(References for the above calculations are Harvey, 1986, and Tan, 1996).

2.5 Water table measurements

Water table measurements were used to describe the hydrology of the study area and also provided a proxy for continuous water content data for model validation.

A series of ten wells was installed in July 1999 to monitor the elevation of the water table. The wells spanned a topographic transect from the low marsh into the forested upland **(figure 4)**. Wells were 213 cm in length (7 ft.) and were installed to an approximate depth of 150 cm. Wells were constructed of 5-cm (2-in.) diameter PVC pipe. The lower portion of each well was factory-slotted with a diameter of 0.1 cm. The upper portion was hand-drilled with a 0.6 cm bit (_-inch) along the entire length, including the above-ground portion. Wells were wrapped in nylon screening to keep sediment from clogging the holes.

Water table data were gathered by hand measurements and well-loggers. Hand measurements were more precise but less frequently available. Logger measurements were correlated to hand measurements to improve their precision. Logger measurements provided long-term data, but were available for only a few points on the transect at a time. The loggers were repositioned periodically to obtain coverage of all wells. Hand measurements were made along the entire transect to build an understanding of the hydrology of the study area and to ensure the point measurements were correctly placed in the context of the surrounding area.

2.5.1 Hand measurements of water table elevation

Water table elevations were recorded along the entire transect approximately daily during low tide for 5 weeks in July and August 1999. Whole-transect hourly measurements during low tide were obtained in August 1999, and August and September 2000. These measurements were obtained by hand using either a salinity meter or a sonic well level indicator. The indicator was lowered into the well until it contacted the surface. The length of cable extended was recorded as water table depth from the top of the well. Similarly, a salinity probe with an incremented cable can be used. The salinity reading jumps from zero to a positive value when the probe contacts the water table.

Measurements of ‘depth from top’ were converted to water table elevation by subtracting the reading from the measured height of the well. This gave water level with respect to the marsh surface. With surveyed surface elevations at each well, water levels with respect to the surface were converted to elevation with respect to mean sea-level (MSL). Precision of hand measurements was $\pm$ 1 cm, based on replicate measurements.

2.5.2 Logger measurements of water table elevation

“Solinst M5 leveloggers” were used to record hourly water table elevations in various wells from July 1999 until December 2000, with a maximum of three wells logged simultaneously (**figure 15**). The loggers were suspended from steel pins inserted near the top of each well. Loggers were suspended with stainless steel cable that would not stretch or shrink during repeated inundation and exposure.

A pressure transducer in the logger measures weight [M] and stores data with an internal recording device. The loggers divide this weight by the density of water [$M\ L^{-3}$] and multiply by the area of the transducer [L^2] to get a ‘length’ of water and atmosphere above the transducer. For brackish water, the loggers use a water density of 1.020 g cm^{-3}.

The water table elevation was derived from the length of water above the logger by first determining the position of the logger in the well. The surveyed surface elevation and the well height were added. From this sum, the depth to the pin, the cable length, and the length of the logger (to the transducer) were subtracted. This was the elevation of the transducer and was the point of measurement. The length of water above this point, minus the “length” of barometric pressure, was the elevation of the water table.

2.5.3 Correction of logger measurements for barometric pressure

The weight of the atmosphere (ie, barometric pressure) was subtracted from each reading. Barometric "length" was measured with a logger in the top of the well at either 60 or 70 m from the creek, where tidal inundation did not reach the tops of the wells. Later, barometric pressure measured in millibars (mb) at the NOAA station in Wachapreague (~20 km north of the site) was correlated to the logger measurement of barometric pressure in units of centimeters of water. Use of Wachapreague data enabled use of a logger for measurement of the water table in an additional well and for water table data to be salvaged when the barometric logger malfunctioned.

When time series of these two measurement-types were compared, a time lag was evident. Time was added to the Wachapreague data in increments of 0.01 days, and the correlation of the time series was maximized at 0.16 days (3.84 hours). For the most part, the lag corresponded to the different time standards of the two data sources. Data from Wachapreague were on Greenwich Mean Time, and logger data were on Eastern Daylight Time.

The mean difference between hourly measurements at the two locations for Days 190-232, 1999, was subtracted from the Wachapreague measurements to convert to centimeters of water:

mean difference =

$$\textit{average}\ [\ \textit{Barometric Pressure}_{Wachapreague}\ \text{(mb)} - \textit{Barometric “length”}_{logger}\ \text{(cm)}]$$

$$\textit{barometric length (cm)} = (\textit{Barometric Pressure}_{Wachapreague}\ \textit{mb}) - (\textit{mean difference})$$

The mean difference was 929.9 (0.4 standard deviation, 0.995 correlation coefficient). The conversion was tested on an independent set of data, Days 238-254, 1999 (**figure 16**). The converted Wachapreague measurements were a good approximation for the time series of barometric length recorded at the study area, and the mean difference was -0.11 cm (0.66 standard deviation). The spikes in the logger measurements in figure 16A were erratic measurements.

2.5.4 Precision of logger measurements of water table elevation

The factors affecting the precision of water table measurements by the loggers were quantified to the extent possible. These factors included precision of the surface elevation survey (**table 2**), precision of the transducers within the loggers, and the effect of using a constant value for water density.

The precision of the pressure transducers was determined by simultaneous measurements with all loggers under only barometric pressure. The transducer precision was 0-2 cm (**figure 17**).

Water density is a function of salinity and temperature. In the absence of hourly salinity and temperature data, the Solinst loggers used a constant density of 1.020 g cm^{-3} to adjust for brackish water. Analysis of salinity and temperature variability in the wells and the effect on water density was undertaken to determine the possible error introduced by the use of a constant value for water density. Salinity was measured 20 cm below the water surface in the wells with a “YSI Model 30” salinity meter. In the marsh (wells 20-49 m from the creek), salinity in summer ranged from 28-37 ppt (parts per thousand), without significant variation with distance from the creek (**figure 18**). Salinity in summer in the transition zone ranged from 23-32 ppt, and in the upland from 4-8 ppt. Data collected in March 2000 (not shown) were in the same range as data from summer, 1999. Measurements of salinity at the same location by Hmieleski (1994) showed a seasonal range of 10-30 ppt in the marsh and 2-10 ppt in the upland. Because the salinity measured during this study in the transition zone was similar to salinity in the marsh (**figure 18**), the range of values for the marsh was also used for the transition zone. Salinity higher than 30 ppt was measured in the marsh during this study, and these values were used for the upper range (instead of 30 ppt measured by Hmieleski, 1994).

Typical observed values for salinity and water temperature and the estimated range of values were used to determine the possible error introduced to water table measurements by using a constant density of 1.020 g cm^{-3} to convert the transducer readings (**table 3**). Using typical conditions, the effect is small in the marsh and transition zone. Water density in the upland was consistently lower than 1.020 g cm^{-3}. Logger readings are thus higher than if a more representative density was used. The error introduced by the density affects the raw logger data. Raw values include both atmospheric pressure and water in the wells and were typically 160-260 cm, with values above 200 cm generally associated with tidal inundation. Density error in units of cm was determined by the percent error times the raw data. For example, a 0.5% error means the reported water table elevation is 1 cm higher than actual for a raw value of 200 cm. This would be typical for measurements in the marsh and transition zone. The water table elevations reported for the upland are probably systematically 2-3 cm lower than actual.

The precision of logger measurements of water table elevation in the marsh was $\pm$ 5 cm. Precision was a combination of survey precision (0.5-2.0 cm), transducer precision (0-2 cm), and density error (0-1.3 cm in the marsh).

2.5.5 Adjustment of logger measurements according to hand measurements of water table elevation

Logger measurements of water table elevation differed from hand measurements (**figure 19**). Because the hand measurements were more precise (and assumed more accurate), logger measurements were adjusted to correspond to hand measurements. There was not a standard adjustment for each logger. Rather, a mean difference for each logger was obtained for each monitoring period (**table 4**; see figure 15 for monitoring periods). The adjustment was the mean difference between coinciding logger and hand measurements during the monitoring period. At a minimum, hand measurements were taken whenever loggers were installed or removed. Often, hand measurements were also taken within the monitoring period.

There were no hand measurements coinciding with logger measurements during the period of Day 304, 1999 to Day 22, 2000. Hand measurements were taken at logger installation, but this logger data was later overwritten. Based on analysis of water table data at 20 m from the creek during this period, the water table time series shows a characteristic spike for inundation, with the rate of change in water table elevation substantially decreased after the tide receded and the water table was below the surface. For this location for this monitoring period, the spike ended below the surface elevation. Therefore, the data were adjusted so the tidal spike ended at the surface. No correction appeared necessary at the other wells monitored during this period (60 and 70 m from the tidal creek).

Water table measurements during inundation illustrated the effect of adjusting the logger measurements to hand measurements. The water table elevation was expected to be the same at all locations that were flooded. However, differences were seen among the wells (**figure 20**). After adjustment, the difference among peak water table elevations centered around zero, indicating no systematic bias. Because the difference in water levels was expected to be zero among wells that were flooded, this comparison also shows the precision of logger measurements was $\pm$ 5 cm.

2.5.6 Well response tests

Well tests were performed to ensure measured values were representative of the actual water table position in the marsh. Wells were tested by adding a slug of water during rising tide (Hemond and Fifield, 1982; Harvey, 1986). The level of water in the well was expected to increase due to the slug, and then to decrease before the water level resumed rising due to the tide. The response time was sufficient at most wells. The well 23 m from the tidal creek did not pass and was excluded from analysis.

2.6 Specific yield estimations

Specific yield is a gravity-driven soil drainage parameter equal to the volume of water drained from a volume of soil per unit decline in total head. Specific yield has been used in other studies of salt marsh hydrology to represent water storage above the water table (**Table 5**). This storage coefficient ("S_y" in this thesis) is important in deriving water table elevation from a water balance model and in determining the saturation deficit from field measurements of the water table elevation:

Modeled water table displacement, cm = (modeled saturation deficit, cm) / (S_y)

Measured water table displacement, cm =

(saturation deficit from water table measurements) / (S_y).

By these relationships, model results can be compared to field measurements.

Water loss decreases (storage increases) for increased values of S_y. This is seen mathematically because S_y is in the denominator, where an increase in S_y decreases the change in modeled water table displacement for a given modeled value of saturation deficit and decreases the saturation deficit from water table measurements for a given measurement of water table displacement.

Two methods were used to determine an appropriate value of S_y at the study site. The first used soil core measurements of the saturation deficit and hand measurements of water table position:

S_y = (saturation deficit, cm) / (water table depth below surface, cm).

In other words, the amount of water removed per unit decline in water table elevation. The average of 16 measurements was 0.12 with a standard deviation of 0.03 (**figure 21**).

The second method used logger measurements of the water table response to precipitation inputs:

S_y = (Cumulative precipitation, cm) / (Cumulative water table response, cm).

In other words, the amount of water table rise per unit of water added. There were only three events to measure this response in which the water table remained below the surface throughout the event. Usually, precipitation was sufficient to bring the water table to the surface, thus truncating the response to precipitation. The Sy values were in the range of 0.10 to 0.11 (**table 6**).

The value employed for S_y in this thesis was 0.1. This value was supported by both methods above and is similar to literature values (**table 5**). The value used here is the same used by Fetsko (1990) for the sandy aquifer underlying the marsh an 2-8 m depth, but differs from the value of 0.03 used by Harvey (1990) in another location in Phillips Creek Marsh (**table 5, figure 3**). However, bulk density and porosity at the study site also differed from Harvey (1990) (see table 9).

2.7 Calculation of potential evapotranspiration

Evapotranspiration was significant as the only water loss in the water balance equation used to model the hourly sediment water content. Use of the Priestly-Taylor (1972) method of estimating potential evapotranspiration (PET) required solar radiation and temperature data:

$$\text{PET} = \alpha \frac{\Delta}{\Delta + \gamma} Q$$

Where $\alpha = 1.26$, a dimensionless empirical coefficient;

Δ = the slope of the relationship between saturation vapor pressure and temperature of the air (mb $^{o}C^{-1}$) and was approximated as

$$\frac{25083}{(T + 237.3)\text{^}2} \exp\left[\frac{17.3T}{T + 237.3}\right]$$

with T the measured air temperature (^{o}C);

$\gamma = 0.66$ mb $^{o}C^{-1}$, an approximation of the psychrometric constant, which combines the heat capacity of the air, air pressure, and the latent heat of vaporization of water (λ);

and Q was the measured incoming solar radiation (kJ cm^{-2} hr^{-1}). (See appendix 5 for correction to the PET method).

It was necessary to divide by the density of water (g cm^{-3}) and λ (kJ g^{-1}) for PET in units of (cm hr^{-1}). The advective effect of the atmosphere is described by α, also referred to as "the drying power of the air", and the radiative effect by $\frac{\Delta}{\Delta + \gamma} Q$. A marsh is a well-watered surface following inundation; therefore, an equation that models potential evapotranspiration, which assumes transpiration is not limited by water availability, approximates actual evapotranspiration in a regularly flooded salt marsh (Brutsaert, 1982; Nuttle and Hemond, 1988; Nuttle and Harvey, 1995).

2.8 Water balance model

The general approach of this thesis was to model the hourly water content for the study area as a means of determining the spatial extent and frequency of occurrence for saturation excess overland flow. A numerical model was developed to calculate the water balance for the sediment at hourly intervals based on tidal and precipitation inputs and losses by evapotranspiration. Saturation deficit was defined as a negative water balance and represented the amount of water necessary to saturate the sediment. Saturation excess was defined as precipitation in excess of the antecedent saturation deficit and was indicated by a positive value for the water balance.

For periods when the marsh was flooded, the saturation deficit was set to zero. Hemond et al (1984) indicated other fluxes could be neglected during periods of inundation. For non-flooded periods the water balance was calculated as the initial water content minus evapotranspiration, plus precipitation. Initial water content for the first time step was zero, because the model was programmed to start following the first tidal inundation in the time series of measurements. Time steps following saturation excess by rainfall also started with an initial water content of zero. Saturation deficit calculations were cumulative, but those for saturation excess were not.

The water balance was set to zero following saturation excess because no provision for runoff was included in the model. If saturation excess was not removed from the water balance after each time step, the model would show up to several centimeters of water on the marsh surface after rain events. This excess would remain until slowly depleted by evapotranspiration or the surface was inundated. This was not an accurate representation of how the surface responds to rainfall. Saturation excess was observed to collect on the surface in depressions in the microtopography and run off when the depth exceeded the depressions. The amount remaining on the surface was limited by the depth of the depressions to be approximately 1 cm. This would not be 1 cm of water uniformly on the surface, but would be small pockets of water. This amount of excess remaining on the surface after runoff events or tidal inundation was neglected in the water balance model, but in the field no water loss from the sediment is expected until these pockets are depleted.

In numerical terms the water balance model was:

If $\text{Tide}_i > \text{Surface}$,

$\text{Water Content}_i = 0$;

Else, if $\text{Water Content}_{i-1} > 0$,

$\text{Water Content}_i = 0 - \text{PET}_i + \text{PPT}_i$;

Else, (if $\text{Tide}_i < \text{Surface}$ and $\text{Water Content}_{i-1} \leq 0$),

$\text{Water Content}_i = \text{Water Content}_{i-1} - \text{PET}_i + \text{PPT}_i$;

i = the hourly time step,

Tide = tidal elevation (MSL),

Surface = elevation of the marsh surface (MSL),

PET = potential evapotranspiration (cm hr^{-1}),

PPT = precipitation (cm hr^{-1}).

The model assumed soil specific yield, vegetation, radiation, air temperature, and rainfall were uniform within the study area. The effects of soil properties were combined into a single term, S_y. Within marsh zones, plant species composition was nearly homogenous, minimizing differences in root water uptake by different species. The distribution of individual plants was so dense as to also be considered uniform, further minimizing spatial differences in water uptake. The study area was small enough that it was reasonable to assume uniform meteorological inputs.

2.9 Saturation deficit calculations

Saturation deficit was determined from soil cores, water table measurements, and the water balance model. The soil core method was the most direct, but measurements were limited to brief periods of field sampling. These data were used to verify the accuracy of the other two methods. Saturation deficit for the entire study period was much easier to obtain from water table measurements, but this was limited to the timing and location of monitored wells. These two methods were used to verify the accuracy of the water balance model. The model allowed extrapolation of the saturation deficit over a broader time and space to analyze temporal and spatial patterns of saturation in the study area. Because the water table remained at the surface during rainfall events that saturated the sediment, saturation excess was not derived from water table measurements.

The following variables and equations were used to determine the saturation deficit.

L_{total} = total core length [L]

L_{sat} = length of core that was saturated (ie, below water table) [L]

= L_{total} - depth to water table from surface

L_{unsat} = length of core that was unsaturated (ie, above water table) [L]

= $L_{total} - L_{sat}$

θ_s = the water content at saturation [$L^3{}_{water}$/ $L^3{}_{total\ core}$]

(θ_s was assumed equal to the average porosity measured at each location; see table 8),

θ = volumetric water content [$L^3{}_{water}$/ $L^3{}_{total\ core}$]

W_{total} = water content of the total core [L] = $L_{total} * \theta$

W_{sat} = water content below the water table [L] = $L_{sat} * \theta_s$

W_{unsat} = water content in the unsaturated zone [L] = $W_{total} - W_{sat}$

If the entire core was above the water table,

Saturation deficit, cm = $(\theta_s - \theta) * (L_{total})$.

When part of the soil core was below the water table,

W_p = Potential water content for the length above the water table when saturated [L]

= $L_{unsat} * \theta_s$

Saturation deficit, cm = $W_p – W_{unsat}$

Using the water table measurements,

S_y = 0.1, dimensionless water storage term analogous to the specific yield

Saturation deficit, cm = (Depth to water table from surface, cm) * (S_y).

Soil core compaction during sampling was limited to 10% of the core length. Actual compaction for each core was not recorded. To determine the effect of sample compaction on the saturation deficit, 10% was added to the measured length of each core. The core volume was adjusted according to the adjusted length. The porosity and volumetric water content were re-calculated with the measured mass of water, mineral, and organic content. The saturation deficit calculations were repeated with the adjusted porosity, water content, and core length. The adjustment for compaction gave an upper bound to the saturation deficit derived from soil cores. The saturation deficit derived without regard to compaction was a lower bound.

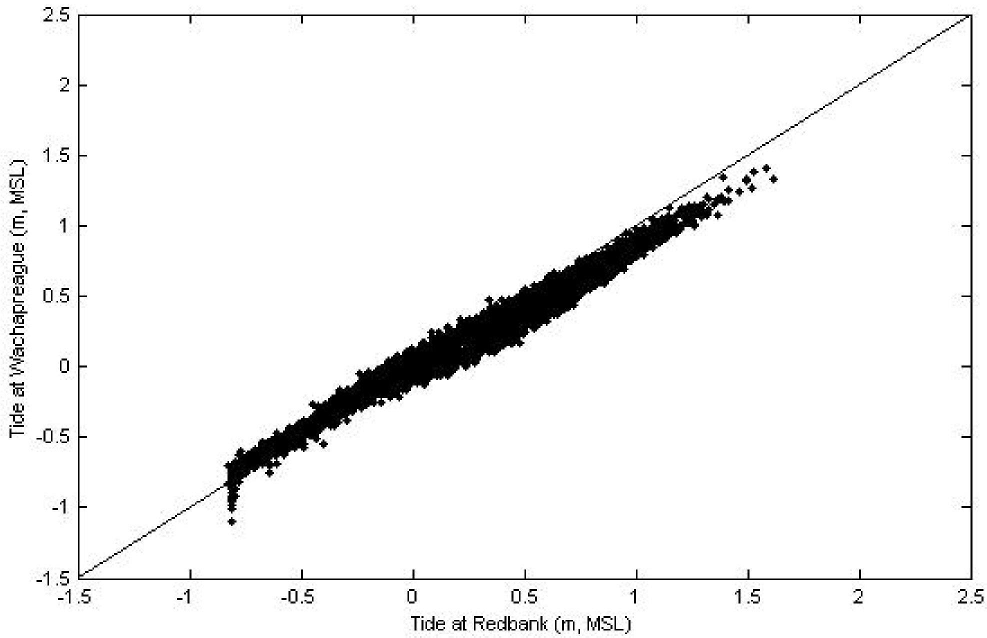

Figure 12. Comparison of tidal elevations at Wachapreague and Red Bank, VA. (Comparison is for Days 42-208, 1999, with one hour added to Wachapreague data to compensate for a time lag).

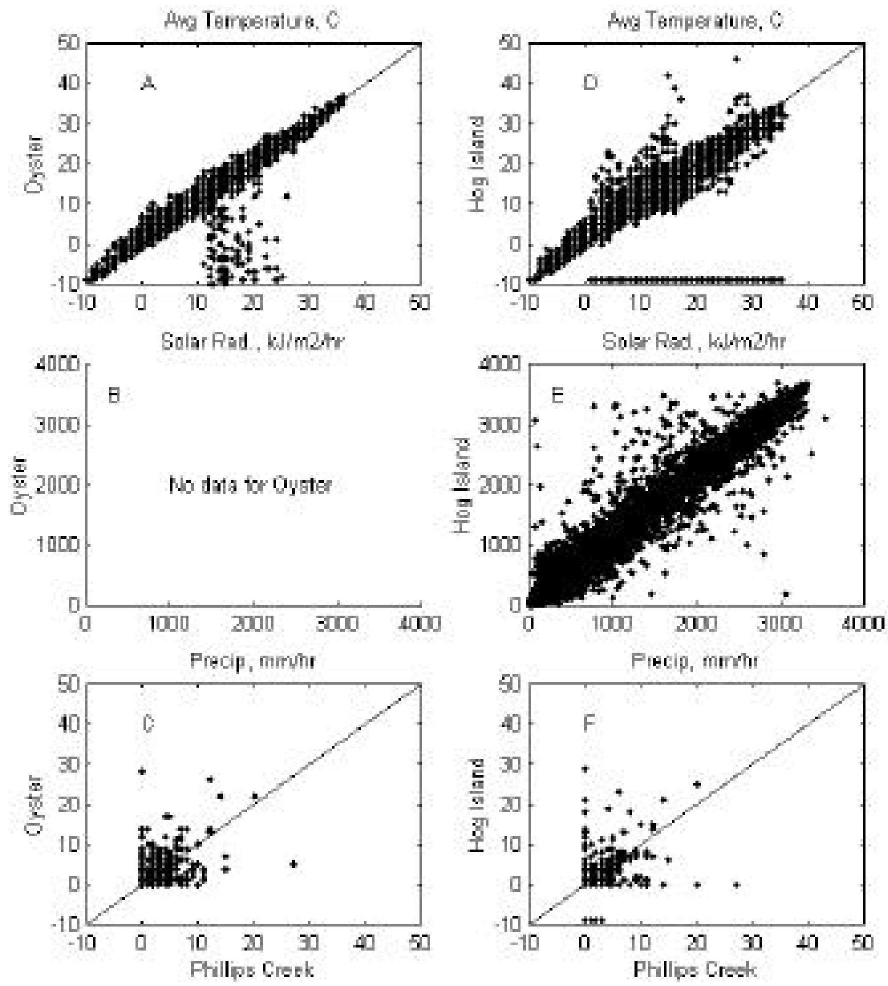

Figure 13. Comparison of hourly air temperature, solar radiation, and precipitation among meteorological stations within the Virginia Coast Reserve

A. Average hourly air temperature (C) at Phillips Creek (x-axis) and Oyster (y-axis).
B. Could not compare solar radiation between Phillips Creek and Oyster.
C. Hourly precipitation (mm) at Phillips Creek (x-axis) and Oyster (y-axis).
D. Average hourly air temperature (C) at Phillips Creek (x-axis) and Hog Island (y-axis).
E. Solar radiation (kJ m^{-2} hr^{-1}) at Phillips Creek (x-axis) and Hog Island (y-axis).
F. Hourly precipitation (mm) at Phillips Creek (x-axis) and Hog Island (y-axis).

Table 1. List of data substitutions from Hog Island and Oyster used to fill gaps in the meteorological data for Phillips Creek Marsh.

Year	mm/dd-mm/dd	Julian Day	Source	Data Replaced
1999	12/19-12/22	353.0-356.5	Oyster	Air temperature
	12/19-12/22	353.0-356.5	Hog Island	Solar radiation
	12/22-12/23	356.54-357.17	Hog Island	Air temp, Solar rad.
	12/23-12/31	357.21-365.96	Oyster	Air temperature
	12/23-12/31	357.21-365.96	Hog Island	Solar radiation
2000	06/18-06/28	170.0-180.96	Hog Island	Air temperature
	06/29-07/18	181.0-199.96	Oyster	Air temperature
	07/19-09/27	200.0-271.96	Hog Island	Air temperature
	09/28-09/30	272.0-274.96	NO DATA AVAILABLE	
	10/01-10/30	275.0-304.96	Oyster	Air temperature
	11/10	315.0-315.96	Hog Island	Air temperature
	11/14	319.0-319.96	Hog Island	Air temperature
	11/25-11/27	330.0-332.96	Hog Island	Air temperature
	12/10-12/17	345.0-352.96	Hog Island	Air temperature

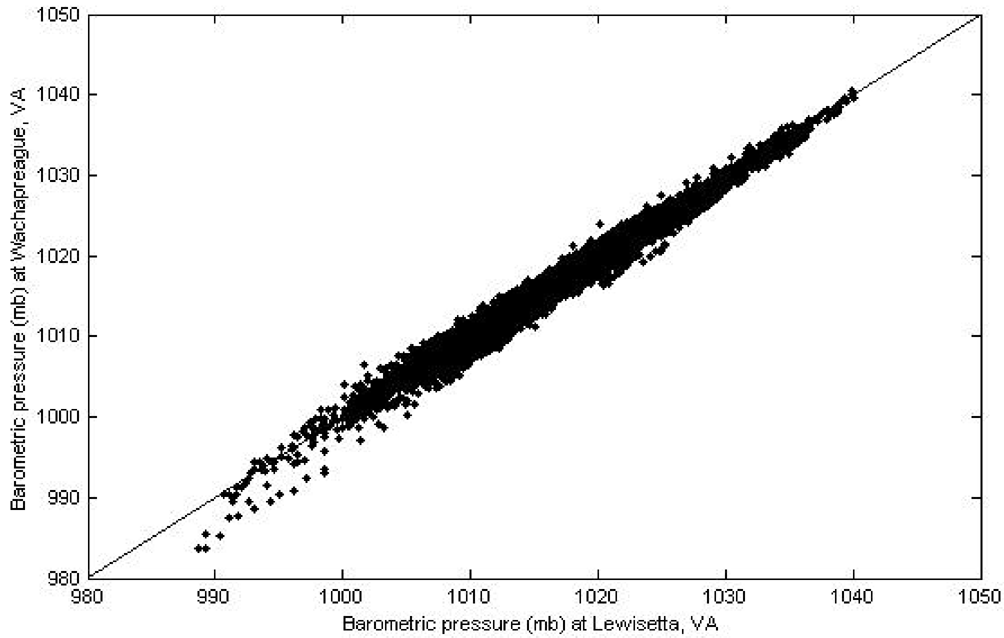

Figure 14. Comparison of barometric pressure recorded at Wachapreague and Lewisetta, VA, 2000.

Table 2. Precision of topographic surveying.

Distance from creek (m)	Surface elevation (cm, MSL) (March, 2000)	Surface elevation (cm, MSL) (August, 1999)	Difference (cm)
20	37.86	38.56	0.7
23	46.56	47.06	0.5
27	63.96	63.36	0.6
31	73.96	72.96	1.0
35	77.56	78.06	0.5
39	79.16	81.06	1.9
43	81.16	82.46	1.3
		average difference	**0.9**
		observed range	**0.5 - 1.9**

A

B

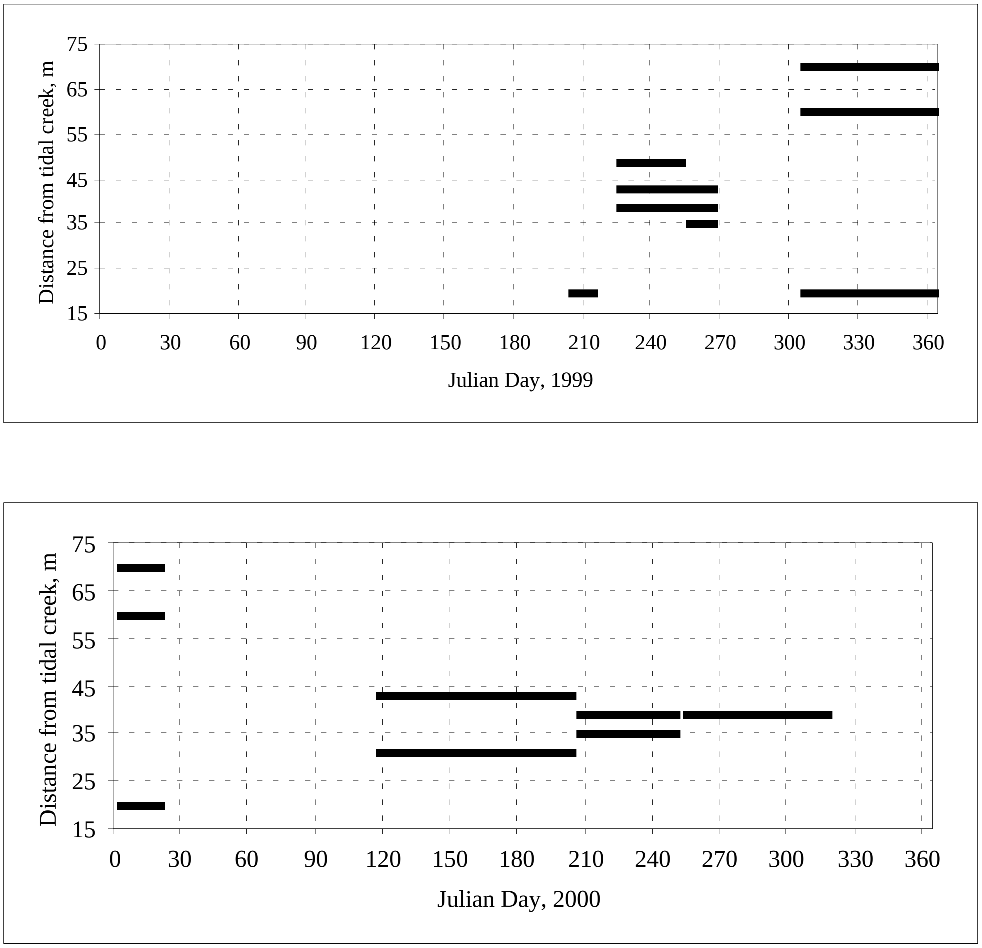

Figure 15. Location and monitoring periods of long-term water table measurements.

A. 1999 monitoring periods
B. 2000 monitoring periods

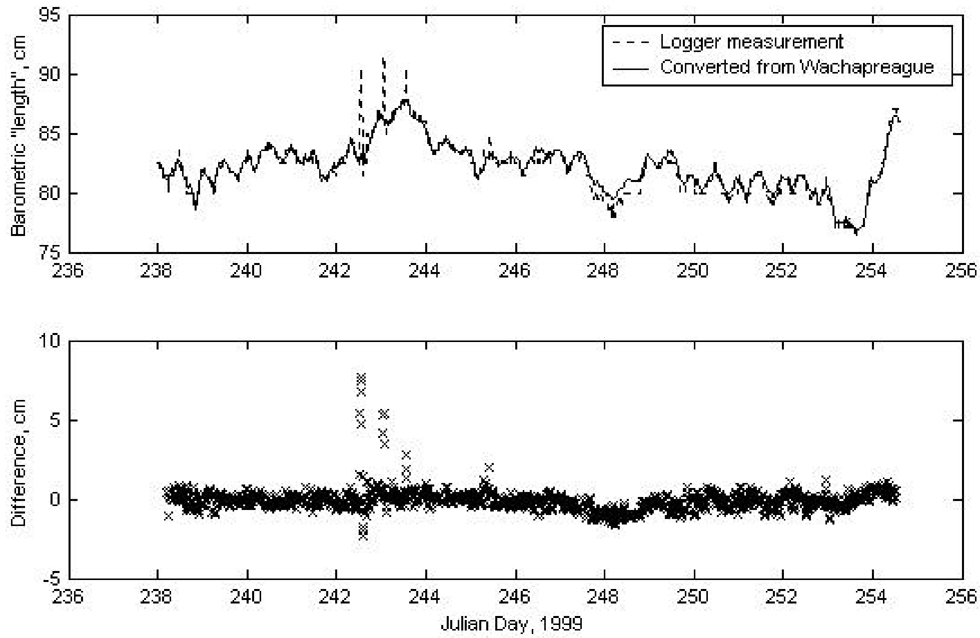

Figure 16. Comparison of the barometric “length” recorded by wells loggers and converted from barometric pressure measurements at Wachapreague.

A. Time series for each measurement type
B. Difference between the two measurement types

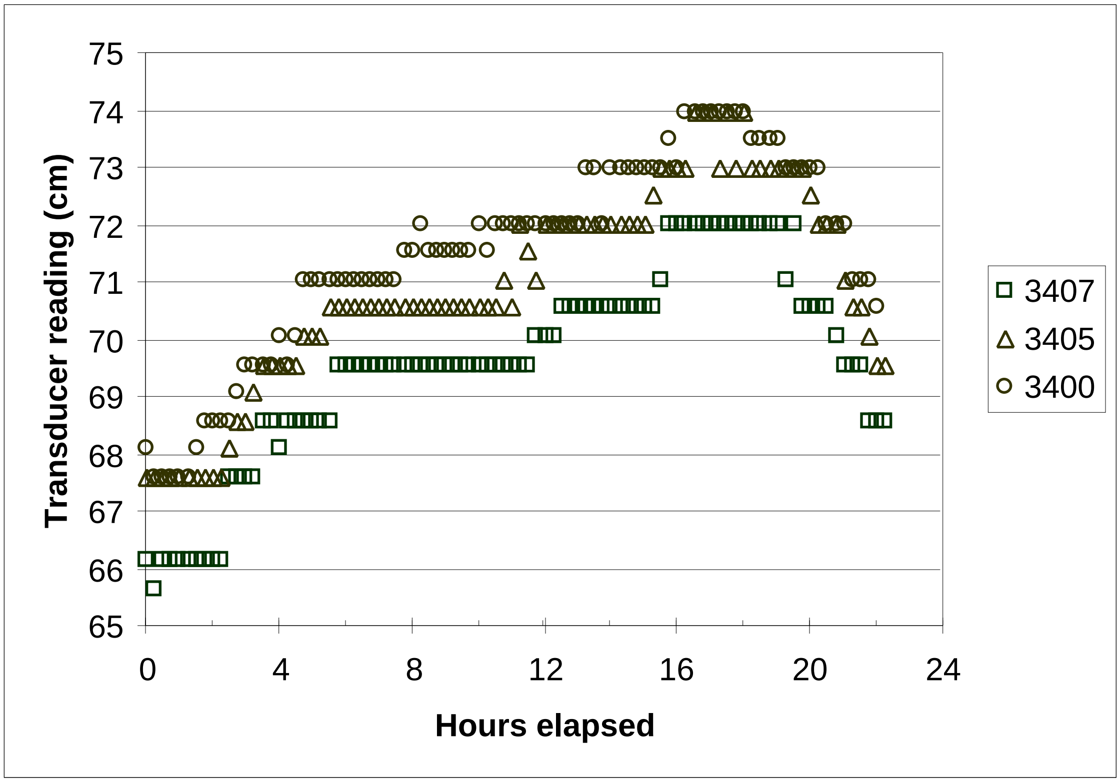

Figure 17. Variability among logger transducer readings. (Legend refers to logger serial numbers).

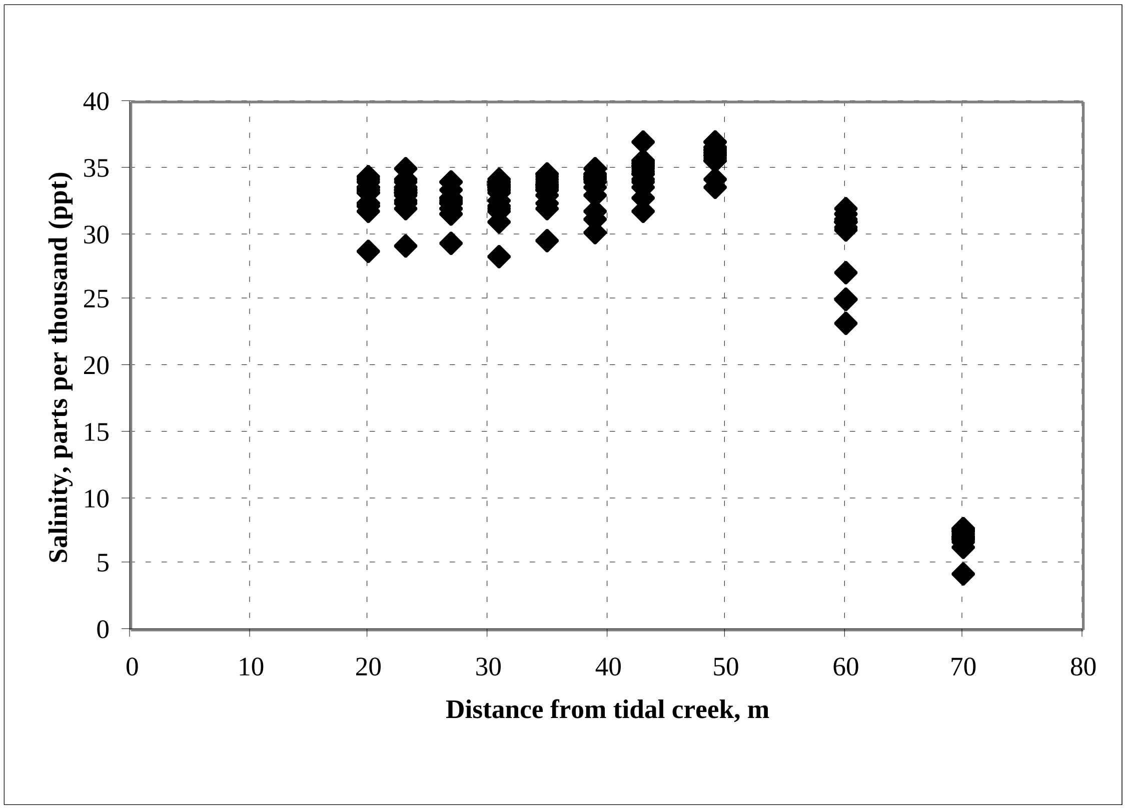

Figure 18. Salinity at 20 cm below the water surface in wells. (Measurements were made during low tide, July 30 to August 13, 1999).

Table 3. Possible effect of water density on water table measurements by loggers.

Location	Conditions	Season	Salinity (ppt)	Water temperature (^oC)	Density* (g cm^{-3})	Effect (%)**
marsh	typical	summer	33	15	1.024	0.4
marsh	typical	winter	33	10	1.025	0.5
transition	typical	summer	30	15	1.022	0.2
transition	typical	winter	30	10	1.023	0.3
upland	typical	summer	7	15	1.004	-1.6
upland	typical	winter	7	10	1.005	-1.5
marsh	range ***	summer	25-40	15-20	1.017-1.030	(-0.3)-(1.0)
marsh	range	winter	10-40	5-10	1.007-1.032	(-1.3)-(1.2)
transition	range	summer	25-35	15-20	1.017-1.026	(-0.3)-(0.6)
transition	range	winter	10-35	5-10	1.007-1.028	(-1.3)-(0.8)
upland	range	summer	5-10	10-15	1.002-1.007	(-1.8)-(-1.3)
upland	range	winter	2-10	5-10	1.001-1.008	(-1.9)-(-1.2)

* Density values as a function of water temperature and salinity from Appendix A in Fischer et al (1979)

** Effect refers to percent change in raw transducer readings for given density,
as compared to density of 1.020 g cm-3 used by logger. Effect = [(density-1.02)/density] *100%

*** Range refers to the expected range of densities for the given ranges in salinity and water temperature.
The highest density in the range includes the upper salinity bound and lower temperature bound;
vice-versa for lowest density.

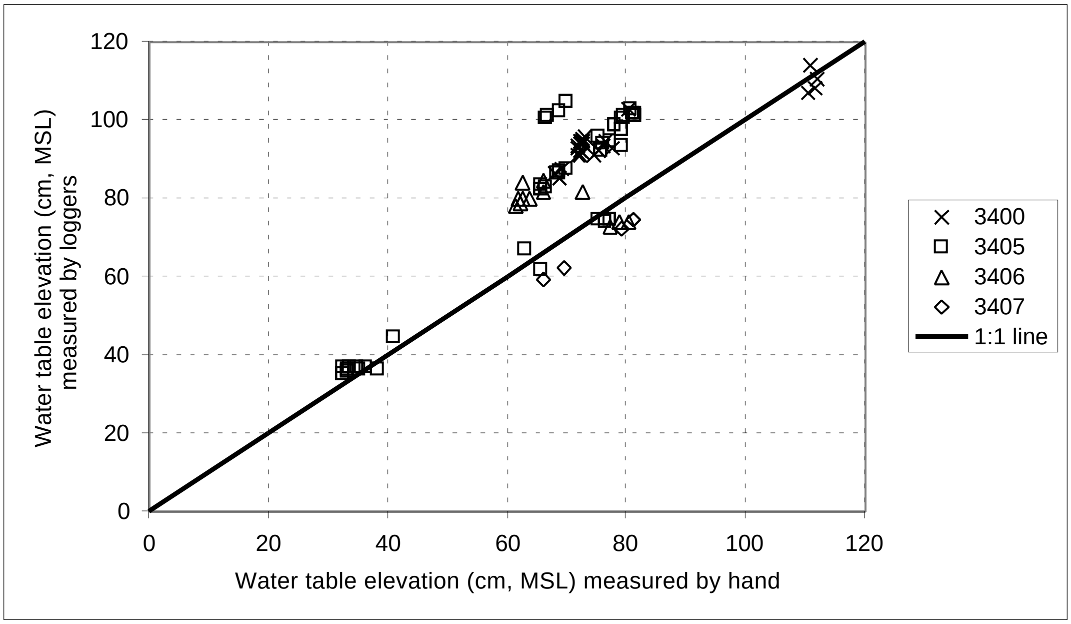

Figure 19. Comparison of hand and logger measurements of water table elevation for all monitoring periods. (Legend refers to logger serial numbers).

Table 4. Adjustment added to logger measurements of water table elevation.

Logger #	Location *	Julian Day	Year	Adjustment (cm)	Standard Deviation (cm)
3400	60	304-022	1999, 2000	0 **	---
3400	35	206-252	2000	-22.0	1.9
3400	31	117-206	2000	-21.1	1.3
3405	20	204-216	1999	-2.4	1.5
3405	39	224-238	1999	+1.7	1.2
3405	39	238-254	1999	+2.0	0.5
3405	35	254-268	1999	+2.5	0.3
3405	70	304-022	1999, 2000	0 **	---
3405	43	117-206	2000	-20.0	1.3
3405	39	206-252	2000	-21.3	1.5
3405	39	253-320	2000	-34.3	0.6
3406	49	224-238	1999	+1.8	2.0
3406	39	254-268	1999	+5.0	1.1
3407	43	224-238	1999	+6.9	0.4
3407	43	238-254	1999	+5.6	0.2
3407	43	254-268	1999	+6.5	0.0
3407	20	304-022	1999, 2000	+6.5 **	---

* Distance from tidal creek (m)

** There were no hand measurements coinciding with logger measurements during this period.

B

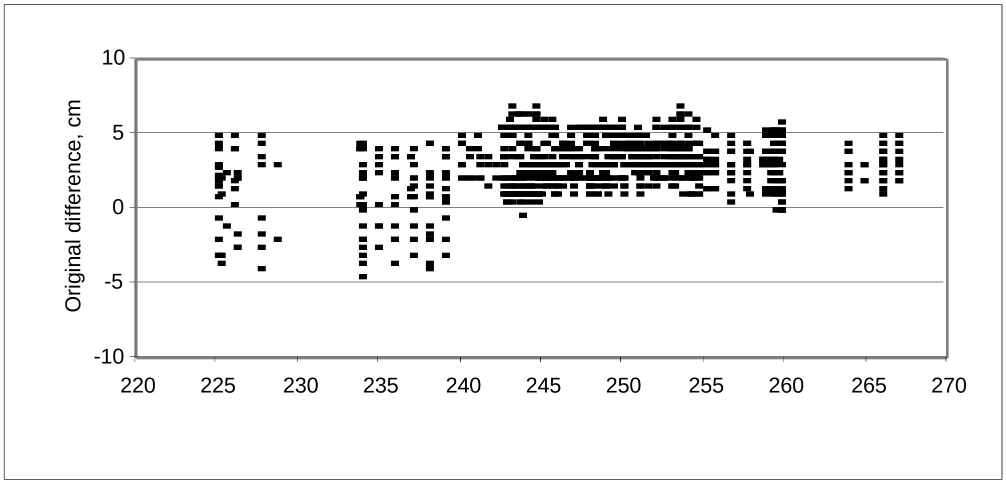

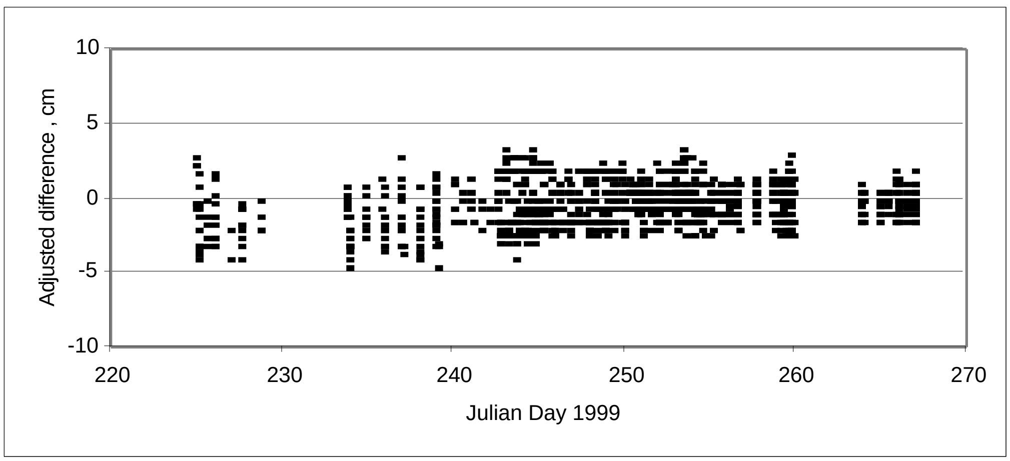

Figure 20. Difference in peak water levels during inundation among wells measured by well loggers.

A. for both original data
B. for data adjusted to hand measurements.

Table 5. Specific yield values used in salt marsh hydrology studies.

Source	**Location**	**Specific yield (S_y) value**
Harvey, 1986; Harvey et al, 1987	Carter Creek, VA	0.03
Knott et al, 1987	Great Sippewissett and Ebben Creek, MA	0.10
Nuttle and Hemond, 1988	Belle Isle, MA	0.11-0.16
Fetsko, 1990	Phillips Creek, VA	0.1
Harvey, 1990	Phillips Creek, VA	0.03
Nuttle and Portnoy, 1992	Cape Cod, MA	0.1

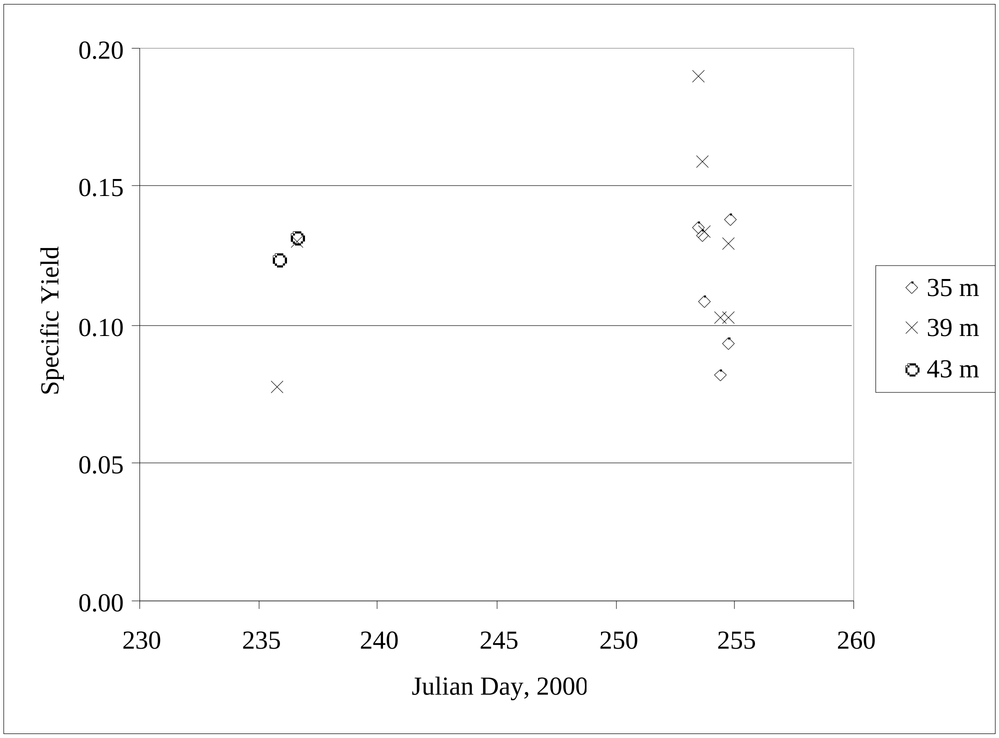

Figure 21. Specific yield calculated with saturation deficit from soil cores and water table displacement. (The average specific yield was 0.123, with n=16 and 0.029 standard deviation. Legend refers to distance from tidal creek for both soil cores and water table measurements).

Table 6. Water table response to precipitation inputs.

Year	Day	Distance to creek (m)	Precipitation (cm)	Water Table Response (cm)	Sy (cm/cm)
2000	179	31	3.0	26.2	0.11
2000	179	43	3.0	26.7	0.11
2000	192	43	1.4	14.1	0.10

Results

3.1 Comparison of tidal elevation at Wachapreague and Phillips Creek Marsh

Tidal elevations at Wachapreague provided a good approximation for the study area. The mean difference between hourly water level measured with well loggers and the water level for the site converted from the Wachapreague tide gauge was 3.7 and 4.1 cm, respectively, for 1999 and 2000. The difference was partly due to variation in the onset of the tides at the measurement locations. Peak tidal elevations were usually similar. Inundation recorded at the study area was usually also indicated by the Wachapreague data, and vice versa (**figure 22A**; see also the agreement between tidal elevation from Wachapreague data and water level recorded at the site for all data in appendix 2).

Exceptions sometimes occurred, in which inundation at the study area was indicated by tidal elevations from one measurement location, but not the other (**figure 22B**). There were 16 exceptions in 248 days of measurements in the midmarsh at 80 cm elevation (MSL), or approximately 3% of the 476 tidal cycles in that period. The duration of inundation at the two locations was also similar. In 113 days of measurements at 80 cm elevation in the study area (Days 207-319, 2000), the total duration of inundation indicated by the Wachapreague data was 88 hours greater than total duration recorded at the site. On average, that was 0.4 hours difference on each of the 217 tidal cycles in that period.

3.2 Microtopographic characteristics and observations of rainfall-runoff events

Sediment mounds, created by crabs during burrowing, ranged in height from 2-4 cm with a surface area of 25-500 cm^2 **(figure 23**). Crab burrow density was 40 m^{-2} in the low marsh (~25 m from the creek) and 3 m^{-2} in the interior (~40 m from the creek) (**table 7**). This corresponded well to the density of 41 m^{-2} observed by Katz (1980) in low marsh. (Note, Katz (1980) used burrow counts to estimate crab density and reported this number, but gave the conversion equation). Plant stems were clumped on the sediment mounds, but also occurred in the depressions. Plant stem density was 158 and 583 m^{-2} in the low marsh and interior, respectively (**table 7**).

Saturation excess was observed to collect in depressions in the microtopography. Dye placed in the depressions flowed in rills when the excess overcame the depth of the depressions. The apparent depth of the depressions was 1 cm, based on analysis of flowpaths among depressions in contour plots of microtopography (**figure 23).** The mounds remained exposed above the saturation excess. Dye placed on sediment mounds was shed into the adjacent depressions. Sediment particles were disturbed by the impact of rain and were transported in the rills.

3.3 Physical soil properties

Marsh soil porosity was high, with low bulk density and low organic content (**table 8, figure 24**). Results were similar to other studies in Phillips Creek Marsh (**table 9**); however, porosity at the study area was slightly higher, and bulk density lower, than other studies. The high porosity values might reflect inappropriate values assumed for mineral and organic matter density. Surface soil layers, approximately the top 30 cm, typically had a high silt component with variable sand and clay content (**table 10**). The sand component of marsh sediments below 30 cm depth was typically 50% or more (**table 10**).

An exception to this pattern of soil layering was found at the upper extent of the marsh, adjacent to the transition zone (textural data 53m from the creek), where sandy sediment was found both in the surface layer and at depth, and clay content increased at depth (**table 10**). At 5-10 cm depth near this location (49 m from the creek) porosity was lower and bulk density was higher than at other locations (**figure 24, table 8**). Porosity and bulk density were consistent among other locations and at both depths at each location (**figure 24, table 8**).

3.4 Soil moisture and saturation deficit from soil core measurements

Soil cores were taken in the summer, 2000, to assess soil moisture dynamics during periods when the marsh was not inundated for several days. Soil moisture values were not adjusted for compaction. Soil moisture content was high and did not vary significantly with distance from the creek (**figure 25 A,B,D,E**). Moisture content remained high throughout the sampling periods, while water table elevations generally decreased (**figure 25C, G**).

For the period of Day 235-237, 2000, soil moisture 39m from the creek decreased during the period. Soil moisture 43m from the creek did not decrease during the period.

This location (43 m from the creek) showed a rising water table around Day 236.5 (**figure 25C**), earlier than the other location (39 m from the creek). For the period of Day 253-255, 2000, at locations 35 and 39m from the creek, soil moisture decreased over time. The water table elevation decreased over the sampling period (**figure 25F**), indicating water removal. Evapotranspiration for the two periods was normal (**figure 25D, H**).

Soil moisture values for the soil cores were converted to saturation deficit values to provide a basis for comparison of other methods of deriving the saturation deficit. Saturation deficit from the soil moisture values of the cores was adjusted for compaction of the cores. The adjustment increased core length by 10%, the maximum compaction allowed during field sampling. The volume increased accordingly, and the volumetric soil moisture decreased. The saturation deficit before adjustment is a lower bound, representing less water removed and higher soil moisture compared to adjusted cores. The adjusted saturation deficit is an upper bound (more water removed, lower soil moisture). Averages of replicate cores were used to create the bounds and were used later to test the other methods of deriving the saturation deficit (**figure 26**).

3.5 Water table characteristics

The most prominent characteristic of the water table was that it remained near the surface throughout the study period. Depth from the surface to the water table during marsh exposure ranged from 0-40 cm (**appendix 2**). There was not much time for water removal from the soil by evapotranspiration between daily or semidiurnal periods of inundation. Depth to the water table generally increased as time since the last tidal inundation increased.

3.5.1 Water table characteristics during periods of regular inundation

Inundation was considered regularly-occurring for once- or twice- daily episodes of tidal flooding at a given elevation on the transect. Regular inundation was a standard occurrence within the low and mid marsh (**appendix 2**). Regularly inundated periods were separated by occasional drying periods. Drying periods were defined by a lack of inundation for more than two successive semi-diurnal tidal cycles.

Measurements of water table position were made by hand along the entire transect during summer, Days 207-225, 1999 (**figure 27A**). During this monitoring period, the study area was regularly inundated and PET was normal (**figure 27B, C**). Measurements were made during low tide, but were not necessarily a low-tide minimum value. This short-term coverage of the whole transect complimented long-term continuous monitoring by well loggers that was limited to only a few locations at a time. The daily low-tide water table position was near the surface at all locations (**figure 27A**). Water table elevation with respect to MSL was higher in the transition zone (60 m from the creek) than in either the marsh or upland. At most locations in the marsh, depth from the surface to the water table was typically 5 cm, such that water table elevation with respect to MSL generally increased with increased surface elevation. Depth to the water table during this monitoring period was about 25 cm at locations 27 and 43 m from the creek.

Hourly measurements of water table position by a well logger 39 m from the creek on Days 233-238 (August 21-26), 1999, illustrated water table dynamics during a period of once-daily inundation (**figure 28**). Inundation occurred in the evening of Day 233 (around 233.75). Overnight, PET was negligible and the water table elevation remained near the surface. On Day 234, PET was normal and the water table elevation was drawn down below the surface. The location was again inundated around Day 234.75. Overnight PET and water table drawdown were negligible. PET and water table drawdown were seen on Days 235 and 236, followed on each day by late afternoon inundation and negligible overnight PET and water table drawdown. The water table elevation was near the surface at the start of Day 237. Rainfall occurred on Day 237, and PET was minimal. The water table remained near the surface. Whenever the water table was near the surface, the unsaturated zone was small, and the saturation deficit was also small.

Hourly measurements of water table position by a well logger 35 m from the creek on Days 211-215 (July 29-August 2), 2000, illustrated water table dynamics during a period of semi-diurnal inundation (**figure 29**). During this period, inundation occurred both at night, when PET was negligible, and during the day, when water input by tides coincided with PET. This location was inundated on the morning of Day 211 (around 211.3). Following inundation, rainfall occurred and PET was low. The water table elevation stayed near the surface. The location was inundated at the end of Day 211. Inundation ended near midnight (Day 212.0) and subsequent PET was zero. The water table elevation remained near the surface overnight. The location was inundated on Day

212 (around 212.4), coinciding with the onset of PET. Following inundation, PET was still high, and the water table elevation was drawn down below the surface. PET during inundation did not affect the water table. The location was inundated at the end of Day 212. This inundation ended near midnight (Day 213.0). Subsequent PET and water table drawdown were negligible. The location was again inundated on Day 213, followed by PET and water table drawdown during the afternoon. Following inundation at the end of Day 213, water table drawdown did not occur overnight. Drawdown again followed day-time inundation on Day 214, when PET was high.

3.5.2 Water table characteristics during drying periods

Water table measurements 35 m from the creek on Days 259-264 (September 16-21), 1999, illustrated water table dynamics of a drying period (**figure 30**). Following inundation around Day 259.75, PET and water table drawdown proceeded until the following inundation at the end of Day 263. During the drying period, PET was normal and tidal elevations were below the surface elevation at this location. The water table elevation was drawn down more than during periods of regular inundation. This increased drawdown was not associated with above-normal PET; rather, with an absence of tidal inundation.

Drying periods were common, but infrequent (**table 11**). Characteristics of drying periods were quantified from logger measurements of water table elevation at locations with a surface elevation of approximately 80 cm (MSL) from three monitoring periods in 1999 and 2000, totaling 247 days. Fourteen drying periods were observed in this period from the water table elevations in appendix 2. This indicates a return interval of 17.6 days. The average number of days between drying periods was 13.4 (8.9 standard deviation), with a range of values from 0 to 30. This indicates the timing of drying periods is highly variable. The average duration was 4.0 days (1.7 standard deviation). Average maximum saturation deficit, derived from logger measurements of water table elevation using $S_y = 0.1$, was 1.9 cm (0.8 standard deviation) during the drying periods. Average maximum saturation deficit from the water balance model using logger measurements for inundation was 2.6 cm (2.0 standard deviation).

Even though the marsh was not flooded for several days during drying periods, the water table remained within 40 cm of the surface (**table 11**). The water table drawdown during drying periods sometimes appeared limited at 15-25 cm below the surface. If reached, the water table did not go below this limit, even when subsequent PET was indicated. For example, the water table at 35 m on Day 260, 1999 (**figure 30**), was drawn down to about 10 cm below the surface. The water table was not drawn down significantly further than this on days 261-263, even though normal PET was indicated. Other examples can be seen in appendix 2 during drying periods starting on Day 229, 1999, and Days 160, 172, 220, and 252, 2000.

3.5.3 Tidal signal in the water table measurements

When the water table at any location remained below the surface during high tide (ie, location was not inundated), there was a clear semi-diurnal signal in the water table that corresponded to tidal elevation. This was a common, but irregular, occurrence.

Because it was only apparent when the water table was below the surface, the signal was most evident during drying periods, when the water table remained below the surface for several days. However, the tidal signal was not seen during all drying periods (**table 12**). The signal was most distinct and the water table fluctuated over a wider range, with a typical amplitude of 5-10 cm, at 43 m from the creek (**figure 31**). At this location, the water table signal was directly in phase with tidal elevation, rising when the tide rose and falling when the tide fell. At other locations, the signal was dampened in amplitude and not directly in phase with the tide, sometimes continuing to rise after the tide began to fall.

The regular sequence of a higher-high tide followed by a lower-high tide appeared to switch on Day 177, 2000 (**figure 31C**). A lower-high occurred when a higher-high was expected. For the following tidal cycles, the pattern remained switched until it switched back on Day 189. This switching was also seen in tide data from NOAA stations 8638863 (Chesapeake Bay Bridge Tunnel, across the mouth of the Chesapeake Bay) and 8632200 (Kiptopeke, VA, at the southern end of the Delmarva Peninsula). Additionally, higher-high and lower-high tides appeared to switch at all three stations for other periods. No explanation is proposed here; for this thesis it was sufficient to verify the data were not in error.

3.5.4 Groundwater discharge from the upland

Episodic discharge to the marsh (“return flow”) kept the water table close to the surface 43 m from the creek on Days 260-264, 1999 (**figure 32C**), when there were no tidal or precipitation inputs (**figure 32D**). PET for the period was normal (**figure 30**), and significant water table drawdown occurred at the two locations closer to the creek (**figure 32 A, B**). Return flow was in response to Hurricane Floyd on Day 259, which inundated the upland and produced a large amount of precipitation.

3.5.5 Seasonal variation in water table elevations

The water table record from logger measurements 39 m from the creek for Days 206-320, 2000, was used to compare summer and winter characteristics. The break between summer and winter was set on Day 275 (October 1). This day was approximately the inflection point in the solar radiation data for the year (**figure 11**). In general the probability distribution for water table position was similar for both summer and winter, indicating little seasonal variation (**figure 33**). The difference in the two probability curves was only 0.05 probability of water table depth exceeding a given value. The hourly inundation frequency was about 35% for the summer period and about 30% for winter (seen in figure 33 as one minus the probability the water table was at or below the surface). The time series of water table elevation for the summer and winter periods were also similar (**figure 34**).

3.6 Saturation deficit derived from water table measurements

The saturation deficit derived from water table measurements was generally within the bounds from the soil cores (**figure 35**). A specific yield of 0.1 and hand measurements of the water table position were used to derive the saturation deficit for these comparisons. Agreement with the soil core method validated the use of water table measurements to derive the saturation deficit.

The saturation deficit derived from logger measurements of water table position showed the effect of elevation and distance from the tidal creek (**figure 36**). The saturation deficit was lowest at the low elevation (38 cm elevation; 20 m from the tidal creek) and higher at upper elevations (74-81 cm elevation; 31, 35, 39 and 43 m from the tidal creek). However, the saturation deficit was also low 49 m from the tidal creek (79 cm elevation).

The measurements used to derive the saturation deficit probabilities shown in figure 36 were not all made concurrently. They were made in different monitoring periods (**figure 15**) and therefore experienced different tidal regimes. For example, the probability distributions for saturation deficit at 31 and 43 m from the creek were very similar, as were the probability distributions for 35 and 39 m. The wells 31 and 43 m from the creek were monitored together, and the wells 35 and 39 m from the creek were monitored together (**figure 15**). The difference in probability distributions between the pairs of stations corresponded to less frequent tidal inundation when 31 and 43 were monitored (**figure 37**). Less frequent inundation meant more time for water loss by evapotranspiration and less frequent saturation by the tides, leading to a greater frequency of saturation deficit.

Concurrently monitored stations differed from other concurrently monitored stations, but within monitoring periods, stations experienced the same tidal regime. Data for individual monitoring periods show that increased distance and elevation increased the saturation deficit (**figure 38**). The differences between concurrently monitored stations was small because the changes in distance and elevation were small. In a later section, modeling was used to show the effect of increased elevation over a greater range in elevation.

3.7 Model validation

A water balance equation was used to model the sediment water content, with hourly PET losses and tidal and precipitation inputs. PET values for the model were calculated by the method of Priestly and Taylor (1972) and were similar for both years of the study (**figure 39**, see appendix 5 for correction to PET method). To ensure the model results were representative of the soil moisture dynamics in the study area, the modeled saturation deficit was compared to bounds on the saturation deficit from the soil cores and to the saturation deficit derived from hand-measurements of the water table position. These are point measurements in time and space. Model results were also compared to long-term measurements of the water table position, for a broader validation.

The model results using logger measurements for tidal inputs were used to calculate the saturate deficit for comparison to the saturation deficit derived from soil cores and from hand measurements of water table position. Only presence or absence of inundation was obtained from the logger measurements. The source of tidal data for these comparisons to soil cores was not highly significant, because soil samples were collected during drying periods when there was no tidal inundation.

Two locations on the transect of wells in the study area were used in each of two sampling periods to compare the three methods of calculating the saturation deficit. In the first period , Days 235-237 (August 22-24), 2000, the three methods produced similar results at the location 39 m from the creek (**figure 40A**). The modeled saturation deficit was within the soil core bounds and very similar to the water table-derived saturation deficit. Modeled saturation deficit 43 m from the creek began within the soil core bounds and was very similar to the water table-derived saturation deficit (**figure 40B**). On Day 236, the water table at this location began to rise in response to the incoming tide, but prior to inundation (**figure 40C**). Accordingly, the soil core bounds and water table-derived saturation deficit show the saturation deficit to decrease, but the model showed the saturation deficit to increase.

In the second sampling period, Days 253-255 (September 9-11), 2000, the two location studied, 35 and 39 m from the creek, both showed similar results (**figure 40E, F**). At these two locations, the modeled saturation deficit initially was within the soil core bounds and was similar to the water table-derived saturation deficit. During the period, however, the modeled saturation deficit was greater than the soil core bounds and the water table-derived saturation deficit. The modeled saturation deficit exceeded the upper soil core bound by about 0.25 cm of water. The modeled and water table-derived saturation deficits diverged during this period, even though both used $S_y = 0.1$.

Model results were compared to the logger measurements of the water table position at all monitored locations in the marsh (wells 20-49 m from the creek) for all monitoring periods. Model results were generated separately using logger measurements for tidal inputs to the model and using water levels converted from the tidal elevation recorded at Wachapreague. Model results using Wachapreague inputs were expected to be less accurate because there were differences in the timing and magnitude of tidal elevations from these data and water levels measured at the study area (**figure 22**).

Using the logger measurements for tidal inputs tested the model assumptions that tidal and precipitation inputs were the only significant sources of water to the sediment, that evapotranspiration was the only significant loss of water, that PET was a good approximation of actual evapotranspiration, and that $S_y = 0.1$ was an approximate parameter for water storage in the unsaturated zone. By exclusion, the model also assumed groundwater input and drainage were not significant.

The basis for comparison was water table depth below surface, a negative value. Modeled saturation deficit was converted to water table displacement by dividing by S_y. The difference between the methods was calculated as modeled water table position minus measured water table position. A negative difference indicated modeled water table depth was lower than observed. Such cases meant the model showed greater drawdown and saturation deficit. Water table depth with respect to surface was used for the comparison because it eliminated differences based on surface elevation among wells on the transect.

Measured and modeled water table elevations were compared for periods when the surface was exposed. The model was not programmed to predict water levels during inundation. The range of the difference for values modeled with logger inputs was more narrow (**figure 41**). With either input, the difference between measured and modeled values was usually within the range of ± 5 cm (**table 13**). The precision of logger measurements was ± 5 cm, and this value was used as a guideline. The mean difference with logger inputs was -0.9 cm (7.0 standard deviation), with 84% of the modeled values within ± 5 cm of the corresponding measured values. For values modeled with Wachapreague inputs, the mean difference was -2.0 cm (7.9 standard deviation), with 75% of the values within ± 5 cm of the measured value. For either input source, there were discrete periods with a negative difference of 30-60 cm ("spikes" in figure 41). These periods corresponded to drying periods (**table 11**).

Model results were a better approximation of water table measurements with logger inputs for inundation than with Wachapreague tide data, but logger inputs were available only for the monitoring periods and were applicable only to the elevations monitored. Use of Wachapreague data allowed model coverage of both years of the study at all elevations in the study area. This provided a more thorough analysis of spatial and temporal characteristics of saturation excess.

3.8 Model sensitivity analysis

Variables used in the model were altered systematically to see which had significant effects on the model results. Each variable was changed independently. Measured values of hourly inputs from 1999 (tidal elevations converted from Wachapreague data, and air temperature and solar radiation measured in Phillips Creek Marsh) and typical values of parameters (surface elevation and specific yield) were used in the sensitivity analysis (**table 14**). Each test value (X*) was a percentage added to or subtracted from the value typically used in the model (X). Test values ranged from half to one-and-a-half times the typical value (X^*/X = 0.5 to 1.5).

The water table elevation, derived from the modeled saturation deficit using the specific yield, was used to compare model results over the range of each variable. Water table elevation was used instead of the saturation deficit so specific yield could be included in the sensitivity analysis. The mean difference between modeled water table elevation using the typical values and the test values was used to quantify the effect of the altered variable. Changes in water table elevation of ± 5 cm were not considered significant, as this was the range of variability of logger measurements of water table position.

Within the range of observed variability for each variable (**table 14**), model sensitivity was within ± 5 cm (**figure 42**). This indicated that the observed variability did not significantly affect model results used to characterize soil saturation by rainfall. The model was most sensitive to decreasing the tidal elevation and increasing the surface elevation, both of which reduce the frequency and duration of tidal inundation.

3.9 Model results

Wachapreague tide-based model results were used to further discern spatial and temporal characteristics of saturation excess, in the absence of continuous water table data for the entire study area. The probabilities of saturation deficit and excess were based on hourly values and included periods of inundation. (See appendix 5 for correction to PET method).

The water balance model was applied across a range of discrete surface elevations from 40 to 80 cm at 10 cm intervals. With both 1999 and 2000 inputs, the modeled probability of saturation deficit increased as elevation increased (**figure 43A, C**). For any elevation, the probability that the saturation deficit exceeded -0.01 cm was considered equivalent to the probability of marsh surface exposure. The marsh surface was exposed more frequently at higher elevations. The probability for saturation deficit exceeding -0.01 cm was approximately 0.70 at 80 cm elevation and 0.36 at 40 cm elevation. The increased frequency of exposure at higher elevations corresponded to an increased probability of higher saturation deficit values. For example, the probability for saturation deficit exceeding 2 cm was about 0.15 for 80 cm elevation and 0.0 for 40 cm elevation. The mean hourly saturation deficit modeled at 80 cm elevation was -0.75 cm (1.25 standard deviation) and -0.92 cm (1.43 standard deviation), in 1999 and 2000, respectively. Periods of inundation were not included in calculating the means.

Saturation excess was modeled when the water balance was positive. That is, when an hourly precipitation input exceeded the combined saturation deficit at the start of the hour and PET losses during the hour. Unlike the modeled saturation deficit, modeled saturation excess did not change significantly with elevation (**figure 43B, D**). Saturation excess was modeled for approximately 2-3% of the hours in each year. This was a small proportion of the total time; however, it was significant, corresponding to roughly 4 hours in a given week. Using 1999 data, saturation excess was modeled at 80 cm elevation for 67% of all hours with rainfall and 83% of hours with rainfall that also coincided with an exposed surface. Percentages were 48**%** and 59%, respectively, in 2000 (**table 15**).

The modeled values for amount of saturation excess were not cumulative. The total accumulation of saturation excess in an event was taken as the sum of the hourly values. Saturation events were defined as starting with the first hour of saturation during rainfall events and stopping when the site was inundated or when a break in rainfall of more than 8 hours occurred. Evapotranspirative losses were included during events. Similarly, rainfall events were defined as starting with the first hour of rainfall and stopping when the site was inundated or when a break in rainfall of more than 8 hours occurred.

There were 93 rainfall events per year in both 1999 and 2000. The mean rainfall sum per event was 1.3 cm (1.8 standard deviation) and 1.1 cm (1.2 standard deviation), in 1999 and 2000, respectively. The rainfall event sums exceeded the mean modeled saturation deficit and the mean measured saturation deficit at 80 cm elevation in the mid marsh (**table 16**). Model results indicated 74 and 65 rainfall events saturated the study area at 80 cm elevation in 1999 and 2000, respectively (**figure 44**). These represent 80% and 70% of rainfall events in each year, respectively.

A little more than half of the rainfall events in each year occurred when the marsh surface at 80 cm elevation was exposed throughout the event (56% in 1999 and 58% in 2000). There were three rainfall events in 1999 and four in 2000 for which the marsh surface at 80 cm elevation was inundated throughout the event (preventing saturation excess and runoff). However, six of these seven events were only one hour in duration. Therefore, the marsh surface was either fully or partially exposed during most rainfall events. On an hourly basis, 81% of the hours with rainfall in 1999, and 80% in 2000, coincided with marsh surface exposure at 80 cm elevation in the study area.

Overland flow was not observed in the field until saturation excess overcame the depth of depressions in the microtopography. The typical depth of the depressions was 1 cm (**figure 23**). At 80 cm elevation, there were 23 and 24 events in 1999 and 2000, respectively, with modeled saturation excess greater than this 1 cm threshold for runoff (25% and 26% of the total rainfall events in each year, respectively). It was assumed the other saturation events would not cause runoff.

3.10 Tidal and meteorological conditions associated with runoff events

The weather associated with saturation events was analyzed for temporal characteristics of tidal and meteorological conditions that were conducive to runoff. Three types of precipitation-generating weather were identified, using data on rainfall, wind, barometric pressure, and deviations of the measured tidal level from the predicted (astronomical) tide. Convective storms were defined by a short duration and without a significant change in tidal deviations, wind, or barometric pressure. Often convective storms had high intensity rainfall. Cyclonic storms were defined by a significant decrease in barometric pressure, with winds from the northeast and a positive tidal deviation (Davis and Dolan, 1993). Frontal storms were defined by a significant decrease in barometric pressure, usually without a significant change in tidal deviations or wind.

Without the spatial distribution of barometric pressure to positively identify frontal systems, it was sometimes difficult to distinguish frontal storms from cyclonic storms.

The weather associated with the modeled events for 1999 was analyzed (**appendix 3**). There was not one weather type that caused the greatest runoff. Each of the three types of weather was associated with at least one of the seven events with saturation excess greater than 3 cm in 1999 (**table 17**). Weather also affected the saturation deficit, as offshore winds and/ or high barometric pressure kept the tide from flooding the marsh at the study area (negative tide deviations on Days 9-14 and 64-67, 1999, in appendix 3).

3.11 Modeled spatial characteristics of saturation excess events

Modeling was used to represent the development of the saturated area during rainfall events. Survey data were used to define 10-cm contours of elevation across the study area (**figure 4**). Saturation values were assigned to contours based on elevation. Inundation was modeled for a contour when the upper contour bound was inundated. Saturation excess values were hourly and not cumulative.

During periods when the entire study area was regularly inundated, there was not much spatial variation in the saturation deficit. The entire study area was inundated on Day 252, 1999. Five hours after inundation, the saturation deficit was slightly greater at upper elevations, which were exposed first, but was relatively uniform (**figure 45A**). In the next hour, 1.5 cm of rain occurred, and the saturated area was also relatively uniform (**figure 45B**).

Following drying periods, the saturation deficit was typically greater at upper elevations. Due to the differential antecedent saturation deficit, it was possible for saturation to occur at lower elevations while not at higher elevations. Following a drying period, four cm of rain occurred over a 24 hour period, starting on Day 105, 2000. The antecedent saturation deficit was greater at upper elevations than lower elevations (**figure 46A**). Seven hours later, the lower elevations were saturated, but the upper elevations were not (**figure 46B**). Fifteen hours into the event, the entire area was saturated (**figure 46C**).

It was also possible for saturation by rainfall to occur only at upper elevations while lower elevations were flooded. On Day 226, 2000, the entire area was inundated. Prior to the onset of rain, the entire area was exposed, with a relatively uniform saturation deficit (**figure 47A**). In the first hour of the event, only 0.1 cm of rain occurred (**figure 47B**). By the fourth hour, 1.2 cm of rain had fallen. The upper elevations were saturated by rainfall, but the lower elevations were inundated by the next incoming tide (**figure 47C**). One hour later, the entire area was inundated.

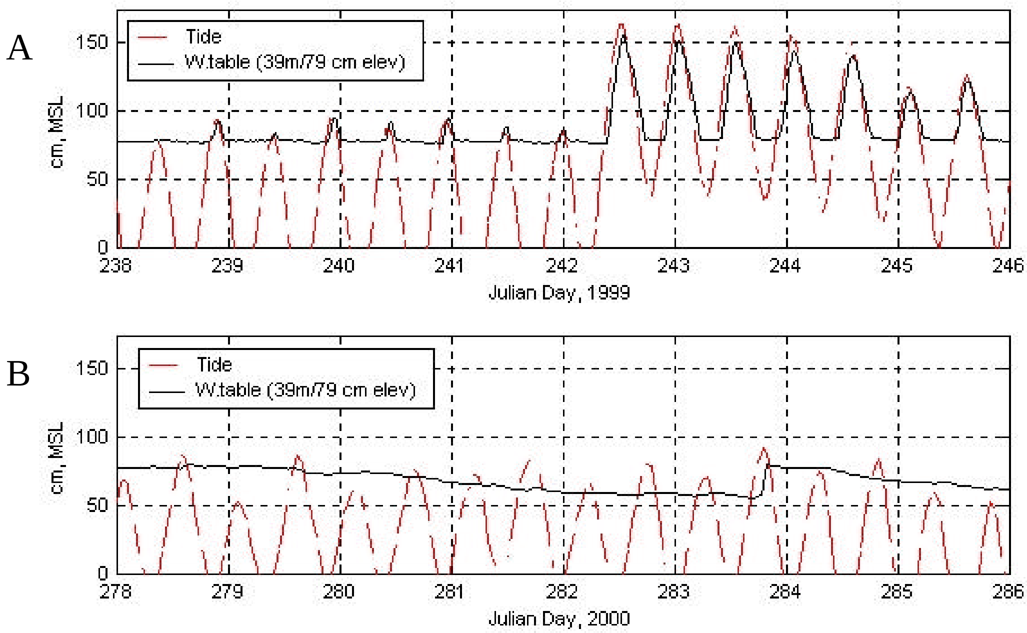

Figure 22. Water level at the study area from converted Wachapreague tidal levels and from water table measurements. (Key to legend: Distance from creek/ surface elevation).

A. Days 238-246, 1999
B. Days 278-286, 2000

Table 7. Crab burrow and plant stem densities for low and mid marsh.

A. Crab burrows

Location	Raw count	Area (m^2)	Density (m^{-2})
Low Marsh	32	0.65	49
	35	1.0	35
	35	1.0	35
	41	1.0	41
		average	**40**
		st. dev.	**7**
Mid Marsh	3	0.5	6
	2	0.5	4
	0	1.0	0
	3	1.0	3
	2	1.0	2
		average	**3**
		st. dev.	**2**

B. Plant stems

Location	Raw count	Area (m^2)	Density (m^{-2})	Average Stem Height (cm)
Low Marsh	83	0.5	166	92.5
	75	0.5	150	78.0
	76	0.5	152	70.5
	82	0.5	164	61.5
		average	**158**	**76**
		st. dev.	**8**	**13**
Mid Marsh	132	0.25	528	35.0
	148	0.25	592	38.0
	136	0.25	544	31.6
	145	0.25	580	40.9
	165	0.25	660	40.4
	149	0.25	596	34.6
		average	**583**	**37**
		st. dev.	**46**	**4**

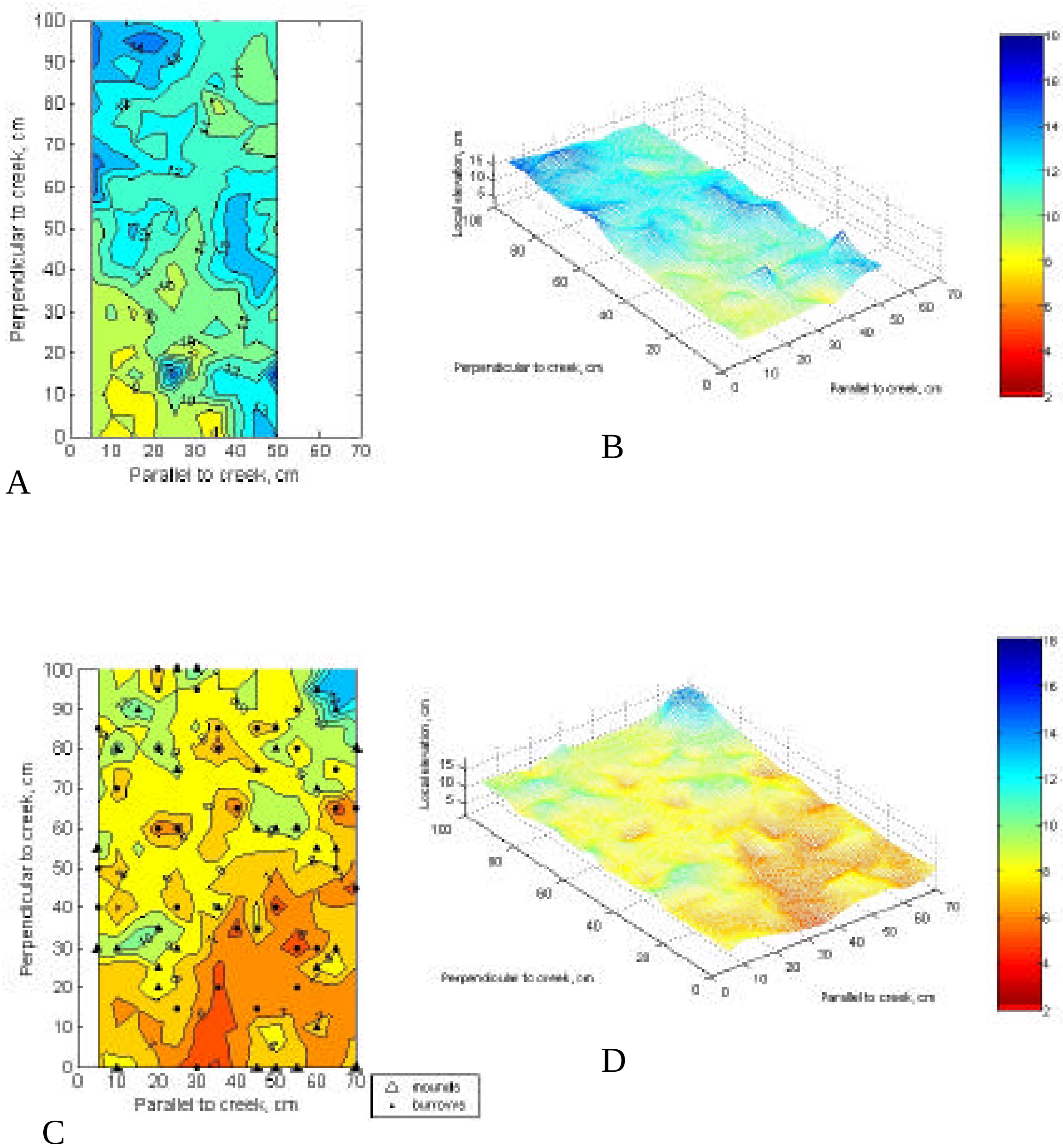

Figure 23. Microtopography in the low marsh and mid marsh (continued next page).

A. Low marsh contour map (replicate #1)
B. Low marsh relief map (replicate #1)
C. Low marsh contour map (replicate #2)
D. Low marsh relief map (replicate #2)

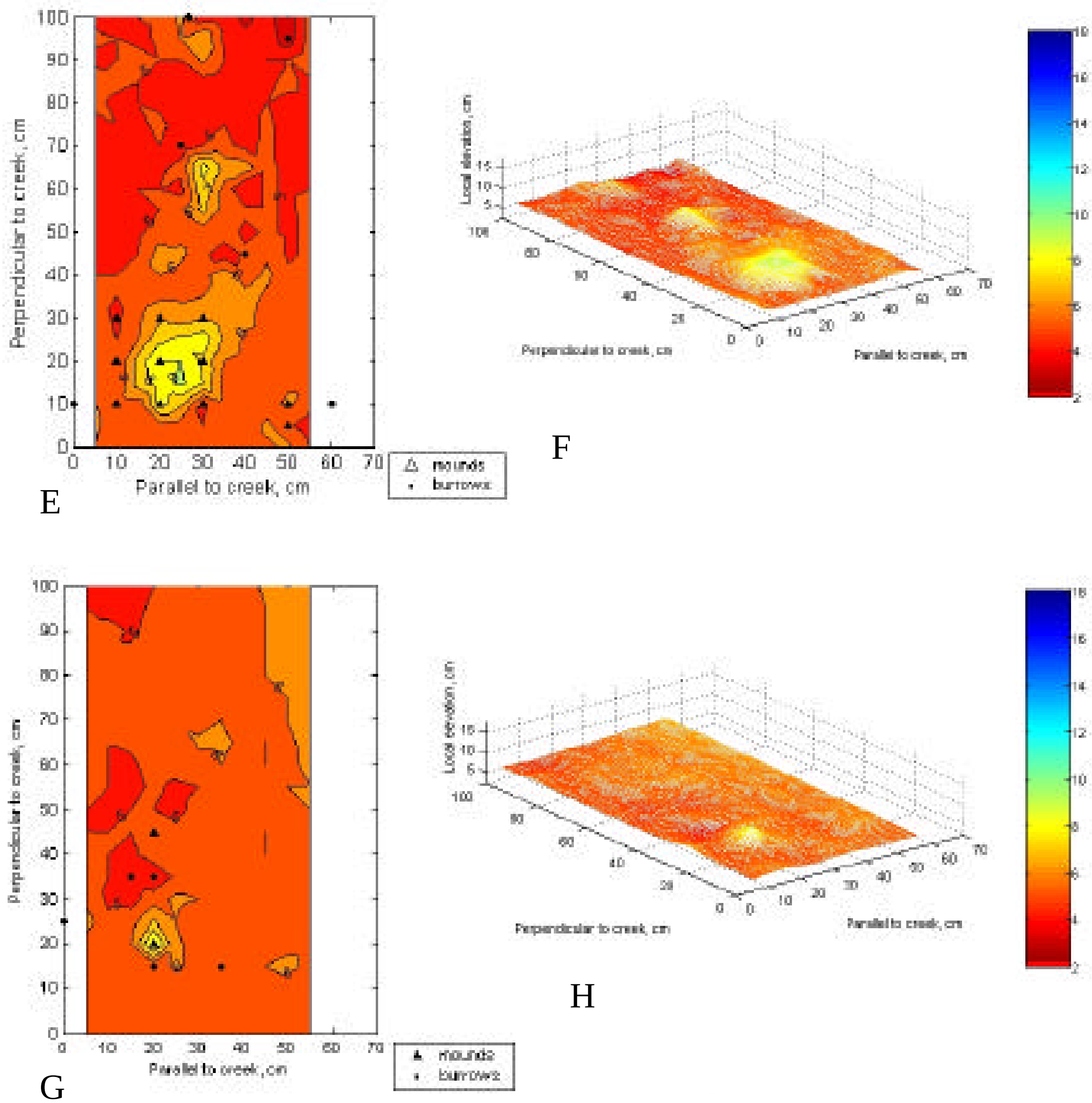

Figure 23. (continued) Microtopography in the low marsh and mid marsh.

E. Mid marsh contour map (replicate #1)
F. Mid marsh relief map (replicate #1)
G. Mid marsh contour map (replicate #2)
H. Mid marsh relief map (replicate #2)

Table 8. Sediment porosity and bulk density 0-10 cm depth.

A. Soil porosity [Vol./Vol.] 0-5 cm depth.

Distance from creek (m)	27	31	35	39	43	49
average	0.80	0.82	0.82	0.81	0.82	0.78
standard deviation	0.00	0.02	0.01	0.01	0.01	0.02
number of cores	1	10	19	26	9	6

B. Soil porosity [Vol./Vol.] 5-10 cm depth.

Distance from creek (m)	27	31	35	39	43	49
average	---	0.82	0.82	0.81	0.83	0.61
standard deviation	---	0.01	0.01	0.03	0.01	0.04
number of cores	---	8	17	23	9	6

C. Dry bulk density (g cm^{-3}) 0-5 cm depth.

Distance from creek (m)	27	31	35	39	43	49
average	0.40	0.34	0.32	0.33	0.32	0.44
standard deviation	0.00	0.04	0.03	0.02	0.03	0.04
number of cores	1	10	19	26	9	6

D. Dry bulk density (g cm^{-3}) 5-10 cm depth.

Distance from creek (m)	27	31	35	39	43	49
average	---	0.35	0.34	0.36	0.31	0.91
standard deviation	---	0.02	0.03	0.07	0.02	0.10
number of cores	---	8	17	23	9	6

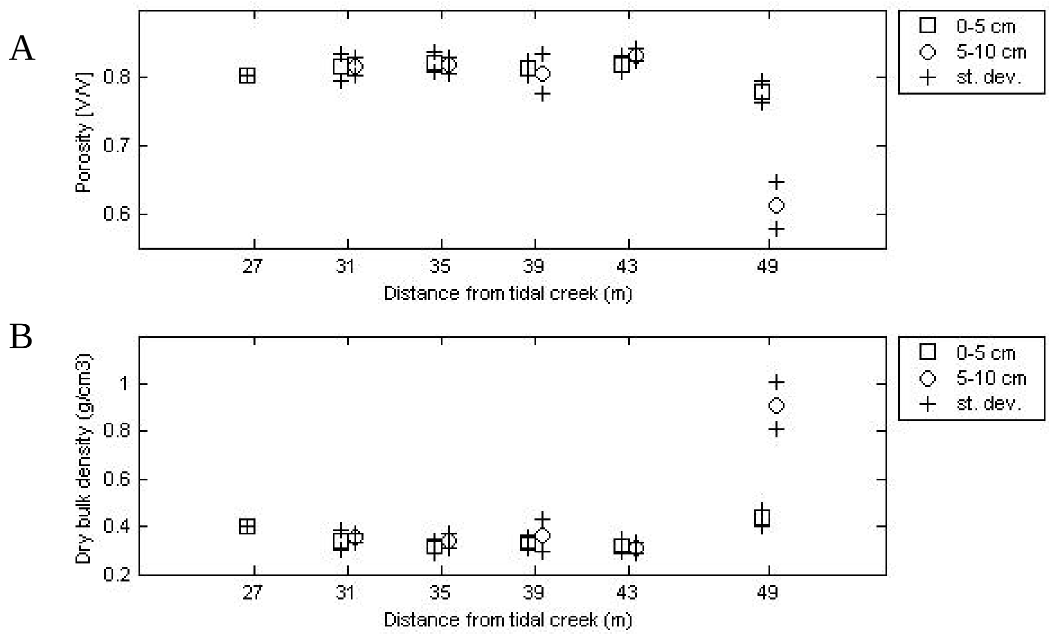

Figure 24. Average sediment porosity and bulk density, 0-10 cm depth.

A. Porosity [Vol./ Vol.]
B. Dry bulk density (g cm^{-3})

Table 9. Comparison of soil properties measured in Phillips Creek Marsh[1].

Source	Station Name	Description	Depth (cm)	Bulk Density (g/cm3)	Porosity	organic matter (% by weight)
This study	39 m	39m from creek 25m from upland	0-10	0.35	0.81	8.6
Kastler (1993)	Interior	30m from creek	0-10[2]	0.69	0.70	9.4
Harvey (1990)	Phil 1	35 m from creek 10m from upland	0-30	1.53	0.42	4.1
Barr (1989)	Phillips Creek 2	marsh interior	0-10[2]	0.39	0.65[3]	24.7

[1] Samples were from different locations in Phillips Creek Marsh (figure 3), but all had short-form *Spartina alterniflora*. Barr (1989) was closest in proximity to this study. Locations for Harvey (1990) and Kastler (1993) were close to one another.

[2] Analysis included approximately 100 cm depth of sediment in 2 cm intervals; only the top 10 cm used here.

[3] Porosity was assumed equal to the reported percent water by weight when saturated. The value for 0-2 cm was half that for depths 2-10 cm. Because porosity was expected to be similar to these depths, even if the top 2 cm had less water, this value was excluded.

Table 10. Soil textural properties[1].

Location[2], Depth[3]	%sand	%clay	%silt	Textural class
20m, 0-30cm	21	36	43	SILTY CLAY LOAM
20m, 26-120	46	23	31	LOAM
20m, 120-	62	17	22	SANDY LOAM
27m, 0-22cm	21	31	48	SILTY CLAY LOAM
27m, 22-26	29	10	61	SILT LOAM
27m, 26-30	49	8	43	LOAM
27m, 30-115	59	20	21	SANDY LOAM
27m, 115-120	76	13	10	SANDY LOAM
27m, 120-	75	15	10	SANDY LOAM
35m, 0-36cm	28	22	50	LOAM
35m, 0-36 (repeat)	34	14	52	LOAM/SILTY LOAM
35m, 36-	55	16	29	SANDY LOAM
35m, 36- (repeat)	62	17	21	SANDY LOAM
43m, 0-30cm	28	10	62	SILT LOAM
43m, 30-105	59	11	29	SANDY LOAM
43m, 105-135	59	18	23	SANDY LOAM
43m, 135-	77	13	11	SANDY LOAM
53m, 0-35cm	56	19	24	SANDY LOAM
53m, 35-95	45	27	28	SANDY CLAY LOAM
53m, 95-	54	26	21	SANDY CLAY LOAM
60m, 0-15cm	44	17	40	LOAM
60m, 15-30	50	13	37	LOAM
60m, 30-70	35	22	43	LOAM
60m, 70-	71	14	14	SANDY LOAM
70m, 0-12cm	--	--	--	ORGANIC LAYER
70m, 12-40	52	13	36	LOAM
70m, 40-60	52	15	33	LOAM
70m, 60-80	50	20	30	LOAM
70m, 80-	75	9	16	SANDY LOAM

1 Soil textural analysis by Dusterhoff (2002)
2 Location=distance from creek (m) and corresponded to the location of a well, except at 53 m.
3 Depth=with respect to surface (cm)

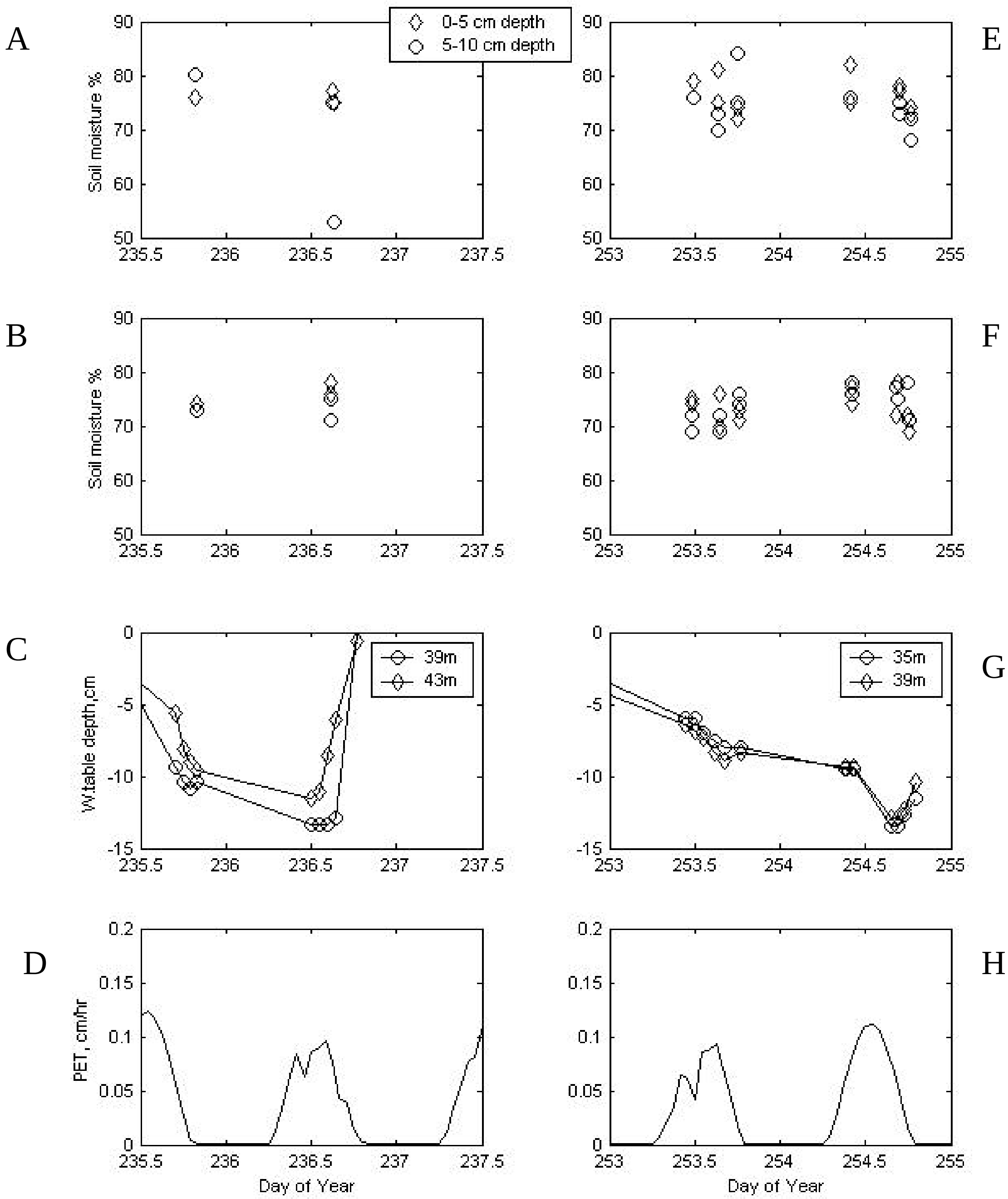

Figure 25. Soil moisture values for two sampling periods, 2000.
A, B, E, F. Soil moisture percent by volume.
C, G. Water table depth from surface (cm).
D,H. Calculated potential evapotranspiration (cm hr^{-1}).

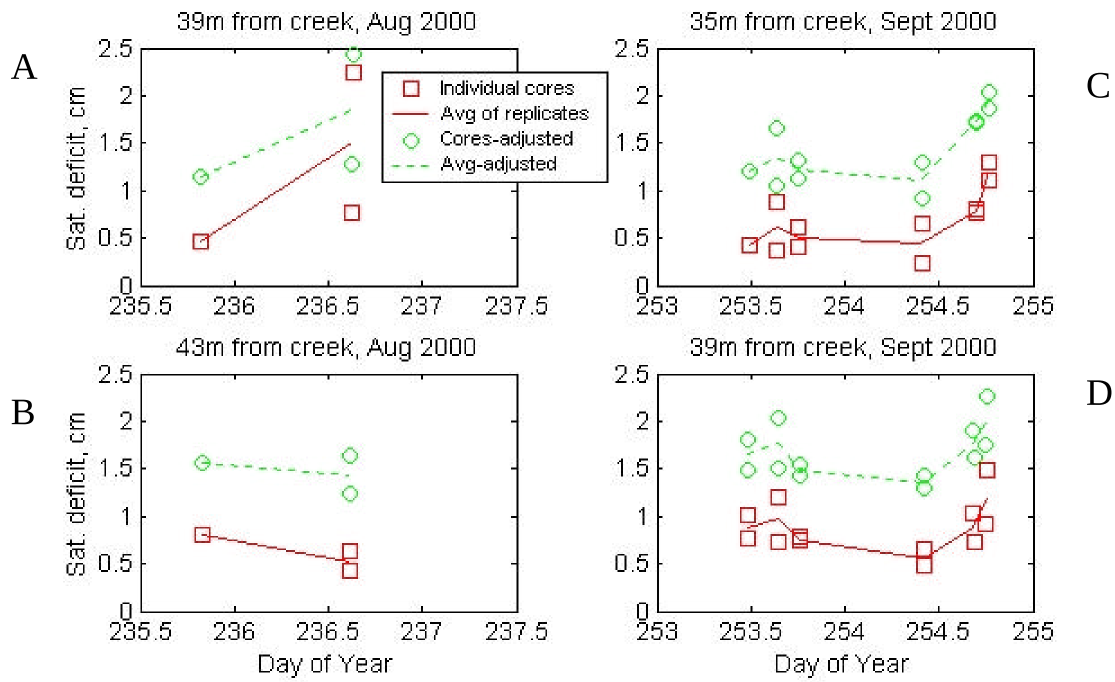

Figure 26. Saturation deficit from soil cores, with and without adjustment for compaction of samples.

A-B. Days 235-237, 2000
C-D. Days 253-255, 2000

A. 39m from creek
B. 43m from creek
C. 35m from creek
D. 39m from creek

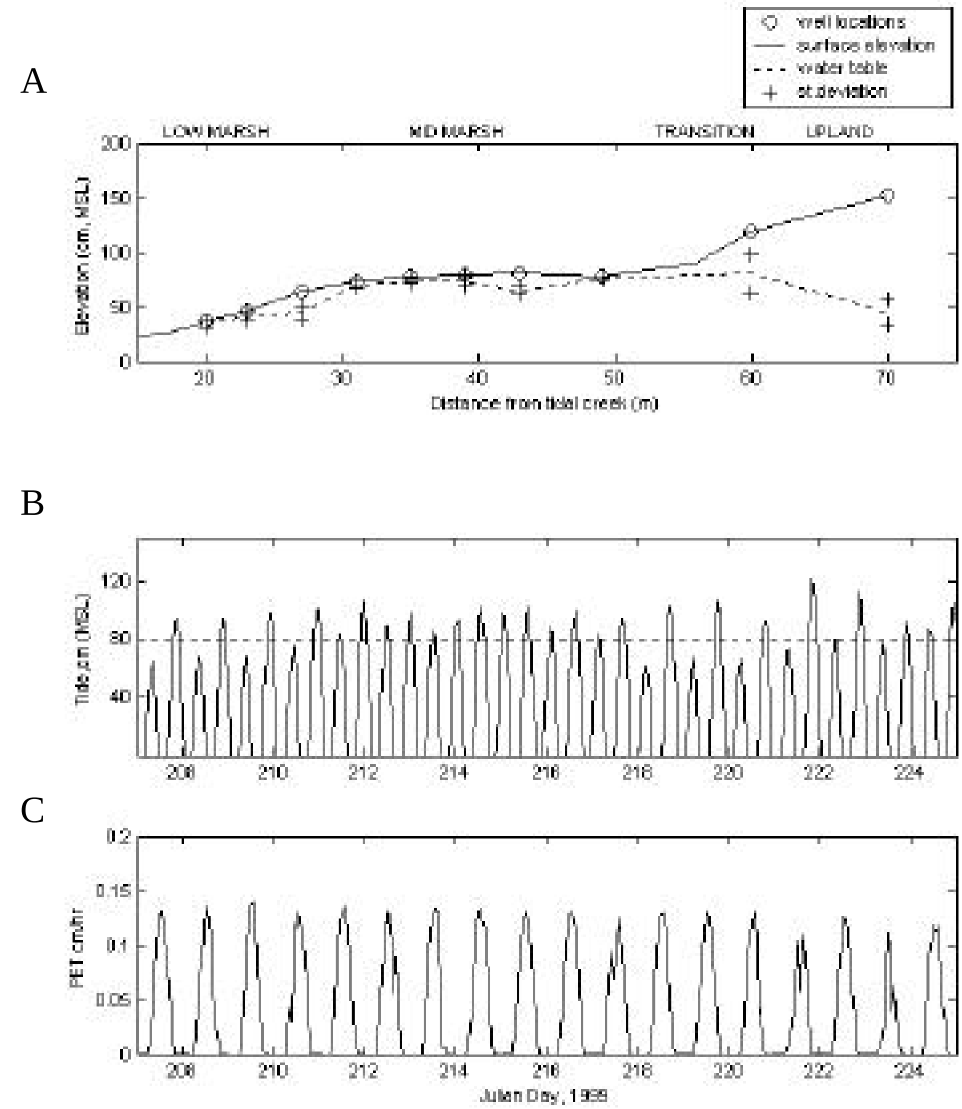

Figure 27. Average daily water table position at low tide, Days 207-225, 1999. (Note, measurements were not necessarily made at the low tide minimum).

A. Average of daily hand-measurements of water table position (cm, MSL) along the transect.
B. Tidal elevations (cm, MSL) for the period from converted Wachapreague data. The line at 80 cm marks the approximate maximum elevation of the mid marsh.
C. Calculated potential evapotranspiration (cm hr^{-1}) for the period

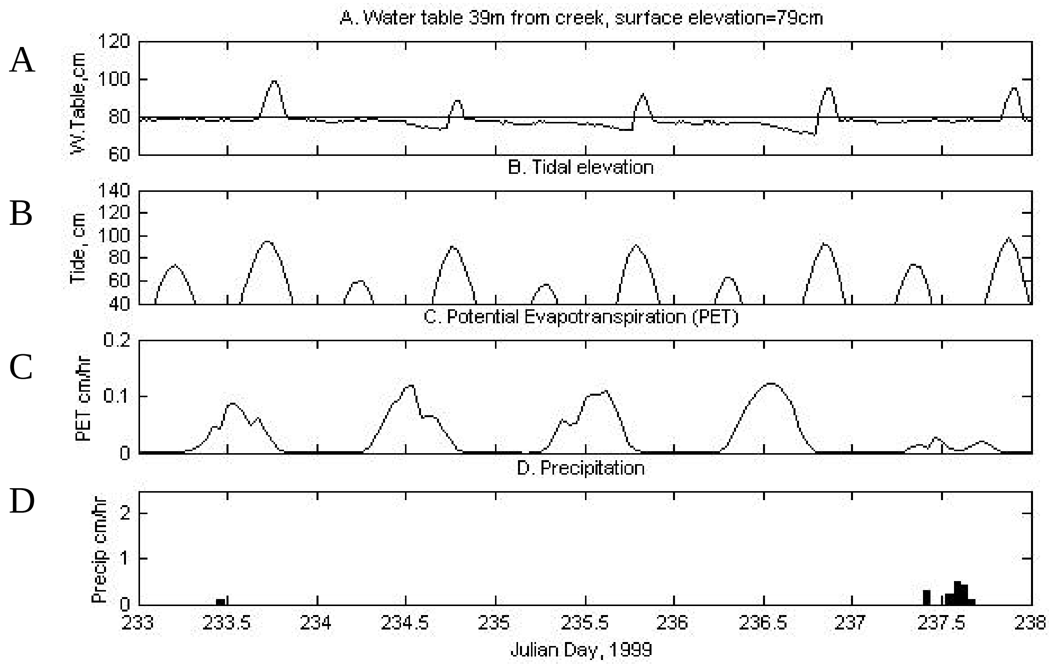

Figure 28. Water table dynamics during a period of daily inundation.

A. Logger measurements of water table elevation (cm, MSL) 39 m from the creek
B. Tidal elevation (cm, MSL) converted from Wachapreague data
C. Calculated potential evapotranspiration (cm hr^{-1})
D. Precipitation (cm hr^{-1})

A
B
C
D

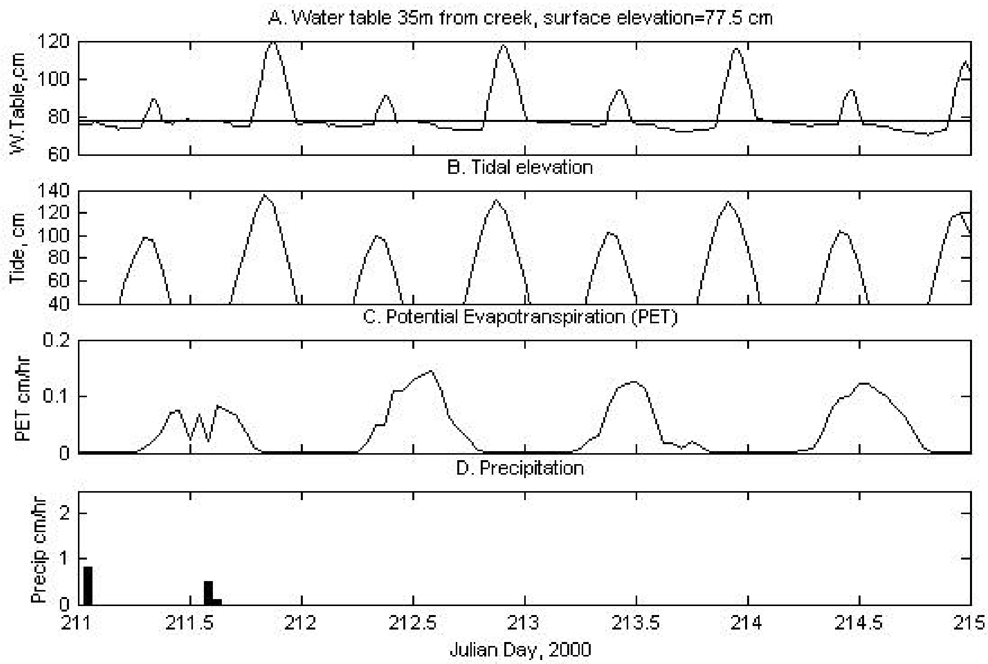

Figure 29. Water table dynamics during a period of semi-diurnal inundation.

A. Logger measurements of water table elevation (cm, MSL) 35 m from the creek
B. Tidal elevation (cm, MSL) converted from Wachapreague data
C. Calculated potential evapotranspiration (cm hr^{-1})
D. Precipitation (cm hr^{-1})

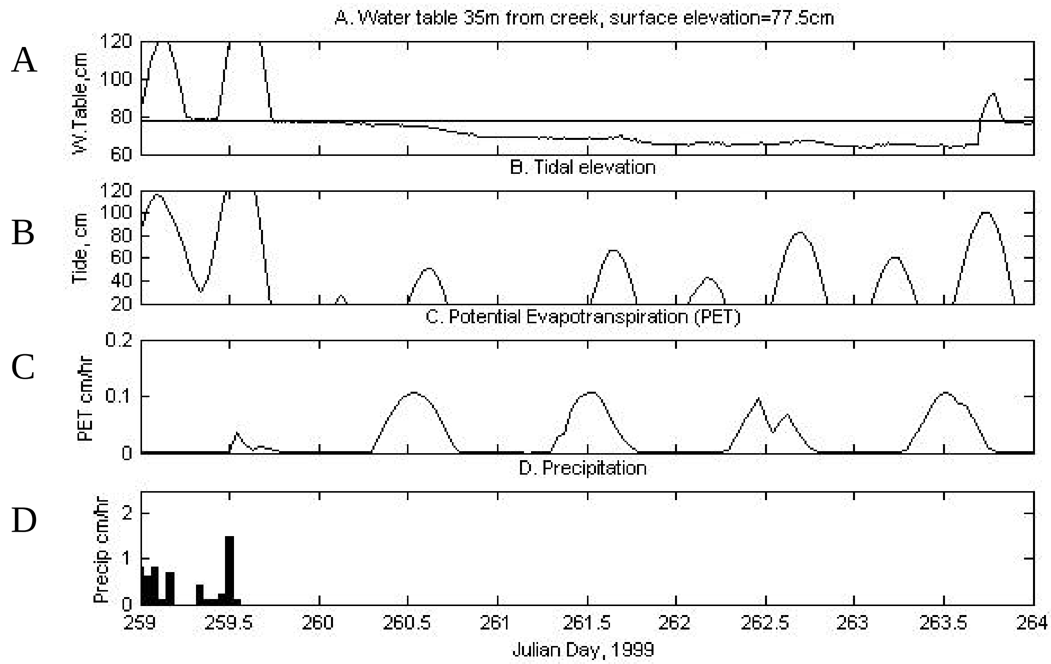

Figure 30. Water table dynamics during a drying period.

A. Logger measurements of water table elevation (cm, MSL) 35 m from the creek
B. Tidal elevation (cm, MSL) converted from Wachapreague data
C. Calculated potential evapotranspiration (cm hr^{-1})
D. Precipitation (cm hr^{-1})

Table 11. Characteristics of drying periods at 80 cm elevation, 1999 and 2000.

Year	Days	Data*	Days since preceding drying period	Duration (days)	Maximum Saturation Deficit (cm) from water table measurements	Maximum Saturation Deficit (cm) from model **	Maximum depth to water table (cm)
1999	229-232	A	---	3.0	1.5	2.8	15
	260-263	A	28	3.5	1.0	2.0	10
2000	147-150	B	30	3.0	1.0	1.5	10
	160-164	B	10	4.5	2.3	5.0	22.5
	172-181	B	8	9.0	4.0	8.3	40
	191-194	B	10	3.0	2.0	2.3	20
2000	219-224	C	25	5.0	2.5	3.5	25
	234-237	C	10	3.5	1.8	1.3	17.5
	251-255	C	14	4.0	1.3	---	12.5
	263-266	C	8	3.0	1.8	1.8	17.5
	278-283	C	12	5.0	2.3	2.3	22.5
	283-287	C	0	4.0	2.3	1.8	22.5
	294-297	C	6	3.0	1.3	1.0	12.5
	310-312	C	13	2.0	1.3	0.8	12.5
average			**13.4**	**4.0**	**1.9**	**2.6**	**18.6**
st.dev.			**8.9**	**1.7**	**0.8**	**2.0**	**7.9**
range			**0-30**	**2.0-9.0**	**1.3-4.0**	**0.8-8.3**	**10-40**

* Key to logger data sources
A. Logger measurements 39 m from the creek, Days 224-268, 1999
B. Logger measurements 43 m from the creek, Days 117-206, 2000
C. Logger measurements 39 m from the creek, Days 206-320, 2000

** Modeling results with logger data for inundation

Table 12. Occurrences of tidal fluctuations in the water table elevation data. *

Year	Day	Distance from Tidal Creek (m)
1999	231	39, 43, 49
	263	35, 39, 43
	304-365	70
	327-328, 344	60
2000	1-23	70
	147-150	43
	161-165	31, 43
	172-181	31, 43
	190-194	31, 43
	278-283	39

* Appendix 2

A
B
C

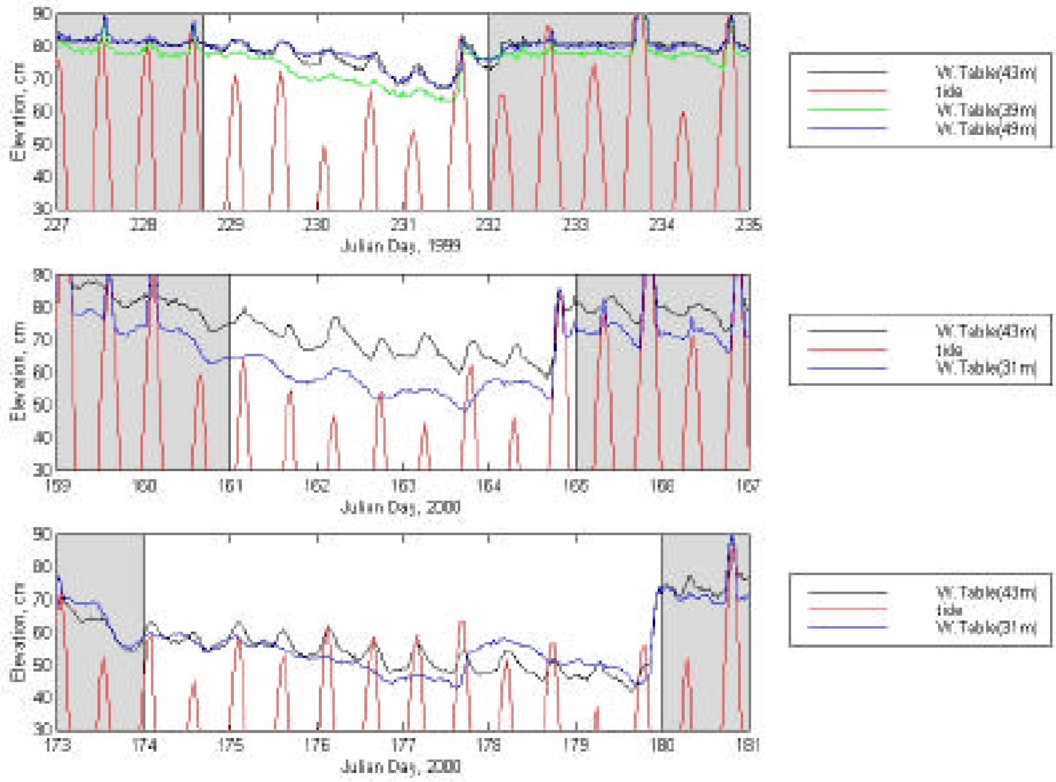

Figure 31. Tidal signal in the water table measurements during 3 drying periods. (Drying periods emphasized in the figure by the non-shaded area. Tidal elevation (cm, MSL) from Wachapreague data and water table elevations (cm, MSL) from logger measurements.)

A. Days 227-235, 1999.
B. Days 159-167, 2000.
C. Days 173-181, 2000.

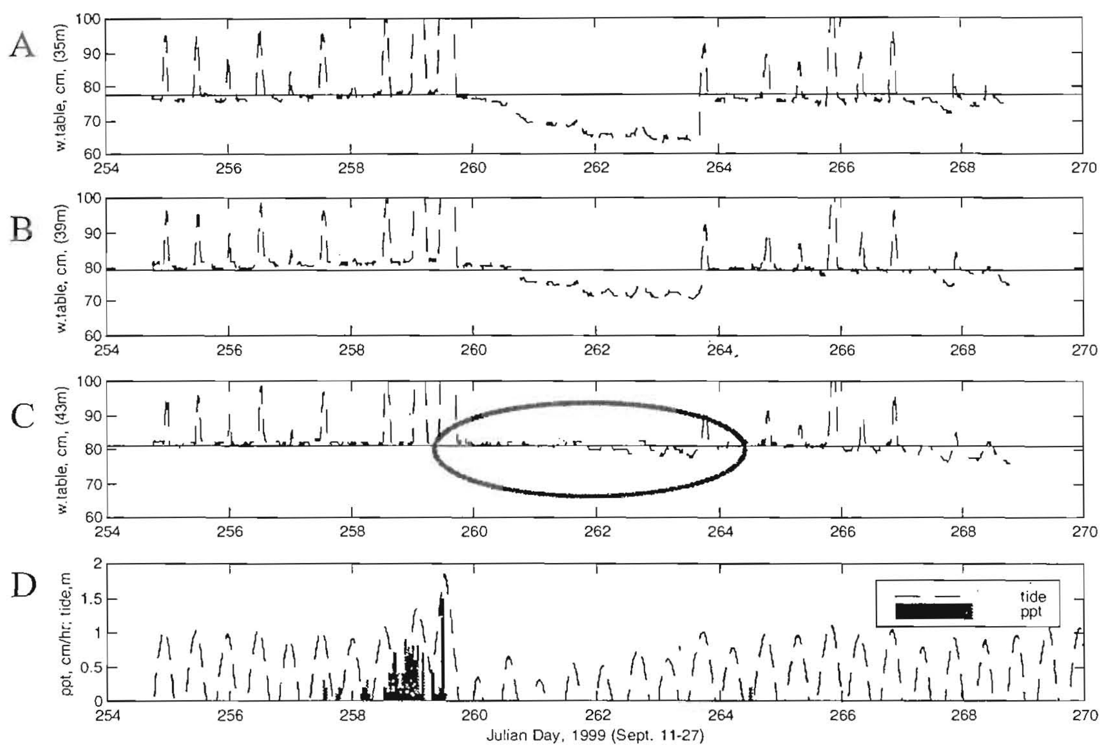

Figure 32. Groundwater discharge to the marsh from the upland and/ or transition zone, Days 260-264, 1999.

(Figure shows water table elevations at 3 wells for the same time period)

A. Water table elevation (cm, MSL) 35 m from the creek (~30 m from the upland)
B. Water table elevation (cm, MSL) 39 m from the creek (~25 m from the upland)
C. Water table elevation (cm, MSL) 43 m from the creek (~20 m from the upland)
D. Tidal elevation (m, MSL) and precipitation (cm hr^{-1})

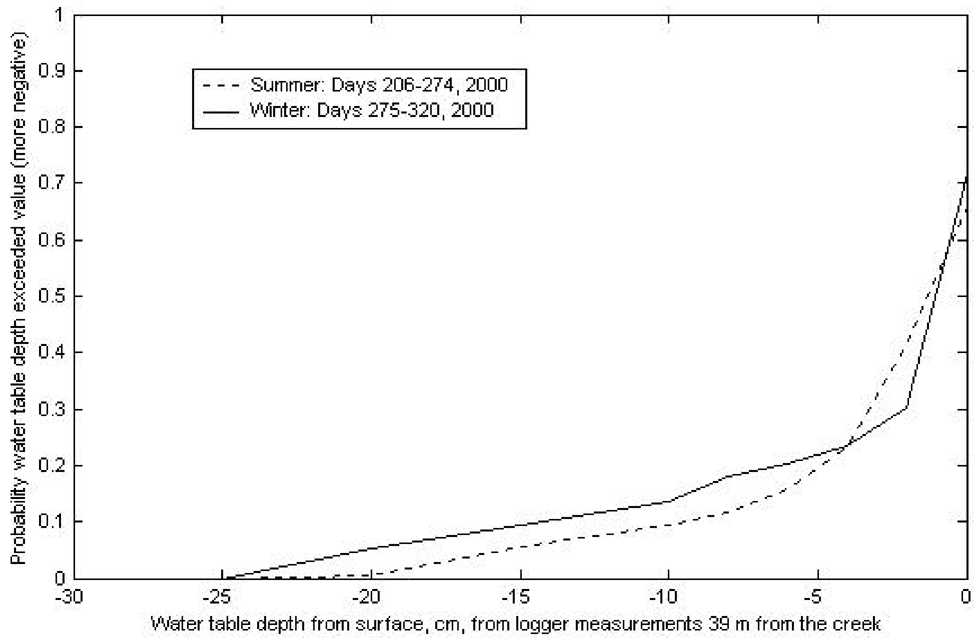

Figure 33. Seasonal variation in the water table position 39 m from the tidal creek (surface elevation 79 cm, MSL).

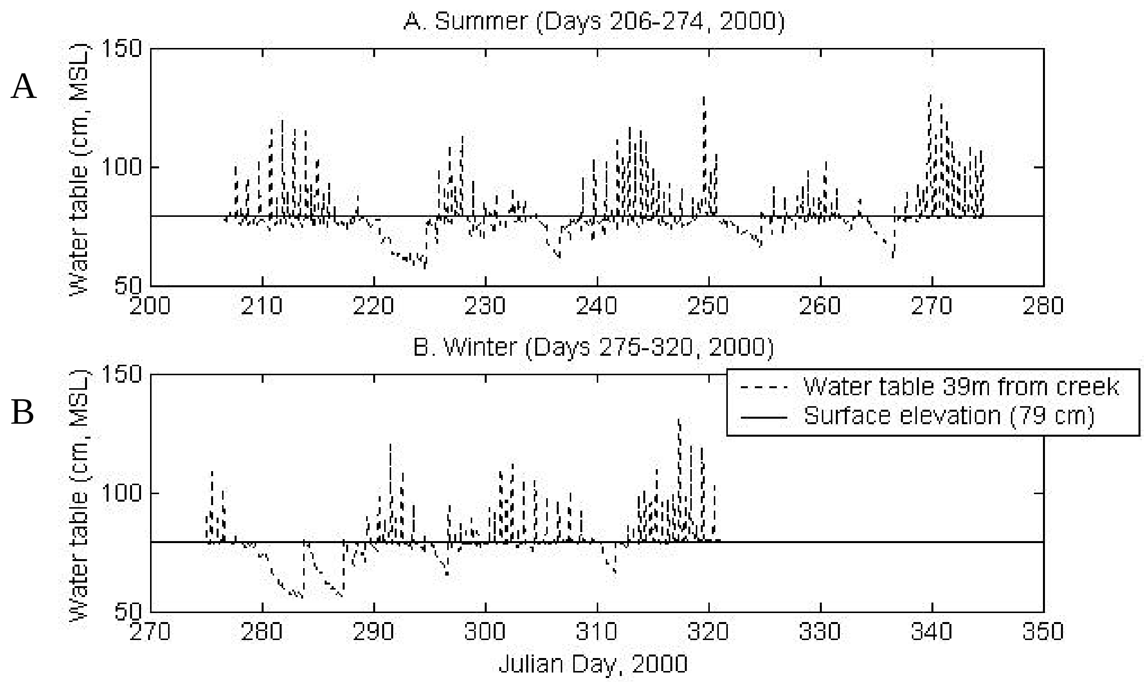

Figure 34. Water table elevations for summer and winter, 2000, 39 m from the creek (surface elevation 79 cm, MSL).
A. Summer (Days 206-274, 2000)
B. Winter (Days 275-320, 2000)

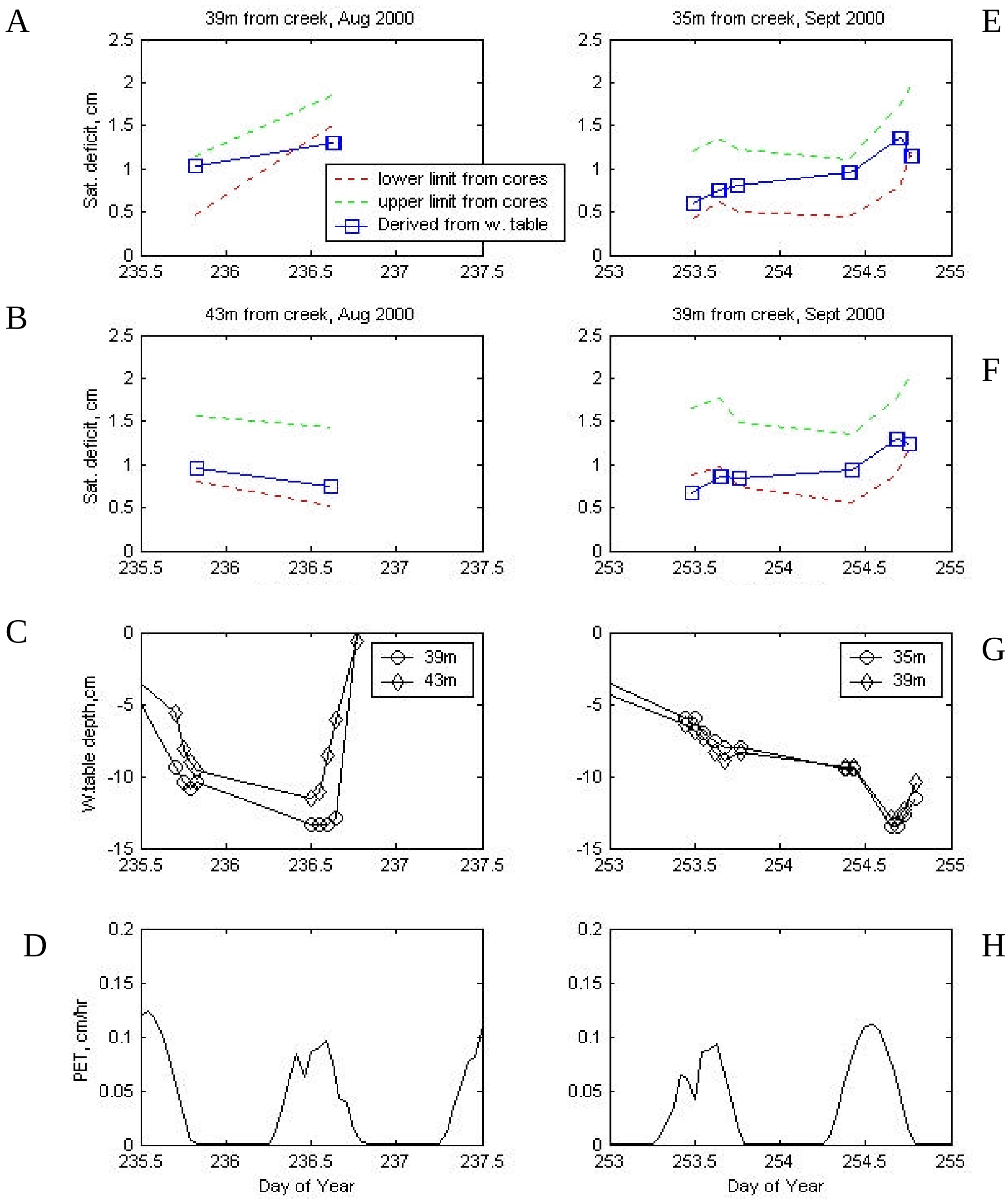

Figure 35. Saturation deficit from water table measurements, with bounds from soil cores, during two drying periods.
A, B, E, F. Saturation deficit (cm) from water table and soil cores.
C, G. Water table depth from surface (cm).
D,H. Calculated potential evapotranspiration (cm hr^{-1}).

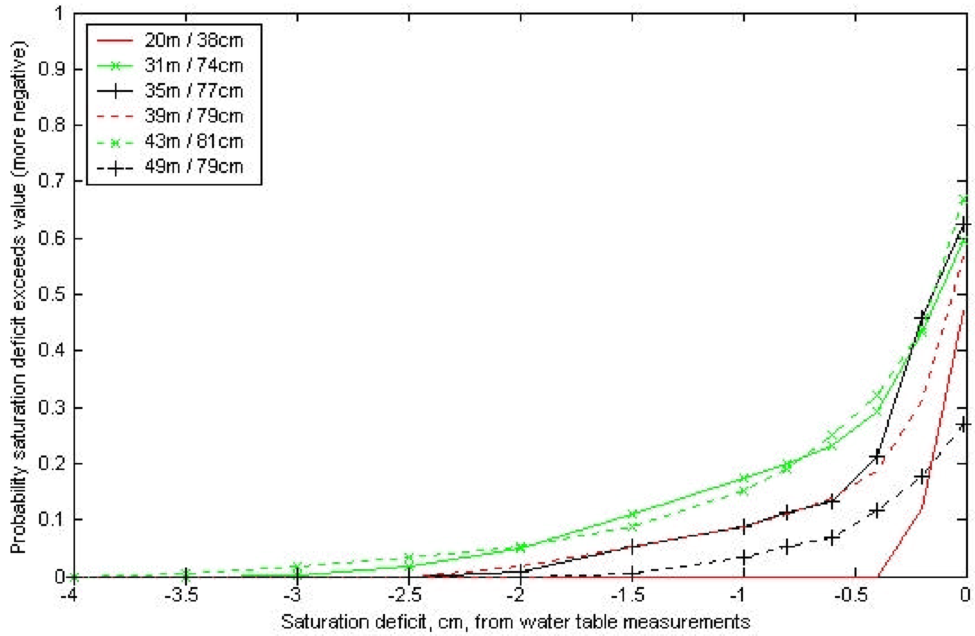

Figure 36. Saturation deficit from water table measurements. (Key to legend: Distance from creek / surface elevation. See Figure 15 for key to monitoring periods).

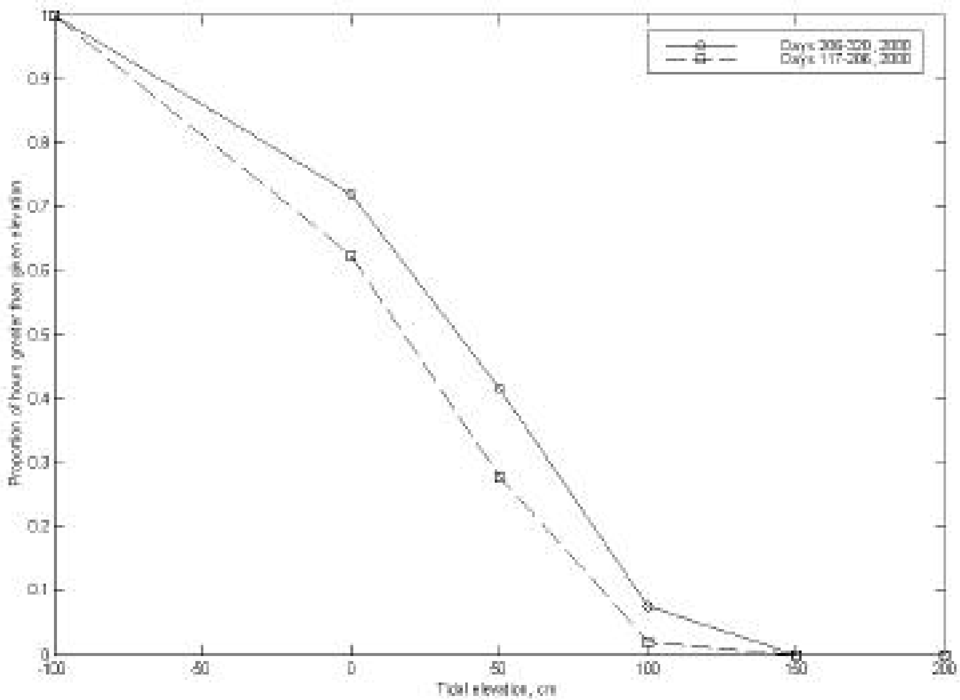

Figure 37. Comparison of inundation frequency for Days 206-320, 2000 (when water table monitored at 35 and 39 m from the tidal creek) and Days 117-206, 2000 (when water table monitored at 31 and 43 m from the tidal creek).

Tidal inundation was less frequent for Days 117-206 when measured saturation deficit was greater (**figure 36**).

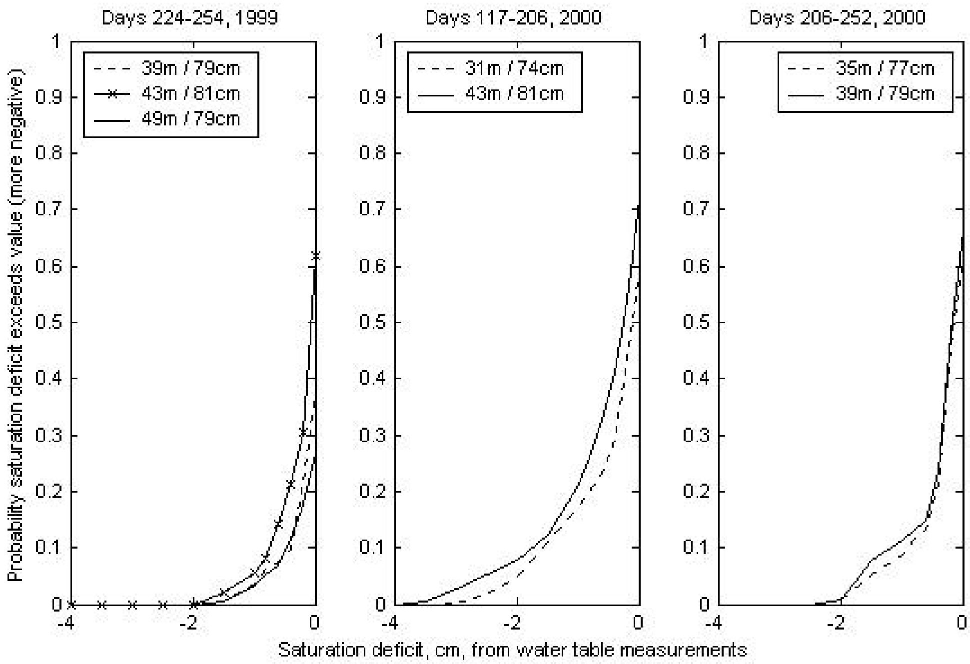

Figure 38. Frequency distribution of saturation deficit from logger measurements of the water table at locations monitored concurrently.

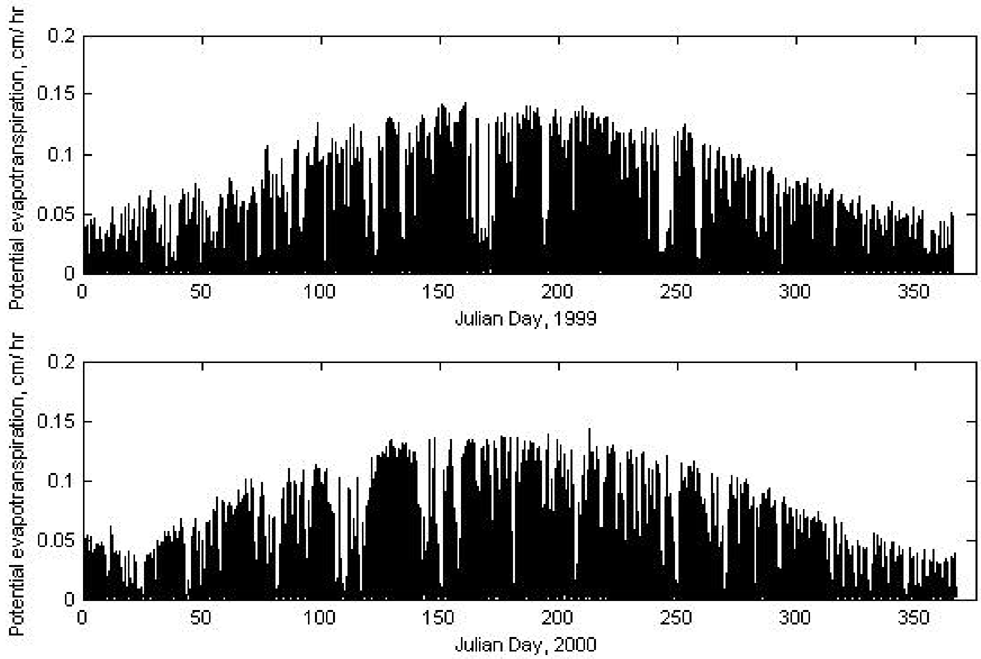

Figure 39. Calculated potential evapotranspiration, 1999 and 2000. (See appendix 5 for correction to PET method).

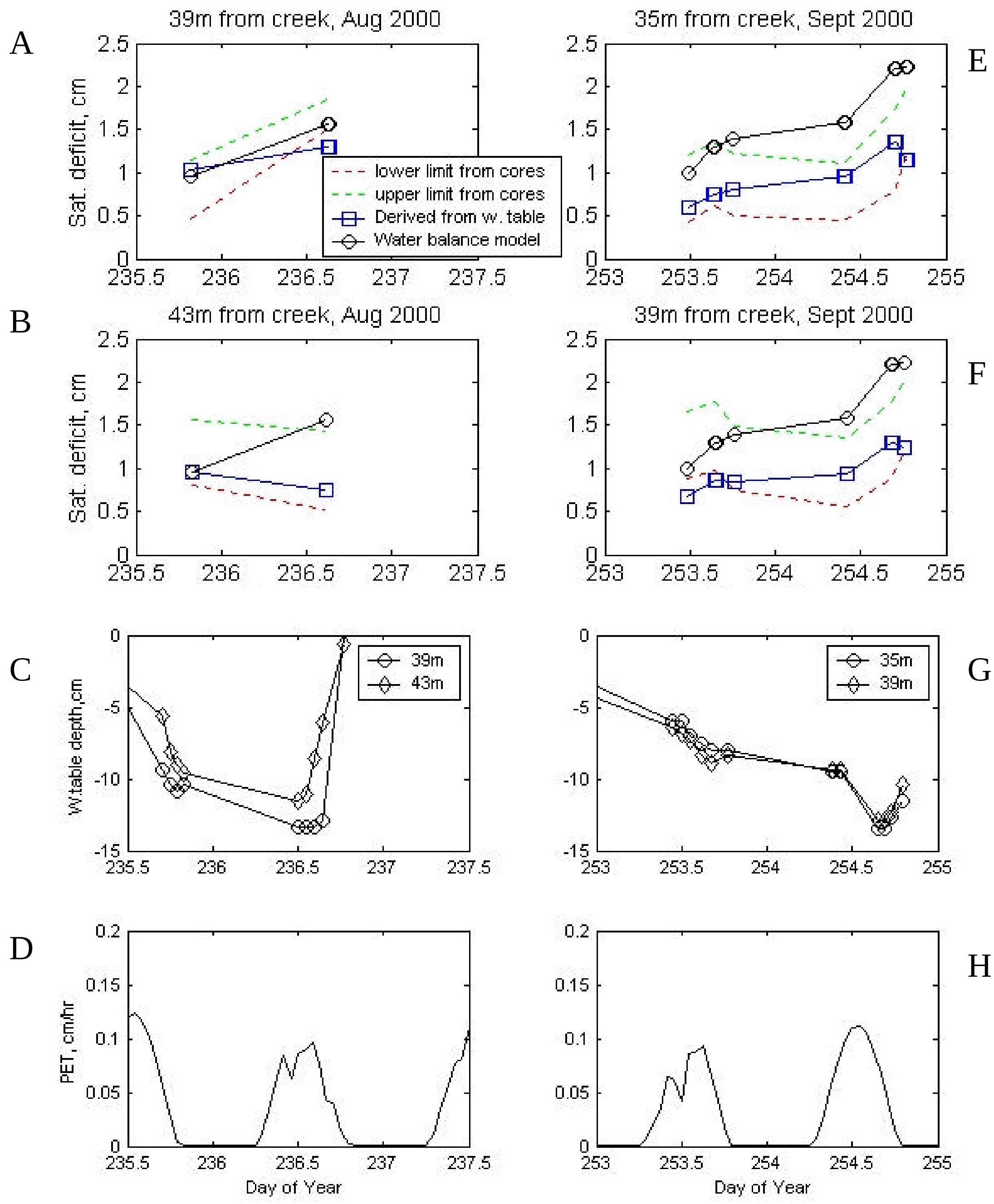

Figure 40. Saturation deficit from model, with bounds from soil cores and water table-derived saturation deficit, during two drying periods.

A, B, E, F. Saturation deficit (cm) from model, water table and soil cores.

C, G. Water table depth from surface (cm).

D,H. Calculated potential evapotranspiration (cm hr^{-1}).

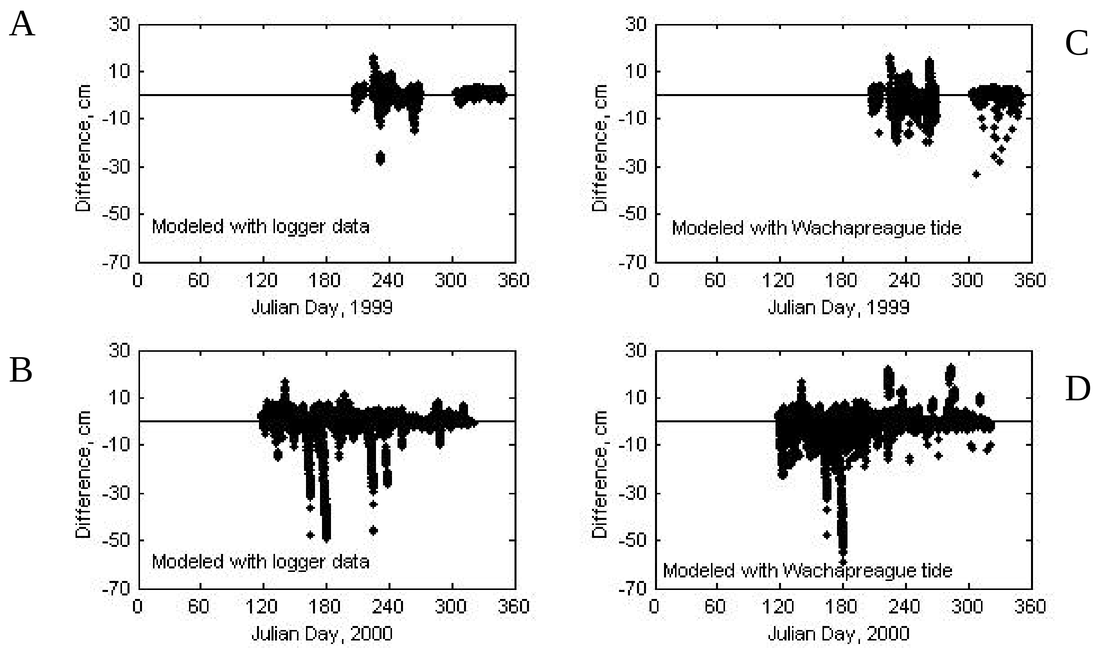

Figure 41. Difference between measured and modeled water table depth with respect to the surface, 1999 and 2000.

A. 1999, with logger inputs for inundation in the model
B. 2000, with logger inputs for inundation in the model
C. 1999, with Wachapreague inputs for inundation in the model
D. 2000, with Wachapreague inputs for inundation in the model

Table 13. Statistics of the difference between measured and model water table elevation.

Indicator of tidal inundation	Mean difference (cm)	Standard deviation (cm)	% of modeled values within ±5 cm of measured values	% of modeled values within ±10 cm of measured values	% of modeled values within ±20 cm of measured values	% of modeled values within ±30 cm of measured values
Logger measurements at monitored wells	-0.9	7.0	84.3	93.2	96.5	98.4
Converted Wachapreague tide data	-2.0	7.9	75.1	88.1	96.2	98.5

Table 14. Values for variables tested in the model sensitivity analysis.

Variable	**Value used to test other variables (X)**	**Observed variability**	**Range of (X*/X) for observed variability**
Tide[1]	Hourly tidal elevations for 1999 at Wachapreague, converted to water level at the study area (cm, MSL)	4 cm mean difference between converted Wachapreague water level and study area; 5% of an 80 cm tide[2]	0.95 - 1.05
Surface elevation	80 cm (MSL)	Survey precision was 2 cm (**table 2**); 3% of 80 cm[2]	0.97 - 1.03
Solar radiation[1]	Hourly data from Phillips Creek marsh meteorological station	± 200 kJ m^{-2} variability among Hog Island and Phillips Creek meteorological stations (**figure 13**); 10% of 2000 kJ m^{-2} [3]	0.90 - 1.10
Air temperature[1]	Hourly data from Phillips Creek marsh meteorological station	± 10 C variability among Hog Island, Oyster and Phillips Creek meteorological stations (**figure 13**); 50% of 20 C[4]	0.50 - 1.50
Specific yield	0.1	Measured values at the study area were 0.12 ± 0.03 (**figure 21**); resultant Sy would be 0.09-0.15, -10% to +50% of 0.1	0.90 - 1.50

[1] All values from 1999 were used for hourly inputs

[2] 80 cm was a significant value for tidal and surface elevation because it was the approximate elevation of the midmarsh (**figure 4**)

[3] Maximum daily solar radiation often reached 2000 kJ m^{-2} even in winter (**figure 11**)

[4] The 10 C range is a larger percentage of lower temperature values and a smaller percentage of higher temperature values. However, lower temperature values result in lower calculated PET values and therefore have less effect on the model.

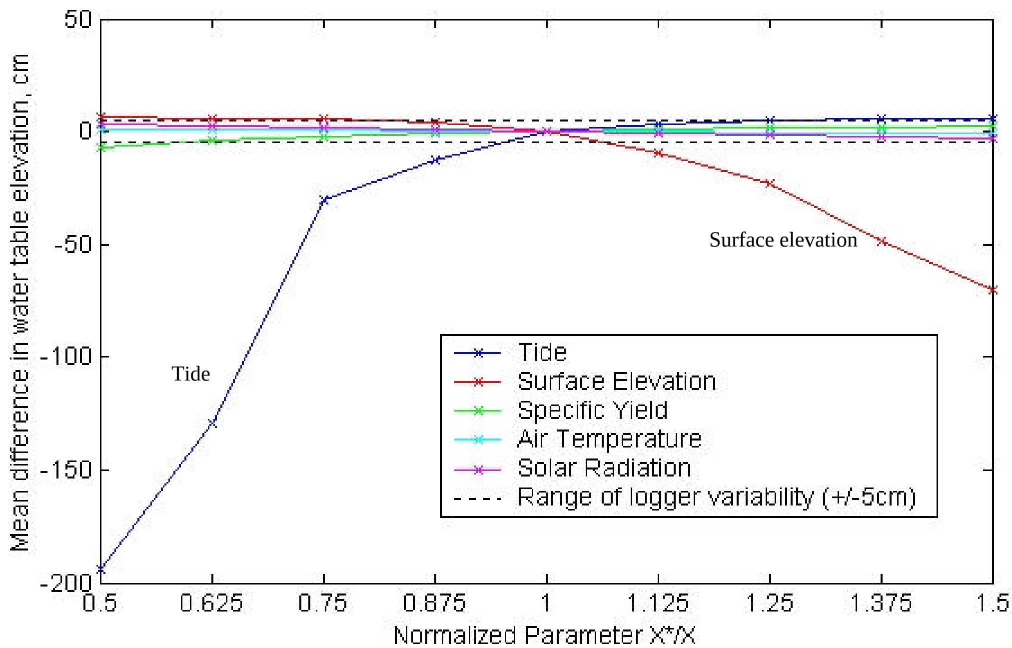

Figure 42. Model sensitivity to systematic variation of parameters.

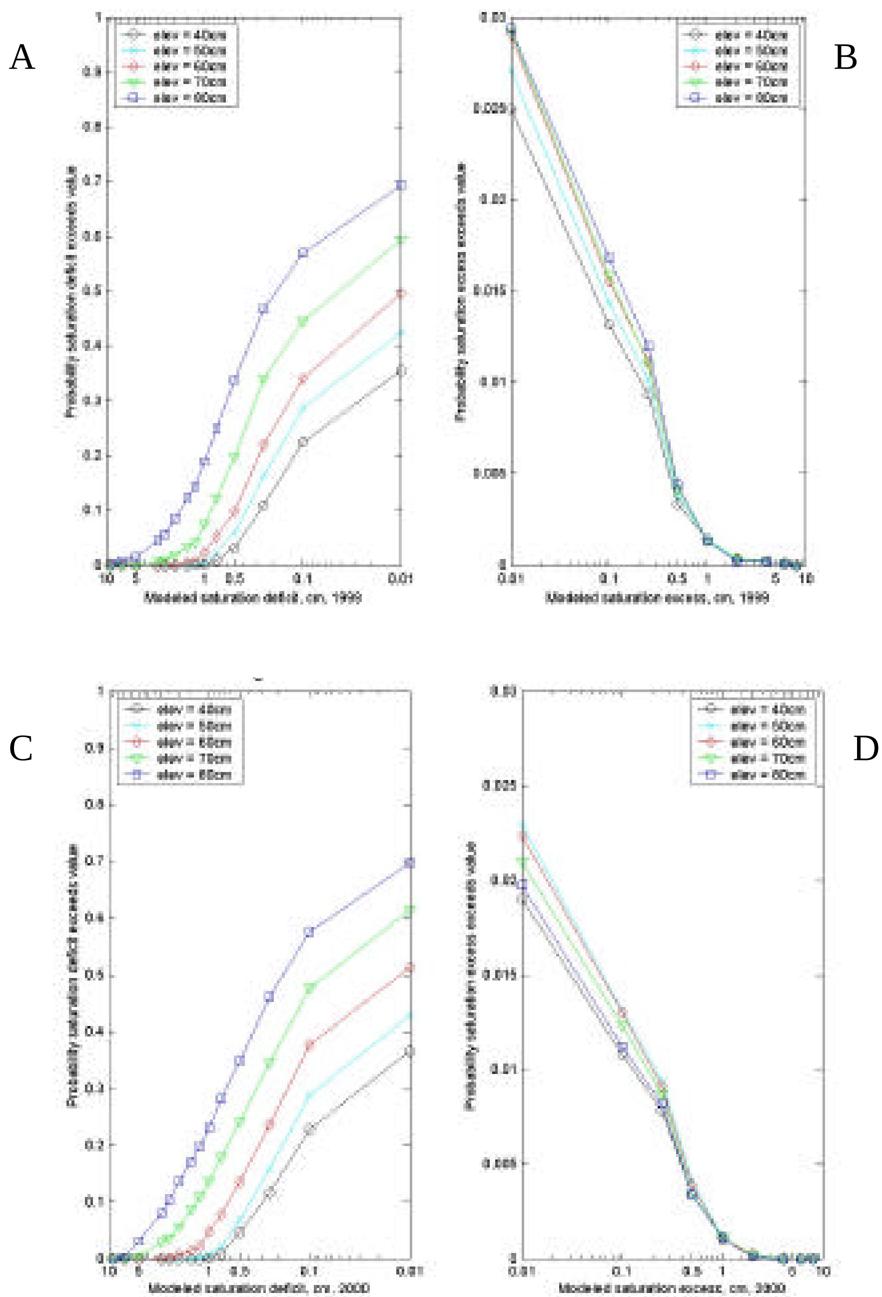

Figure 43. Modeled probability of saturation deficit and excess for 1999 and 2000. (Tidal inputs from converted Wachapreague data; see appendix 5 for PET correction).

A. Modeled saturation deficit, 1999
B. Modeled saturation deficit, 2000
C. Modeled saturation excess, 1999
D. Modeled saturation excess, 2000

Table 15. Probabilities associated with rainfall, modeled with hourly data for 80 cm surface elevation.

	1999	**2000**
(1) Probability of precipitation	0.043	0.040
(2) Probability of surface exposure	0.694	0.698
(3) Probability of precipitation during surface exposure	0.035	0.032
(4) Probability of saturation excess (modeled)	0.029	0.019
(5) Fraction of all hours with precipitation that generated saturation excess (modeled)	0.674	0.475
(6) Fraction of hours with precipitation on an exposed marsh that generated saturation excess (modeled)	0.829	0.594

<u>Key to probability calculations:</u>
(1) Number of hours with precipitation, divided by total hours of record;
    data from Phillips Creek meteorological station
(2) Number of hours water level at the study area was less than 80 cm, divided by total
    hours of record; using water level at study area from converted Wachapreague tides
(3) Number of hours with precipitation that occurred when the water level at the study
    area was less than 80 cm, divided by total hours of precipitation data
(4) Number of hours with a modeled water balance greater than zero, divided by total
    hours of precipitation data
(5) = (4) divided by (1)
(6) = (4) divided by (3)

Table 16. Statistics of rainfall events, measured and modeled hourly saturation deficit, and modeled saturation excess.

	1999	**2000**
Mean hourly modeled saturation deficit (cm) at 80 cm surface elevation	-0.75	-0.92
(standard deviation)	(1.25)	(1.43)
Mean hourly saturation deficit (cm) from logger measurements of water table position at 80 cm elevation	-0.3 *	-0.7 **
(standard deviation)	(0.3)	(0.7)
Number of rainfall events	93	93
Mean rainfall sum per event (cm)	1.3	1.1
(standard deviation)	(1.8)	(1.2)
Mean rainfall event duration (hours)	6.2	6.0
(standard deviation)	(4.3)	(4.3)
Number of modeled saturation excess events at 80 cm elevation	74	65
Number of modeled saturation excess events at 80 cm elevation with greater than or equal to 1 cm of total saturation excess	23	24

* Logger measurements were from Days 224-268, 1999 (39 m from the creek; 79 cm surface elevation)
** Logger measurements were from Days 117-206, 2000 (43 m from the creek; 81 cm surface elevation)
and Days 206-320, 2000 (39 m from the creek; 79 cm surface elevation)

n = 65

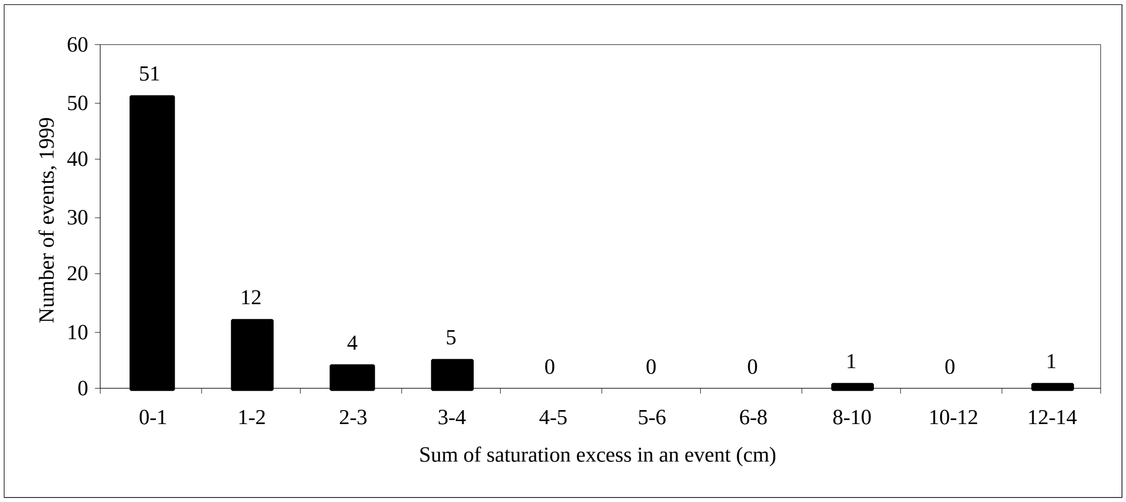

Figure 44. Frequency histograms for total depth of modeled saturation excess at 80 cm

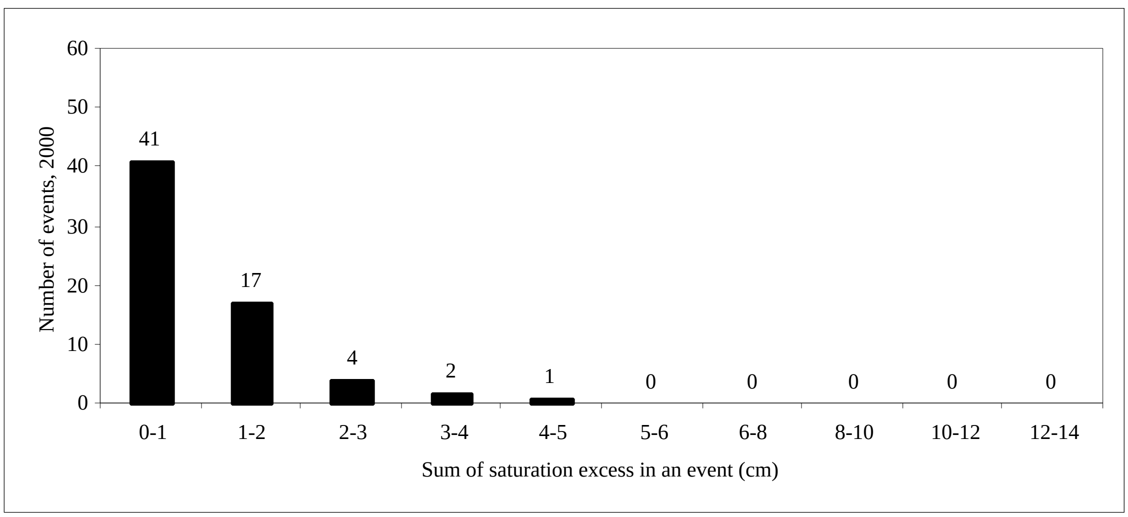

surface elevation, 1999 and 2000 (assuming no surface runoff inputs or outputs).

Table 17. Weather associated with modeled saturation excess events at 80 cm elevation, 1999. (Table lists all events with 1 cm or more of saturation excess).

Start of event (Julian Day)	Sum of modeled saturation excess (cm)	Associated weather

226.2	12.6	Convective
290.6	8.9	Cyclonic
258.6	4.4	Cyclonic *
24.2	3.4	Frontal
250.0	3.1	Convective
203.5	3.1	Convective
86.9	3.0	Frontal
253.0	2.8	Cyclonic
232.1	2.7	Convective
73.9	2.6	Cyclonic
348.1	2.4	Cyclonic
164.5	1.9	Frontal
293.3	1.9	Frontal
171.2	1.7	Cyclonic
252.7	1.5	Frontal
59.8	1.4	Frontal
237.4	1.4	Convective
330.7	1.3	Frontal
86.5	1.2	Frontal
192.0	1.1	Convective
247.9	1.1	Cyclonic
166.5	1.1	Cyclonic
80.5	1.0	Frontal

* Hurricane Floyd

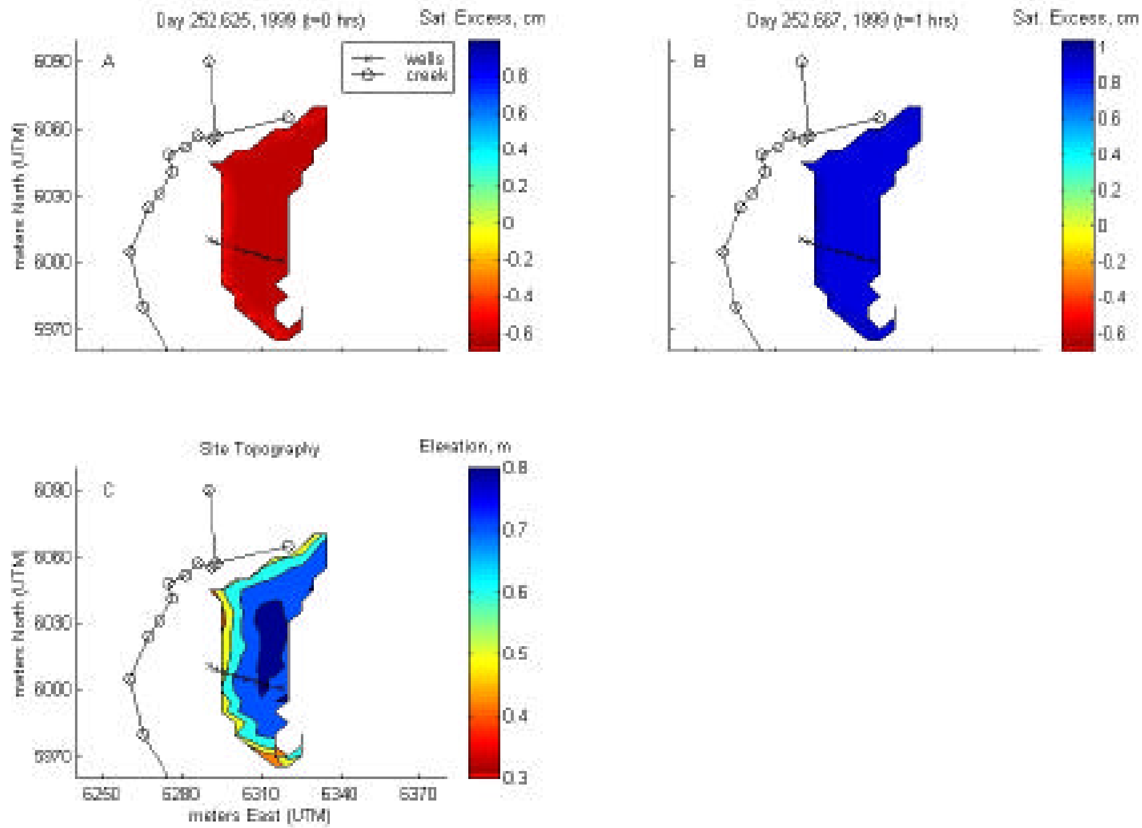

Figure 45. Spatial development of the area saturated by rainfall shortly after inundation.

A. t=0 hours before the onset of rain (antecedent saturation deficit)
B. t=1 hour, the onset of rain
C. site topographic map, for reference

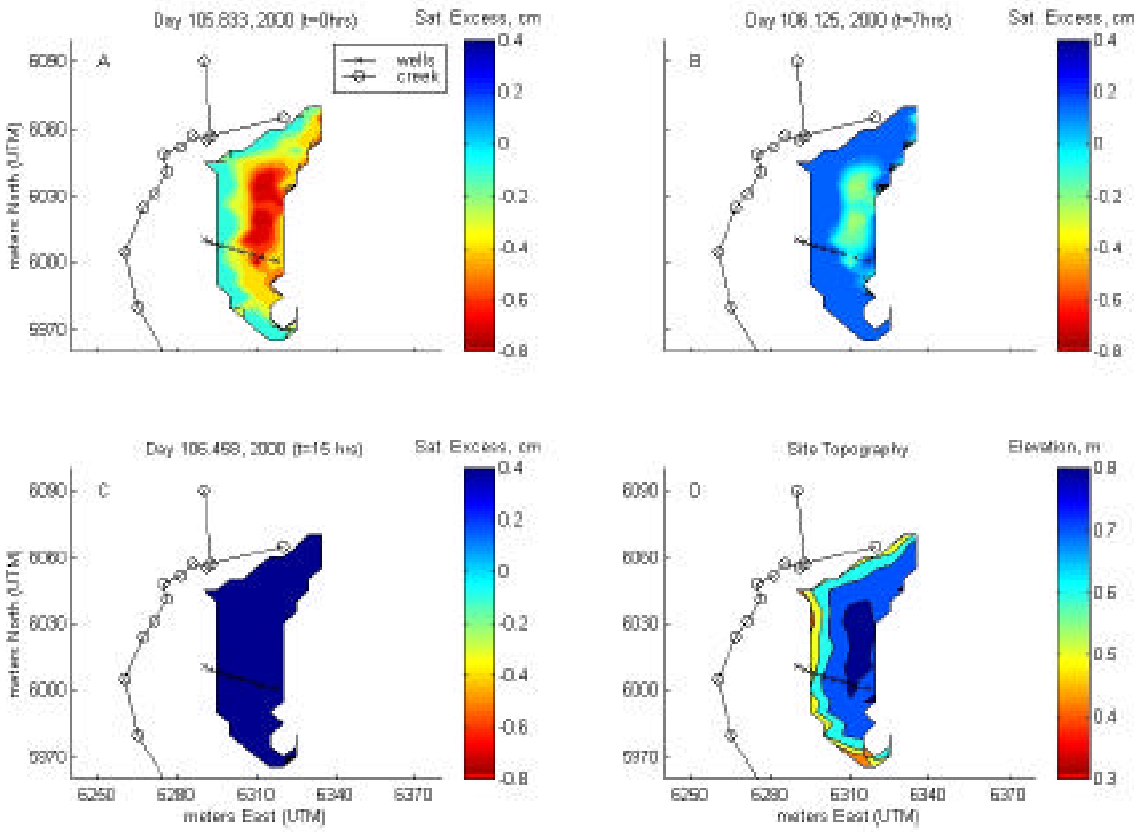

Figure 46. Spatial development of the area saturated by rainfall following a drying period.

A. t=0 hours before the onset of rain (antecedent saturation deficit)
B. t=7 hours after the onset of rain
C. t=15 hours after the onset of rain
D. site topographic map, for reference

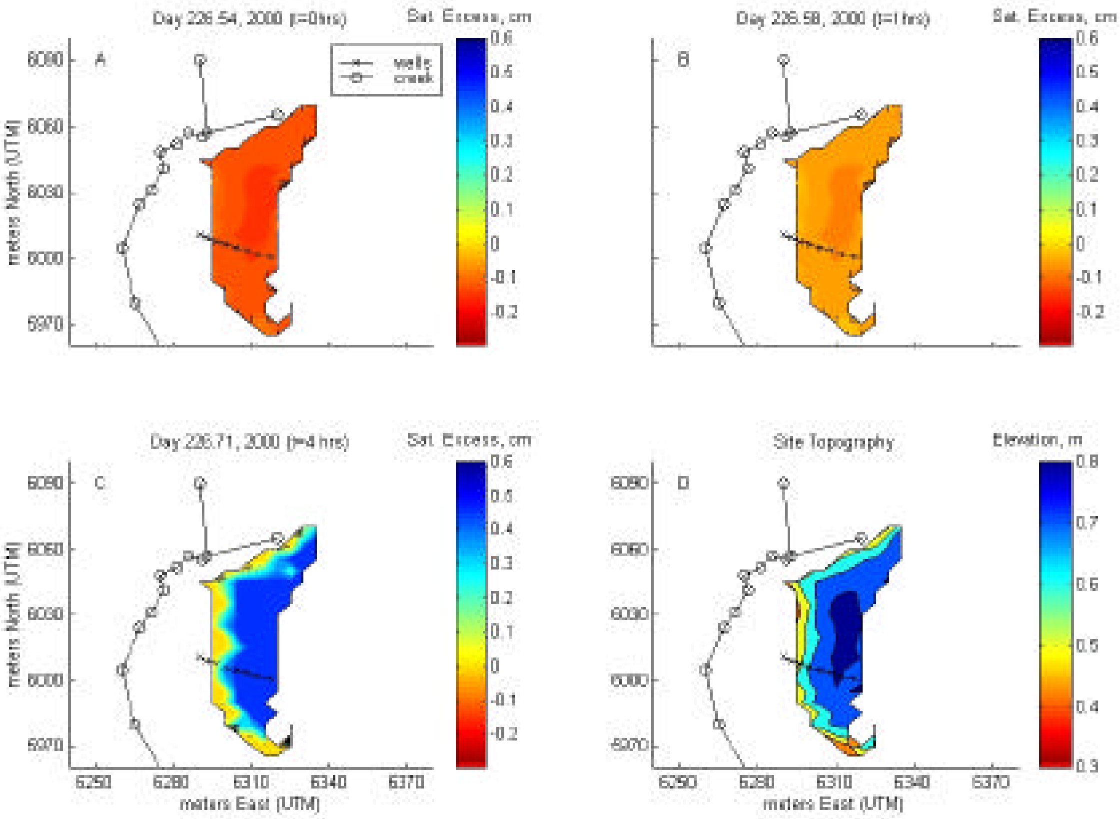

Figure 47. Spatial development of the area saturated by rainfall during partial inundation of the surface.

A. t=0 hours before the onset of rain (antecedent saturation deficit)
B. t=1 hour, the onset of rain
C. t=4 hours after the onset of rain
D. site topographic map, for reference

Discussion

The following questions motivated this research. What conditions were conducive to overland flow? How often did these conditions occur? What were the potential mechanisms for erosion? What were the spatial and temporal characteristics of the saturated area?

Exposure of the marsh surface was a necessary condition for saturation by rainfall. When the marsh was inundated, rain did not affect the surface. Tidal inundation saturated the sediment, but saturation by tides was not expected to erode the sediment. However, frequent saturation by tides had an important effect on the frequency of saturation by rainfall. Regular tidal inundation kept the saturation deficit low so that the amount of rainfall typically required to saturate the sediment was also low.

The general condition for overland flow was for rainfall to exceed the saturation deficit during non-flooded periods. Saturation excess was expected when the water table was near the surface at the onset of rain. Day 237, 1999, illustrated conditions when this was likely (**figure 28**). The study area was inundated at the end of Day 236, saturating the sediment and bringing the water table to the surface. Overnight PET and water table drawdown were negligible. On Day 237, PET was very low and the water table remained close to the surface, indicating a small saturation deficit. Rain in the afternoon was likely sufficient to saturate the sediment, and 1.4 cm of saturation excess was modeled at 80 cm elevation on this day (**table 17**).

The conditions for saturation by rainfall were shown to be met frequently. (See appendix 5 for correction to PET method). There was a high probability that, if rainfall coincided with marsh surface exposure, it would be sufficient to saturate the surface (**table 15**). This occurrence was modeled 74 times in 1999 and 65 times in 2000, out of a total of 93 rainfall events in each year. Field measurements of water table position agreed with the modeled frequency of occurrence. Using the water table as an indicator of the saturation deficit, saturation excess was expected frequently because the water table remained near the surface throughout the period of field monitoring.

The mean hourly saturation deficit was an indication of a typical antecedent saturation deficit at the start of a precipitation event. The mean sum of precipitation in an event was greater than the modeled mean hourly saturation deficit and the mean hourly saturation deficit derived from logger measurements of water table position (both for 80 cm elevation, **table 16**). Because the values for event rainfall exceeded the average hourly saturation deficit, it follows that saturation excess was modeled for 70-80% of all rainfall events. On an hourly basis, saturation excess was modeled for 50-70% of all hours with rainfall (**table 15**). Rain sometimes coincides with inundation, but rain falling onto a flooded marsh did not affect the surface. Saturation excess was modeled for 60-80% of the hours in each year with rainfall during surface exposure.

The saturation deficit was greater during drying periods, making saturation by rainfall less likely at these times. The average maximum saturation deficit of the drying periods in this study was 2.6 cm (**table 11**). This was greater than the mean sum of precipitation in an event (**table 16**). However, saturation by rainfall was still possible during drying periods. There were 14 rainfall events in 1999 and 12 events in 2000 with total precipitation greater than 2.6 cm.

Drying periods were common, but infrequent, with 13 days separating drying periods, on average (**table 11**). The spring-neap tidal cycle, which is approximately bi-weekly, obviously affects inundation potential. However, the large variability of the number of days between drying events suggests other mechanisms are involved. For instance, only 3 of 13 events in table 11 were separated by 12 to 14 days, and the standard deviation was 9 days.

Erosion can be initiated by the transfer of energy from a raindrop to soil particles (Smith and Wischmeier, 1962). The second phase of erosion is transport of disturbed sediment. In the study area, disturbed sediment and water were shed from mounds into adjacent depressions and transported in overland flow (**figure 48**). Chalmers et al (1985) found rainfall runoff was an important transport mechanism for organic matter. Less-dense organic matter is expected to be eroded more frequently and transported further than more-dense mineral matter.

The relative proportions of eroded sediment will vary for a given amount of rainfall based on storm intensity (Smith and Wischmeier, 1962). Raindrop energy generally increases with increased storm intensity. The greater the energy, the greater the erosion potential. The energy of a raindrop is a function of drop size and terminal velocity and determines the potential to dislodge soil particles on impact. Just as tidal inundation absorbs the energy of rain, so that rain on a flooded marsh does not impact the surface, there is some minimum depth of saturation excess that will buffer the surface.

This points to the importance of crab mounds in the erosion process. Crabs create piles of loosened, easily-erodible sediment that protrudes above saturation excess collecting in depressions during rainfall events.

Total saturation excess in an event exceeded 1 cm 23 times in 1999 and 24 times in 2000, approximately 25% of the total rainfall events in each year (**table 16**). These results were based on an assumption that 1 cm of rainfall in excess of the saturation deficit was required for runoff. However, the depth of saturation excess in the depressions might exceed 1 cm for a lesser amount of rain, because saturation excess was concentrated into the depressions as it was shed from adjacent mounds. No attempt was made to quantify surface runoff or the concentration of saturation excess in the depressions. When runoff occurs, it will increase the depth of saturation excess at lower elevations. In a saturation excess event interrupted by inundation, the depressions would be full when the tide receded. If rainfall continued, all subsequent rainfall would go to runoff, without first filling the depressions. For example, a 24-hour duration storm on Days 73 and 74, 1999, was divided into three saturation excess events because the surface was inundated twice during the course of the storm.

Some amount of rainfall would be intercepted by the vegetation, increasing the amount of rainfall necessary to saturate the surface. However, some of the intercepted rainfall would reach the surface as throughfall and stemflow. No attempt was made to quantify these processes.

Spatial variability of the saturation deficit was small, and modeled saturation by rainfall usually included the entire study area. Surface elevation was the only significant spatial control. Increased surface elevation decreased the frequency and duration of tidal inundation, so that the average hourly modeled saturation deficit increased as surface elevation increased (**table 18**). During periods of regular inundation, the difference in length of exposure between upper and lower elevations was only a few hours, which was not enough time for large saturation deficits to develop. During these periods, spatial differences in saturation deficit based on elevation were small.

Drying periods were the only time significant spatial differences in saturation deficit were able to develop. Drying periods were also the only time the saturation deficit exceeded the mean sum of rainfall in an event. The longest the study area went without complete inundation was 9 days (**table 11**). Lower elevations were inundated more frequently than upper elevations, and had fewer and shorter drying periods. For example, drying periods of 3 days and 9 days at 81 cm elevation lasted only 2 days and 7 days, respectively, at 74 cm elevation (Days 147-150 and 172-181, 2000, see appendix 2). Differences in the duration and frequency of drying periods would increase as the difference in surface elevation increased.

Because the entire study area was regularly inundated, a nearly uniform spatial distribution of the saturated area was most commonly found. Two other spatial patterns were also found. In cases when the antecedent saturation deficit was greater at upper elevations, saturation by rainfall occurred sooner at lower elevations, or exclusively at lower elevations. Another pattern occurred when lower elevations were inundated during rainfall. Saturation excess occurred only on the exposed surface at upper elevations. In these cases, runoff from upper elevations was likely to be stopped when it encountered floodwaters at lower elevations. Any sediment suspended in the runoff was likely to be deposited at that point.

The annual probabilities of saturation excess were very similar at all elevations modeled (**figure 43**). In 1999, modeled saturation by rainfall was slightly more frequent at mid and upper elevations than at lower elevations. In 2000, modeled saturation by rainfall was slightly more frequent at mid elevations and less frequent at upper and lower elevations.

Two factors affected the frequency of saturation excess, the average hourly saturation deficit and the duration of tidal inundation that coincided with rainfall events. Mid-elevations (50-70 cm in the study area) might have the optimum potential for saturation excess because they are inundated frequently enough to have a low saturation deficit, on average, at the onset of rain events, but not inundated so frequently as to have the surface shielded from the effects of rain by overlying flood waters. The surface at 80 cm elevation was inundated for some portion of approximately half of the rainfall events (approximately 20% of the hours with rainfall), preventing rainfall from affecting the surface at those times. The shielding effect of inundation was greater at lower elevations, because the duration of inundation during rainfall events was greater there than at higher elevations. Therefore, although the average hourly saturation deficit was lowest at lower elevations (40-50 cm), saturation excess was less frequent at lower elevations. Upper elevations (70-80 cm) had a greater average hourly saturation deficit, but this did not always lead to less frequent saturation excess (**table 18**). In 2000, upper elevations showed less frequent saturation excess than mid elevations. In 1999, however, the mean hourly saturation deficit at upper elevations was lower than in 2000, and saturation excess was not modeled less frequently at upper elevations than at mid elevations in 1999, as it was in 2000.

In general terms, then, there appears to be a mid elevation range most prone to rainfall erosion. Lower elevations are often inundated during rainfall, and upper elevations are not inundated frequently enough to have a low saturation deficit. Mid-elevations have a low average saturation deficit and are frequently exposed during rainfall. (See appendix 5 for correction to PET method, as it relates to the average saturation deficit). This generality can be scaled-up from the small study area to larger areas, because of the dominance of tidal inputs in the determination of the saturation deficit, and the fact that inundation is a fairly simple function of elevation and distance from the tidal creek. As area is scaled-up, however, greater heterogeneity is expected in soil properties (see Table 9 for comparison of different sites within Phillips Creek Marsh) and plant species composition (which will have varying rates of evapotranspiration).

Runoff at this site could also occur by infiltration excess overland flow in certain circumstances. The infiltration rate of water added to the wells for well response tests was 1-3 cm hr^{-1}. This was consistent with the hydraulic conductivity in other marshes (Knott et al, 1987; Harvey et al, 1987; Nuttle and Hemond, 1988). Rainfall intensity was typically less than 1 cm hr^{-1}. There were 27 hours with intensity greater than 1 cm hr^{-1} during 1999 and 2000 combined, but there was only one hour that exceeded 3 cm hr^{-1}. Infiltration excess might have greater relative significance in areas above Mean High Water. Such areas are expected to have greater saturation deficits because they are less frequently inundated. For example, the depth to the water table can exceed 100 cm in the high marsh at Phillips Creek Marsh (Hmieleski, 1994; Stasavich, 1998). Because of the greater saturation deficit, areas above Mean High Water might not experience saturated overland flow, or only for events with rainfall following recent inundation.

Temporal characteristics of saturation excess included the timing of rain with respect to the tides, and the timing of the tides with respect to PET. Rainfall must coincide with marsh surface exposure to saturate the sediment. Because regional storms are often accompanied by tidal surges that inundate the marsh, it was thought such storms might not generate saturation excess. However, meteorological conditions conducive to overland flow included both regional storms accompanied by tidal surges and local convective storms (**table 17**). For the former, runoff was modeled when rain preceded the storm surge and/ or continued after the tide receded. Convective systems typically build in the afternoon and are not connected with tidal elevations.

The timing of tides with respect to PET was also important. PET was the only significant means of water removal from the sediment in the marsh interior. PET drives the saturation deficit and water table drawdown between periods of water input by inundation or rainfall. Day-time inundation coinciding with PET limited water loss from the sediment (**figure 29**). When the surface was exposed by day, evapotranspiration removed water from the sediment.

In the marsh, topographic gradients were low, such that lateral hydraulic gradients and subsurface transport were minimal. The factors assumed important to water table position and the saturation deficit in regularly flooded portions of the salt marsh interior were water inputs by tidal inundation or precipitation and water loss by PET. These assumptions were confirmed by the agreement between measured and modeled water table elevations (**figure 41, table 13, appendix 2**).

Tidal water saturated the sediment. Inundation brought the water table to the surface, while the water table elevation decreased when PET was indicated during exposure of the marsh surface after inundation. Peak tidal elevations during inundation did not affect the water table position. Drawdown was similar 39 m from the creek on Days 234, 235, and 236, 1999, following inundation periods with peak tidal elevations of 98, 88, and 92 cm (MSL), respectively (**figure 28**).

The duration of marsh exposure was less during semi-diurnal tides than during once-daily tides or neap tides. More time of marsh exposure roughly corresponded to more time for water removal by PET, leading to greater saturation deficit and water table drawdown, with the above consideration for the timing of PET with respect to the tides.

During drying periods, water table drawdown was sometimes halted 15-25 cm below the surface, even when additional PET was calculated (**figure 30**). The saturation deficit calculated from water table measurements for these periods was also halted. However, model results showed additional water removal by evapotranspiration and therefore diverged from the field measurements (see appendix 2 and figure 41, Days 231, and 261-264, in 1999; Days 161-165,174-181, 222-225, and 252-255 in 2000). Soil core measurements of the saturation deficit during drying periods were not able to help explain this occurrence because water table drawdown was not halted during four neap-tide sampling periods.

A depth of 15-25 cm corresponds to the root zone of the salt marsh grasses. Salt marsh plant roots are concentrated in the top 10 cm, with a maximum rooting depth of 20-30 cm (Good et al, 1982; Blum, 1993; Tirrell, 1995; Loomis, 1999). Once the water table reached the bottom of the root zone, it is probable that additional water was removed by the roots above the water table when PET was indicated. Because of the low hydraulic conductivity of the sediment, this water could have been removed without affecting the water table position. Another possible explanation for the divergence of model results and water table measurements during drying periods is that as soil moisture decreased, less water was available to the plants (so the marsh was no longer a "well watered surface"), and potential evapotranspiration no longer adequately represented actual evapotranspiration. Also, plants senesce after the growing season, so actual evapotranspiration is expected to be less than potential at these times. Any time evapotranspiration is overestimated, the model will show greater water table drawdown than the field measurements of water table position.

Nocturnal increases in the water table were not seen in field measurements for this study, indicating regular groundwater input was not significant for the area studied. Additionally, the water table measurements were adequately modeled without groundwater input or drainage. Nuttle and Harvey (1995) found significant regional groundwater input in a different part of the marsh (**figure 3**), indicating spatial variability of this input.

There was evidence for small-scale and episodic groundwater seepage at the upper part of the marsh in the study area, fringing the transition zone. The portion of the marsh in the study area within 5 m of the transition zone was nearly always soggy or had ponded water in depressions, corresponding to the description of shallow groundwater discharge and surface seepage from the upland (Harvey, 1990). In 2000, taller *Spartina alterniflora* was observed in the transition zone than in the mid marsh, possibly due to freshwater flushing of the root zone in the transition zone by upland discharge. Summer months in 2000 consistently had higher rainfall than the 30-year average at Painter, VA (**figure 10**), possibly driving discharge from the upland. These evidences of discharge were only seen at the transition zone and upper extent of the marsh adjacent to the transition zone, and not in the marsh interior. Although salinity in the well 49 m from the creek was not different from other wells in the marsh (**figure 18**), surface seepage from the upland could occur without diluting the salinity. Groundwater transport in the shallow subsurface would be expected to affect the salinity.

Days 240-260, 1999, was a period of semi-diurnal inundation when PET was minimized by day-time inundation (**appendix 2**). Water table elevations 39 and 43 m from the creek remained at or very near the surface during this period, but the water table was at or above the surface 49 m from the creek (the upper-most location in the marsh, **figure 4**). Five successive tidal cycles reached the upland on Days 242-244, in weather associated with Hurricane Dennis. Presumably, the combination of upland discharge and minimized PET was responsible for observed water table elevations during this period. There was also evidence of episodic groundwater discharge into the marsh up to 10 m from the upland after a major inundation event on Days 260-264, 1999 (**figure 32**).

No salinity gradient was found in the low or mid marsh in the study area (**figure 18**), which was entirely below Mean High Water (**figure 6**). Lack of a salinity gradient further indicated the entire study area was regularly inundated. The inundation frequency was similar among elevations in the low and mid marsh for the period of the salinity measurements in figure 18, and the upper elevations had similar salinity values as the lower elevations. This was consistent with the conclusion by Leeuw et al (1991) that duration of flooding, which is less at upper elevations, is not a significant parameter with respect to shallow groundwater salinity in a marsh. It was also consistent with the conclusion by Leeuw et al (1991) that dilution of salinity by rainfall is significant only at elevations near and above Mean High Water.

The water table elevation often increased in response to tidal forcing when tidal elevation was not sufficient to inundate the surface or on the rising tide prior to inundation. The magnitude of these fluctuations was greatest 43 m from the creek (in the mid marsh) and 70 m from the creek (in the upland). Hemond and Fifield (1982) and Hughes et al (1998) showed that tidal forcing can be transmitted laterally through shallow unconfined sandy aquifers and, if vertical conductivity is sufficient, into the surface layer. The water table was also seen to rise prior to inundation in results presented by Dacey and Howes (1984, their figure 1) and Harvey et al (1987, their figure 5b). Sediment at the study area was sandier in the upland, possibly indicating higher conductivity and providing a reasonable explanation for the increased magnitude at that location. Sediment texture, porosity, and bulk density 43 m from the creek were not substantially different than adjacent locations with a smaller magnitude tidal signal (**table 8, table 10**).

Soil moisture for Days 235-237, 2000 (**figure 25**), and S_y (**figure 21, table 6**) at this location were also similar to other locations.

Rain events and modeled saturation excess events were more frequent in summer. (Summer, here, was Days 81-264, defined by the equinoxes, so that summer and winter periods had an equivalent number of days). In 1999, 54 of 93 rain events (58%) and 43 of 74 modeled saturation excess events (58%) occurred in summer. In 2000, 58 of 93 rain events (62%) and 40 of 65 modeled saturation excess events (62%) occurred in summer. However, the seasonal differences were not disproportionate; saturation excess was more frequent in summer because rain events were more frequent in summer.

Comparison of summer/ winter water table characteristics (**figures 33, 34**) did not reveal significant seasonal differences. For the period of those measurements, inundation frequency was slightly higher at 80 cm elevation for summer (35%) than winter (30%). In summer, despite more frequent saturation by tides and less surface exposure for water removal by PET, there was a slightly higher probability of the water table reaching depths of 2-5 cm. This is possibly due to the higher PET in summer (**figure 39**). Winter had a higher probability of water table depth exceeding 5 cm, which is consistent with less frequent inundation.

Although the water table measurements did not show significant seasonal differences during the limited time of the record, the mean hourly modeled saturation deficit was higher in summer (Days 81-264) (**table 19**). However, the increased PET and saturation deficit in summer were not significant with respect to the frequency of saturation excess. Even in summer, the mean sum of rainfall per event (**table 16**) was greater than the mean hourly modeled saturation deficit.

The relative positions of the land, sea, and water table surfaces described by Hayden et al (1995) can also be used to describe the controls on saturated overland flow at the study site in Phillips Creek Marsh. Surface elevation was shown to be a significant control on soil saturation, through its influence on tidal inundation. A surrogate for the saturation deficit, the marsh groundwater table, indicated the amount of precipitation necessary to saturate the surface and the amount of rainfall-runoff for a given precipitation event. Runoff can potentially alter the land surface elevation by gradual, episodic erosion.

The sediment budget and surface topography determine marsh development (Brinson et al, 1995). Sediment supply determines if a marsh will increase or decrease in area, while surface topography determines if a marsh will stall or migrate over land at the upland transition during sea-level transgression. Components of the sediment budget include inputs by deposition and organic matter accumulation, modified over time by compaction, and losses by erosion. Overall, Phillips Creek Marsh is depositional (Kastler, 1993; Christiansen, 1998), and erosion is therefore less than the inputs, over time.

To determine a rate for sediment removal by rainfall erosion would require measuring sediment concentrations in actual events or runoff simulations. The amount of runoff and entrained sediment would need to be correlated to the amount of saturation excess. This would help define the significance of rainfall erosion to the sediment budget. Because saturation by rainfall was shown to occur relatively frequently, rainfall erosion has the potential to be a significant process.

The sediment water balance was shown to be dependent on tidal inundation. Potential effects of sea-level rise and increased air temperature were modeled in a very simplified manner, by adding projected increases to measured values from 1999. Estimates for the current rate of mean relative sea-level rise (eustatic plus subsidence) for the Eastern Shore of Virginia include 2.0, 3.1, and 3.5 mm yr^{-1} (respectively, Holdahl and Morrison, 1974; Emery and Aubrey, 1991; and Nerem et al, 1998). Hourly tidal elevations from 1999 were increased by 20 cm. The increase in tidal elevation reflects a 3 mm yr^{-1} increase in mean sea-level minus 1 mm yr^{-1} vertical sediment accretion (Kastler and Wiberg, 1996), for 100 years. The Intergovernmental Panel on Climate Change "best estimate" of surface air temperature increase is 2^{o}C by 2100 (Kattenberg et al, 1995). Hourly values of air temperature for 1999 were increased by 2^{o}C. Potential changes in solar radiation, precipitation, tropical storms, or the rate of sea-level rise were not included.

Changes in air temperature and mean sea level were modeled individually and together (**figure 49**). With an increase in sea-level, the frequency of all values of saturation deficit decreased at all elevations (**figure 49B**). This would likely be due to a combination of more frequent saturation by tides and shorter duration periods of surface exposure for water removal by evapotranspiration. With decreased saturation deficit, and assuming the same rainfall amounts and temporal patterns as in 1999, saturation excess might be expected to be more frequent than without the increased sea-level. Saturation excess, however, did not change very much with increased sea-level. Saturation excess decreased slightly at lower and mid-elevations (**figure 49E**). The decrease would likely be due to decreased frequency and shorter durations of surface exposure. By definition, saturation excess occurs only during periods of rainfall on an exposed surface.

Increased air temperature did not have a significant effect on either saturation deficit or excess (**figure 49C, F**). The combined effect of sea-level rise and air temperature increase therefore was very similar to the change produced by sea-level rise independently. These results are in agreement with the model sensitivity analysis (**figure 42**), which showed tidal elevation was significant but air temperature was not.

While saturation excess in regularly-flooded areas was not shown to change much with increased Mean Sea Level, sediment deposition and organic matter accumulation rates are expected to increase with increased inundation. The former because inundation is the sediment transport mechanism for both regular inundation events and storm surges; and the latter because plant roots are hypothesized to die and grow new roots in response to saline stress and anoxic conditions (Blum, 1993).

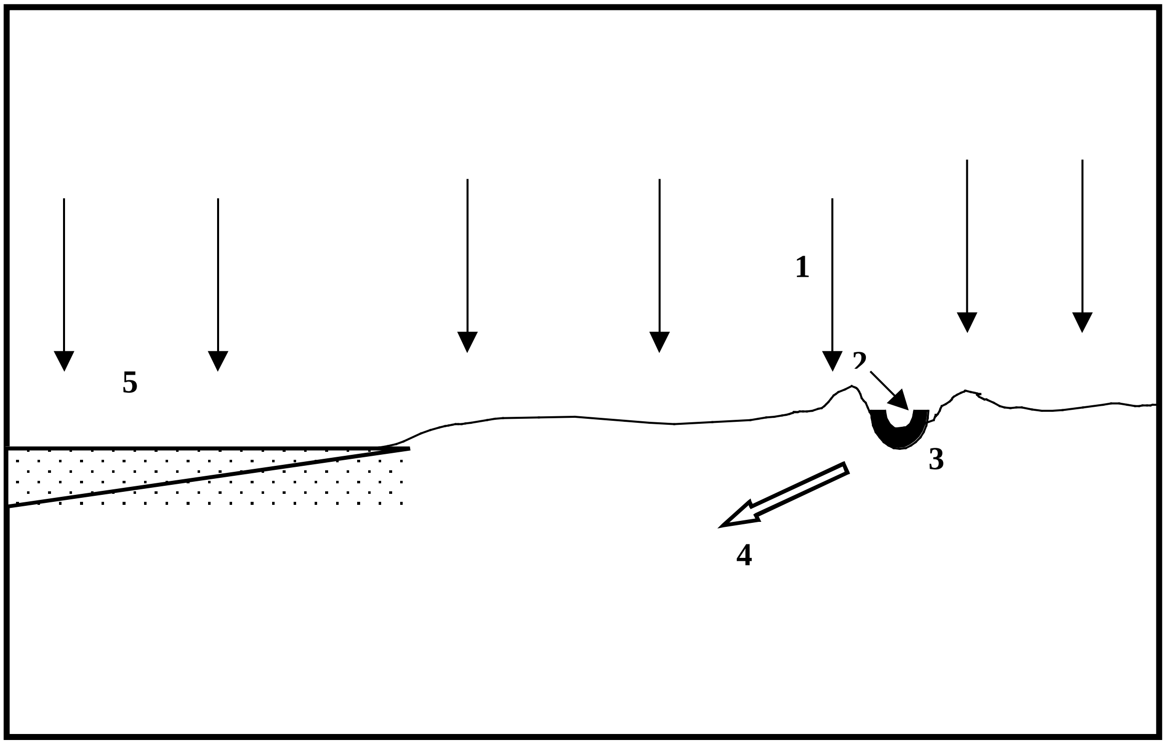

Figure 48. Conceptual diagram of surface runoff by saturated overland flow.

Legend
1. Rain impacts sediment on mounds created by crab burrow excavation
2. Water and sediment are shed from mounds into adjacent depressions
3. Saturation excess collects in depressions
4. Runoff occurs when saturation excess is greater than the depth of the depression
5. Rain falling on flood waters does not yield runoff

Table 18. Mean saturation deficit modeled on an elevation gradient.

	Mean modeled hourly saturation deficit, cm[1] (standard deviation)	
Elevation, cm (MSL)	1999	2000
40	-0.12 (0.18)	-0.13 (0.20)
50	-0.16 (0.22)	-0.16 (0.23)
60	-0.21 (0.29)	-0.26 (0.40)
70	-0.36 (0.54)	-0.54 (0.92)
80	-0.75 (1.25)	-0.92 (1.43)

[1]excluding inundation and saturation excess

Table 19. Mean modeled saturation deficit by season at 80 cm elevation.

	Mean modeled hourly saturation deficit, cm[1] (standard deviation)	
80 cm elevation (MSL)	1999	2000
Summer (Days 81-264)	-1.03 (1.62)	-1.08 (1.61)
Winter (Days1-80, 265-365)	-0.45 (0.53)	-0.75 (1.18)

[1]excluding inundation and saturation excess

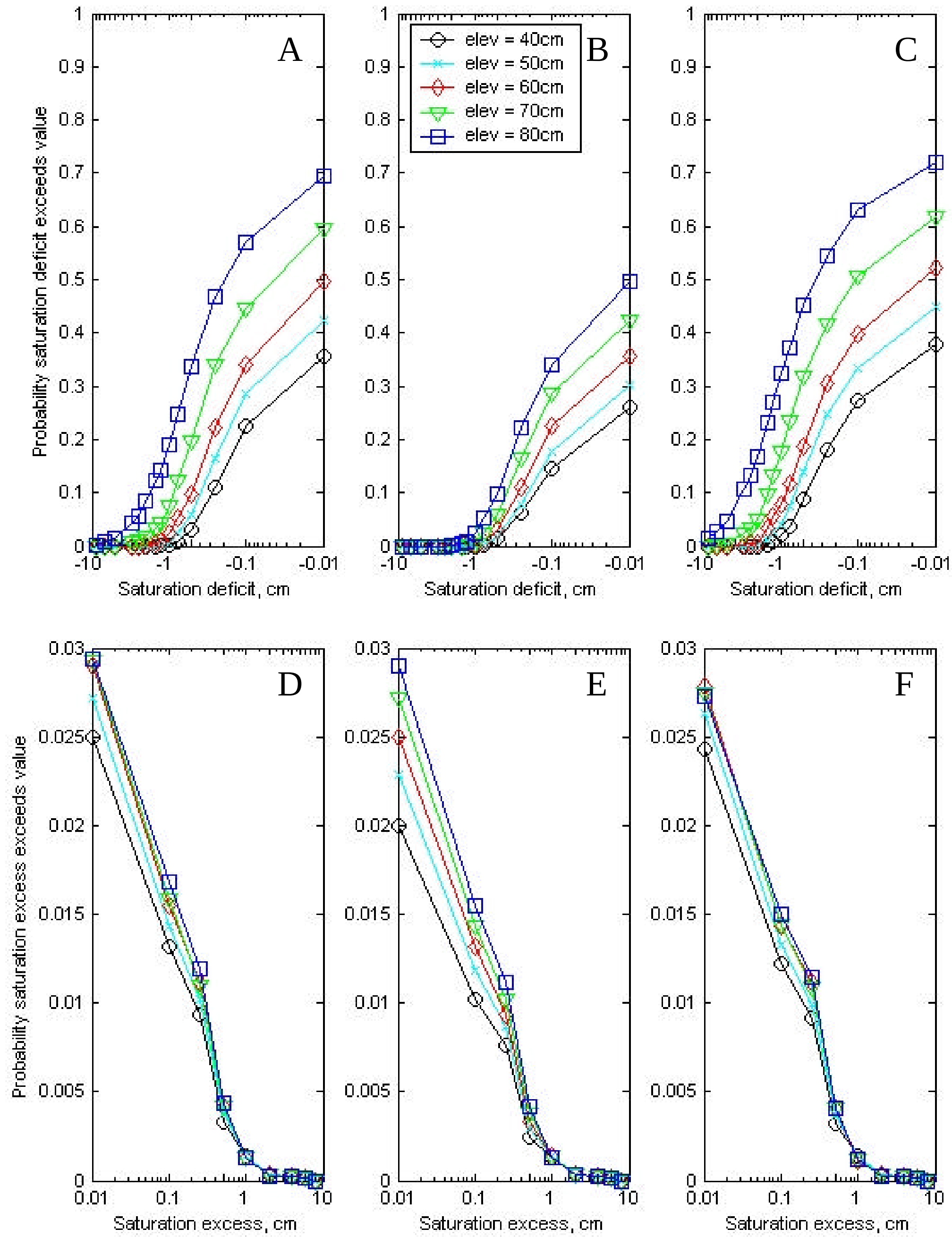

Figure 49. Probabilities of saturation deficit and excess associated with increased air temperature and mean sea-level, using 1999 data.

A. Saturation deficit probability distribution for 1999 tidal elevations and air temperature.

B. Saturation deficit associated with 1999 tidal elevations increased by 20 cm

C. Saturation deficit associated with 1999air temperatures increased by 2 C

D. Saturation excess for 1999 data

E. Saturation excess associated with 1999 tidal elevations increased by 20 cm

F. Saturation excess associated with 1999air temperatures increased by 2 C

Summary and Conclusions

At a study site within a regularly flooded area of the marsh interior, sediment water content was analyzed for 1999 and 2000. The mean hourly saturation deficit was smaller than the mean sum of rainfall in an event, and model results indicated saturation excess was a common occurrence. This thesis showed the spatial extent and frequency of occurrence for rainfall-runoff is sufficient to be a potentially significant means of sediment redistribution on a salt marsh surface. Soil particle displacement by raindrop impact and transport in overland flow were described as a means of erosion. Sediment dynamics are an important part of understanding marsh development over time.

The saturation deficit was controlled by inundation much more so than by evapotranspiration. Inundation regularly saturated the sediment, so the saturation deficit was typically small. The short time between daily or semi-diurnal inundation events prevented evapotranspiration from creating a significant saturation deficit with respect to event rainfall. Rainfall that coincided with marsh surface exposure was usually sufficient to saturate the sediment.

Drying periods, defined by surface exposure of more than one day, were the only times the saturation deficit exceeded the mean sum of rainfall in an event. Still, event rainfall exceeded the average saturation deficit of the drying periods for approximately 15% of rain events in each year. Drying periods occurred irregularly, but approximately bi-weekly, with an average duration of four days.

Within the study area, spatial variability of the saturation deficit was small, and when saturation by rainfall was modeled it usually affected the entire area. The upper extent of the saturated area is likely to be controlled by the upper extent of regular inundation (Mean High Water) and the lower extent by marsh surface exposure during the rain event. This points to a possible optimum for rainfall erosion in a mid-elevation zone.

Soil saturation was modeled for approximately 75% of the total rainfall events in each year, and runoff for 25%. This might be a conservative estimate for the number of runoff events, because concentration of saturation excess in surface depressions was neglected. Runoff is expected when saturation excess is greater than the depth of the depressions in the microtopography. Because runoff is not uncommon, rainfall erosion deserves further attention; specifically, ascertaining sediment transport rates and amounts to determine if erosion is a significant part of the annual sediment budget for the marsh.

In this study, tidal inundation had the greatest effect on the saturation deficit, suggesting that other locations that are regularly inundated will also show frequent saturation excess by rainfall. The value for S_y determined for the study area was within the range of values reported for other studies, further suggesting the results of this study will be generally applicable in other locations.

Literature Cited

Allen, J. R. L. 1989. Evolution of salt-marsh cliffs in muddy and sandy systems: a qualitative comparison of British west-coast estuaries. Earth Surface Processes and Landforms 14: 85-92.

Allen, J. R. L. and Pye, K. 1992. Coastal marshes: their nature and importance. Chapter 1 in *Saltmarshes: morphodynamics, conservation, and engineering significance*. (Allen, J. R. L. and Pye, K., eds.) Cambridge Univ. Press, Cambridge, Great Britain. 184 pp.

Barr, L. H. 1989. Sedimentation and fallout Cesium-137 cycling in a Virginia salt marsh. MS Thesis, Univ. of Virginia, Charlottesville, VA. 181 pp.

Bertness, M. D. 1991. Zonation of *Spartina patens* and *Spartina alterniflora* in a New England salt marsh. Ecology 72: 138-148.

Blum, L. K. 1993. *Spartina alterniflora* root dynamics in a Virginia marsh. Marine Ecology Progress Series 102: 169-178.

Brinson, M. M., Christian, R. R., and Blum, L. K. 1995. Multiple states in sea-level induced transition from terrestrial forest to estuary. Estuaries 18: 648-659.

Brutsaert, W. H. 1982. Evaporation into the Atmosphere: Theory, History, and Applications. D. Reidel Pub. Co., Boston, MA.

Chalmers, A. G., Wiegert, R. G. and Wolf, P. L. 1985. Carbon balance in a salt marsh: interactions of diffusive export, tidal deposition, and rainfall-caused erosion. Estuarine, Coastal, and Shelf Science 21: 757-771.

Chorley, R. J. 1978. The hillslope hydrological cycle. Chapter 1 in *Hillslope Hydrology* (Kirkby, M. J., ed.) 393 pp.

Christiansen, T. 1998. Sediment deposition on a tidal salt marsh. Ph.D. dissertation. Univ. of Virginia, Charlottesville, VA, 134 pp.

Christiansen, T., P. L. Wiberg, and T. G. Milligan. 2000. Flow and sediment transport on a tidal salt marsh surface. Estuarine, Coastal and Shelf Science 50: 315-331.

Dacey, J. W. H., and Howes, B. L. 1984. Water uptake by roots controls water table movement and sediment oxidation in short *Spartina* marsh. Science 218: 487-489.

Davis, R. and Dolan, R. 1993. Nor'easters. American Scientist 81: 428-439.

DeLaune, R., Patrick, J. W. H. and Buresh, R. 1978. Sedimentation determined by Cs-137 dating in a rapidly accreting salt marsh. Nature 275: 532-533.

Dusterhoff, S. R. 2002. Controls on near-surface soil-moisture dynamics in coastal environments. MS thesis, Univ. of Virginia, Charlottesville, VA, 93 pp.

Emery, K. and Aubrey, D. 1991. Sea levels, land levels, and tide gauges. Springer-Verlag. Berlin. 237 pp.

Fetsko, M. E. 1990. A water balance estimate at Brownsville, Virginia. MS thesis, Univ. of Virginia, Charlottesville, VA, 195 pp.

Fischer, H. B., List, E. J., Koh, R. C. Y., Imberger, J. and Brooks, N. H. 1979. Mixing in inland and coastal waters. Academic Press, New York. 483 pp.

French, J. and Spencer, T. 1993. Dynamics of sedimentation in a tide-dominated backbarrier salt marsh, Norfolk, UK. Marine Geology 110: 315-331.

Good, R. E., Good, N. F., and Frasco, B. F. 1982. A review of primary production and decomposition of the belowground marsh component. Pages 139-157 in: *Estuarine comparisons*. (Kennedy, V. S., ed.) Academic Press, New York.

Harvey, J. W. 1986. Subsurface hydrology in a regularly flooded *Spartina alterniflora* marsh. MS Thesis. Univ. of Virginia, Charlottesville, VA, 62 pp.

Harvey, J. W., Germann, P. F., and Odum, W. E. 1987. Geomorphological control of subsurface hydrology in the creekbank zone of tidal marshes. Estuarine Coastal and Shelf Science 25: 677-691.

Harvey, J. W. 1990. Hydrological transport in tidal marsh soils: controls on solute cycling at three scales. Ph.D. dissertation, Univ. of Virginia, Charlottesville, VA, 243 pp.

Harvey, J. W., and Nuttle, W. K. 1995. Fluxes of water and solute in a coastal wetland sediment. 2. Effect of macropores on solute exchange with surface water. Journal of Hydrology 164: 109-125.

Hayden, B. P., Dueser, R. D., Callahan, J. T. and Shugart, H. H. 1991. Long-term research at the Virginia Coast Reserve: modeling a highly dynamic environment. BioScience 41: 310-318.

Hayden, B. P., Santos, M. C. F. V., Shao, G., and Kochel, R. C. 1995. Geomorhpological controls on coastal vegetation at the Virginia Coast Reserve. Geomorphology 13: 283-300.

Hemond, H. F. and Fifield, J. L. 1982. Subsurface flow in salt marsh peat: a model and field study. Limnology and Oceanography 27: 126-136.

Hemond, H. F., Nuttle, W. K., Burke, R. W. and Stolzenbach, K. D. 1984. Surface infiltration in salt marshes: theory, measurement, and biogeochemical implications. Water Resources Research 20: 591-600.

Hmieleski, J. I. 1994. High marsh – forest transitions in a brackish marsh: the effects of slope. MS Thesis. East Carolina Univ., Greenville, NC. 129 pp.

Holdahl, S. and Morrison, N. 1974. Using precise relevelings and mareograph data. Tectonophysics 23: 373-390.

Howes, B. L., Dacey, J. W. H., and Goehringer, D. D. 1986. Factors controlling the growth form of *Spartina alterniflora*: feedbacks between above-ground production, sediment oxidation, nitrogen, and salinity. Journal of Ecology 74: 881-898.

Hughes, C. E., Binning, P., and Willgoose, G. R. 1998. Characterisation of the hydrology of an estuarine wetland. Journal of Hydrology 211: 34-49.

Jordan, T. E. and Correll, D. L. 1985. Nutrient chemistry and hydrology of interstitial water in brackish tidal marshes of Chespaeake Bay. Estuarine, Coasatal, and Shelf Science 21: 45-55.

Kastler, J. A. 1993. Sedimentation and landscape evolution of Virginia salt marshes. MS thesis, Univ. of Virginia, Charlottesville, VA, 119 pp.

Kastler, J. and Wiberg, P. 1996. Sedimentation and boundary changes of Virginia salt marshes. Estuarine, Coastal, and Shelf Science 42: 683-700.

Kattenberg, A., F. Giorgi, H. Grassl, G.A. Meehl, J.F.B. Mitchell, R.J. Stouffer, T. Tokioka, A.J. Weaver, and T.M.L. Wigley. 1995. Climate Models-Projections of future climate. Chapter 6 in *Climate Change 1995: Contribution of Working Group I to the second assessment report of the Intergovernmental Panel on Climate Change*. (J.T. Houghton, L.G. Meira Filho, B.A. Callander, N. Harris, A. Kattenberg, K. Maskell, eds). 572 pp.

Katz, L. C. 1980. Effects of burrowing by the fiddler crab, *Uca pugnax*. Estuarine and Coastal Marine Science 11: 233-237.

Letzsch, W. S., and Frey, R. W. 1980a. Deposition and erosion in a holocene salt marsh, Sapelo Island, Georgia. Journal of Sediment Petrology 50: 529-542.

Letzsch, W. S., and Frey, R. W. 1980b. Erosion of salt marsh creek banks, Sapelo Island, Georgia. Senckenbergiana Maritima 12: 201-215.

Loomis, K. E. 1999. Local geomorphological controls on hydrology, pore water chemistry and *Spartina alterniflora* morphology in a Virginia barrier island salt marsh. MS Thesis, Univ. of Virginia, Charlottesville, VA, 161 pp.

Nerem, R., van Dam, T. and Schenewerk, M. 1998. Chesapeake Bay subsidence monitored as wetland loss continues. EOS 79: 156-157.

Nixon, S. W. 1980. Between coastal marshes and coastal waters- a review of twenty years of speculation and research on the role of salt marshes in estuarine productivity and water chemistry. In *Estuarine Wetland Processes*. (Hamilton, P. and McDonald, K. B., eds). Plenum Press, New York. pp 437-525.

Nuttle, W. K. 1988. The extent of lateral water movement in the sediments of a New England salt marsh. Water Resources Research 24: 2077-2085.

Nuttle, W. K., and Hemond, H. F. 1988. Salt marsh hydrology: implications for biogeochemical fluxes to the atmosphere and estuaries. Global Biogeochemical Cycles 2: 91-114.

Nuttle, W. K., and Portnoy, J. W. 1992. The effect of rising sea-level on runoff and groundwater discharge to coastal ecosystems. Estuarine Coastal and Shelf Science: 34: 203-212.

Nuttle, W. K., and Harvey, J. W. 1995. Fluxes of water and solute in a coastal wetland sediment. 1. The contribution of regional groundwater discharge. Journal of Hydrology 164: 89-107.

Oertel, G. F., Wong, G. F. T., and Conway, G. F. 1989. Sediment accumulation at a fringe marsh during transgression, Oyster, Virginia. Estuaries 12: 18-26.

Pethick, J. S. 1981. Long-term accretion rates on tidal salt marshes. Journal of Sedimentary Petrology 51: 571-577.

Pethick, J. S. 1984. An introduction to Coastal Geomorphology. Edward Arnold Publishers, London. 260 pp.

Pethick, J. S. 1992. Saltmarsh geomorphology. Chapter 3 in *Saltmarshes: morphodynamics, conservation, and engineering significance.* (Allen, J. R. L. and Pye, K., eds.) Cambridge Univ. Press, Cambridge, Great Britain. 184 pp.

Porter, J. H., Krovetz, D. O., Spitler, J., and Nuttle, W. 2001. Meteorological data, Virginia Coast Reserve LTER data set.

Priestly, C. H. B., and Taylor, R. J. 1972. On the assessment of surface heat flux and evaporation using large-scale parameters. Monthly Weather Review 100: 81-92.

Robinson, S. E. 1994. Clay mineralogy and sediment texture of environments in a barrier island – lagoon system. MS thesis, Univ. of Virginia, Charlottesville, VA, 102 pp.

Shea, M. L., Warren, R. S. and Niering, W. A. 1975. Biochemical and transplantation studies of the growth form of *Spartina alterniflora* on Connecticut salt marshes. Ecology 56: 461-466.

Smith, D. D. and Wischmeier, W. H. 1962. Rainfall erosion. Advances in Agronomy 14: 109-148.

Stasavich, L. E. 1998. Hydrodynamics of a coastal wetland ecosystem. MS Thesis. East Carolina Univ., Greenville, NC. 68 pp.

Stevenson, J. C. , Kearney, M. S. and Pendelton, E. C. 1985. Sedimentation and erosion in a Chesapeake Bay brackish marsh system. Marine Geology 67: 213-235.

Tan, K. 1996. Soil sampling, preparation, and analysis. Marcel Dekker, Inc. New York. 408 pp.

Tirrell, R. L. 1995. Response of sediment microbial community to *Spartina alterniflora* roots in a Virginia salt marsh. MS thesis, Univ. of Virginia, Charlottesville, VA, 161 pp.

Tolley, P. M. and Christian, R. R. 1999. Effects of increased inundation and wrack deposition on a high salt marsh plant community. Estuaries 22: 944-954.

Valiela, J., Teal, M. J. and Deuser, W. G. 1978. The nature of growth forms in the salt marsh grass *Spartina alterniflora*. American Naturalist 112: 461-470.

Wiegert, R. G., Chalmers, A. G., and Randerson, P. F. 1983. Productivity gradients in salt marshes: the response of *Spartina alterniflora* to experimentally manipulated soil water movement. Oikos 41: 1-6.

Wray, R. D., Leatherman, S. P. and Nicholls, R. J. 1995. Historic and future land loss for upland and marsh islands in the Cheaspeake Bay, Maryland, USA. Journal of Coastal Research. 11: 1195-1203.

Yelverton, G. F. and Hackney, C. T. 1986. Flux of dissolved organic carbon and pore water through the substrate of a *Spartina alterniflora* marsh in North Carolina. Estuarine, Coastal, and Shelf Science 22: 255-267.

Appendix 1. Method for removing soil cores from the marsh.

A copper pipe and wooden dowel were used to remove soil cores from the marsh. The inside diameter of the pipe was one inch, and the diameter of the dowel was only slightly less. A metal file was used to make teeth in the end of the pipe, making it easier to cut into the mat of roots in the soil. The pipe was slowly rotated and pushed into the ground to a depth of 5-10 cm (depending on how easily the soil compacted).

For cores within the compaction limit, the pipe was removed after moving it back and forth to a 30 or 45^{o} angle from the vertical to break the core at the bottom of the pipe. Soil cores compacted more than 10% were left in the ground. Each core was pushed slowly out of the pipe with the dowel onto a plastic tray. Roots were trimmed with a serrated knife to make the end of the core even, and the core was cut into 5 cm sections. Not all cores were 10 cm in length, due to inability to remove soil at depths when the soil was too easily compacted. The final length of the core was measured and recorded, as well as the depth (eg, 5 cm length, 0-5 cm depth; and 3 cm length, 5-8 cm depth). Initial attempts were to take 20 cm cores, but it was soon discovered to be too difficult to maintain a known volume of soil for a core this length.

Soil cores were sealed in plastic bags individually, and individuals for a given time interval were sealed in a larger bag. A rubber glove was worn to handle the cores to prevent absorbing water from the core into the skin. To minimize water loss in the field, samples were stored on a tray in a cooler with ice, and the cooler was placed in the shade. Samples were stored in a refrigerator in the lab until processed. Plastic bags were labeled in advance to minimize the time of exposure of the core. Because many cores were taken over time, each hole was filled with sand to minimize disturbance to the normal infiltration and drying regime. Replicates of all samples were taken.

Appendix 2. Water table measurements, modeled water table elevation, tidal elevation, calculated potential evapotranspiration, and precipitation.

Key:

All water table elevations (cm, MSL) were plotted with a vertical range of 70 cm, and the specific range was consistent at each location. For example, water table elevations 39 m from the creek were always shown from 40-110 cm. Model results used logger data for tidal inputs and were plotted along with the measured water table elevations.

Tidal elevations at the study site (cm, MSL) were converted from Wachapreague tide data.

Potential evapotranspiration and precipitation were plotted together, with PET in mm hr^{-1} and precipitation in cm hr^{-1}. The scale for these data cut-off values for precipitation at 2.0 cm. Values exceeding 2 cm were inserted as text.

Water table data inventory

Distance from creek (m)			20	27	31	35	39	43	49	60	70
Surface elevation (cm, MSL)			38	64	74	78	79	81	79	118	152
Start Date	Stop Date	Julian Days									
07/23/99	08/04/99	204-216	**X**								
08/12/99	09/11/99	224-254					**X**	**X**	**X**		
09/11/99	09/25/99	254-268				**X**	**X**	**X**			
10/31/99	01/22/00	304-022	**X**							**X**	**X**
04/27/00	07/24/00	117-206			**X**			**X**			
07/24/00	09/09/00	206-252				**X**	**X**				
09/09/00	11/15/00	253-320					**X**				

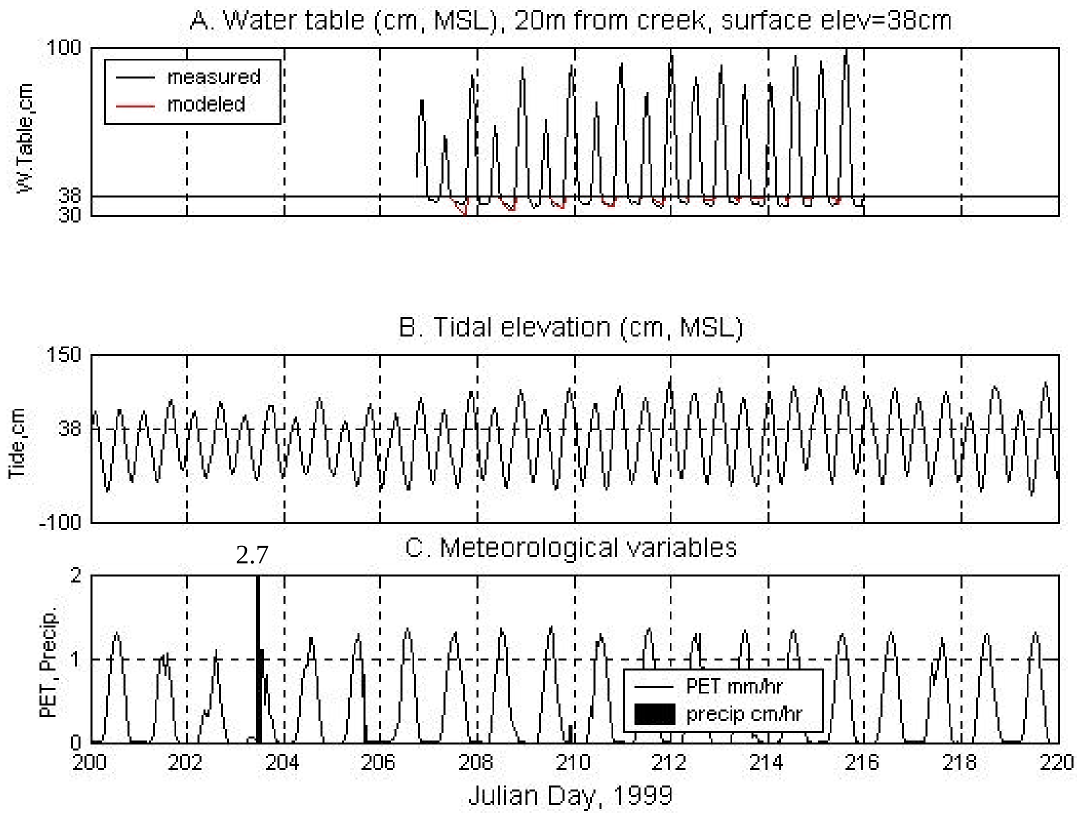
A. Water table (cm, MSL), 20m from creek, surface elev=38cm
W.Table,cm
100
38
30
measured
modeled
B. Tidal elevation (cm, MSL)
Tide,cm
150
38
-100
C. Meteorological variables
2.7
PET, Precip.
2
1
0
PET mm/hr
precip cm/hr
200
202
204
206
208
210
212
214
216
218
220
Julian Day, 1999

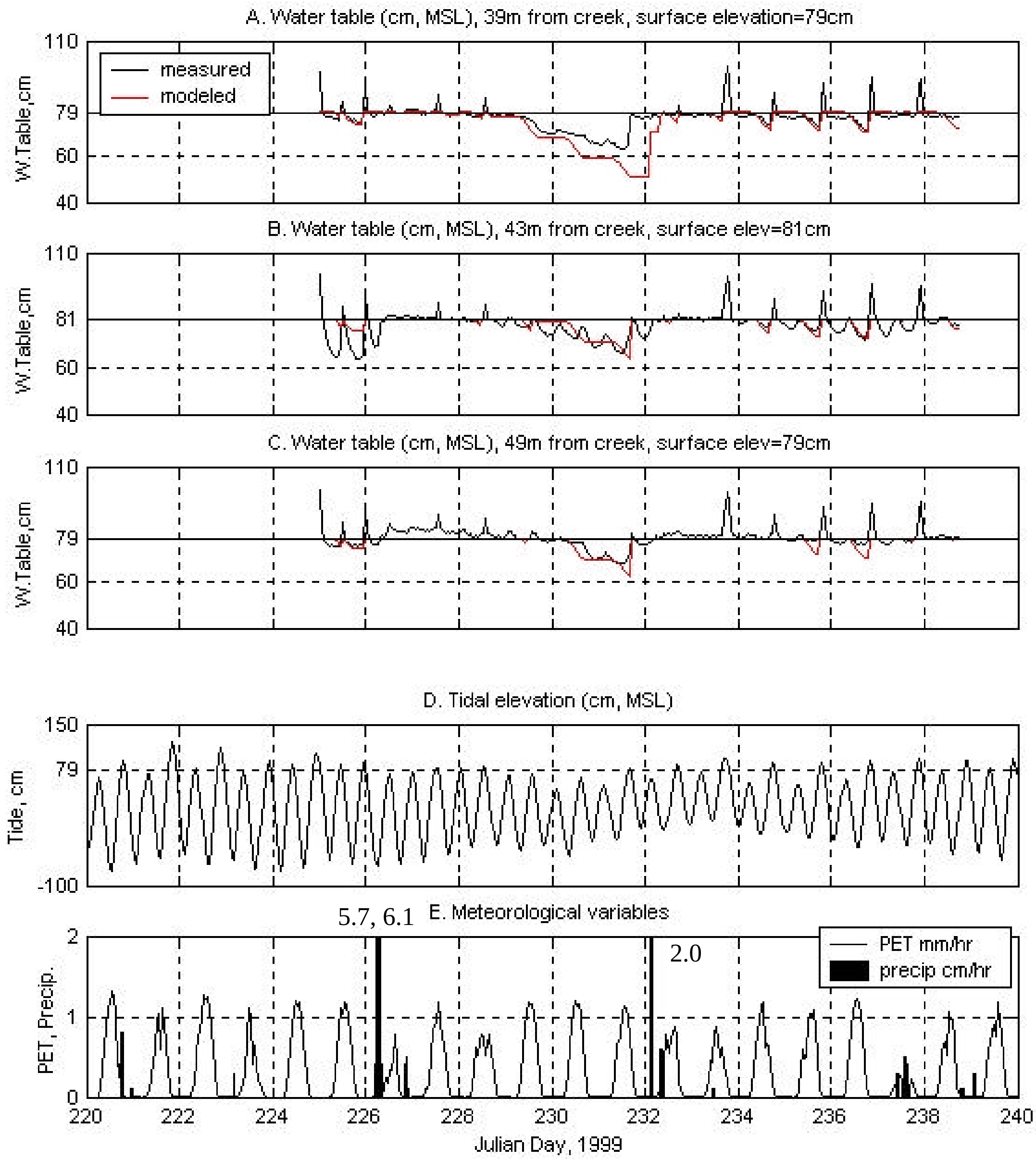
A. Water table (cm, MSL), 39m from creek, surface elevation=79cm
W.Table,cm
measured
modeled
B. Water table (cm, MSL), 43m from creek, surface elev=81cm
C. Water table (cm, MSL), 49m from creek, surface elev=79cm
D. Tidal elevation (cm, MSL)
Tide, cm
5.7, 6.1
E. Meteorological variables
2.0
PET mm/hr
precip cm/hr
PET, Precip.
Julian Day, 1999

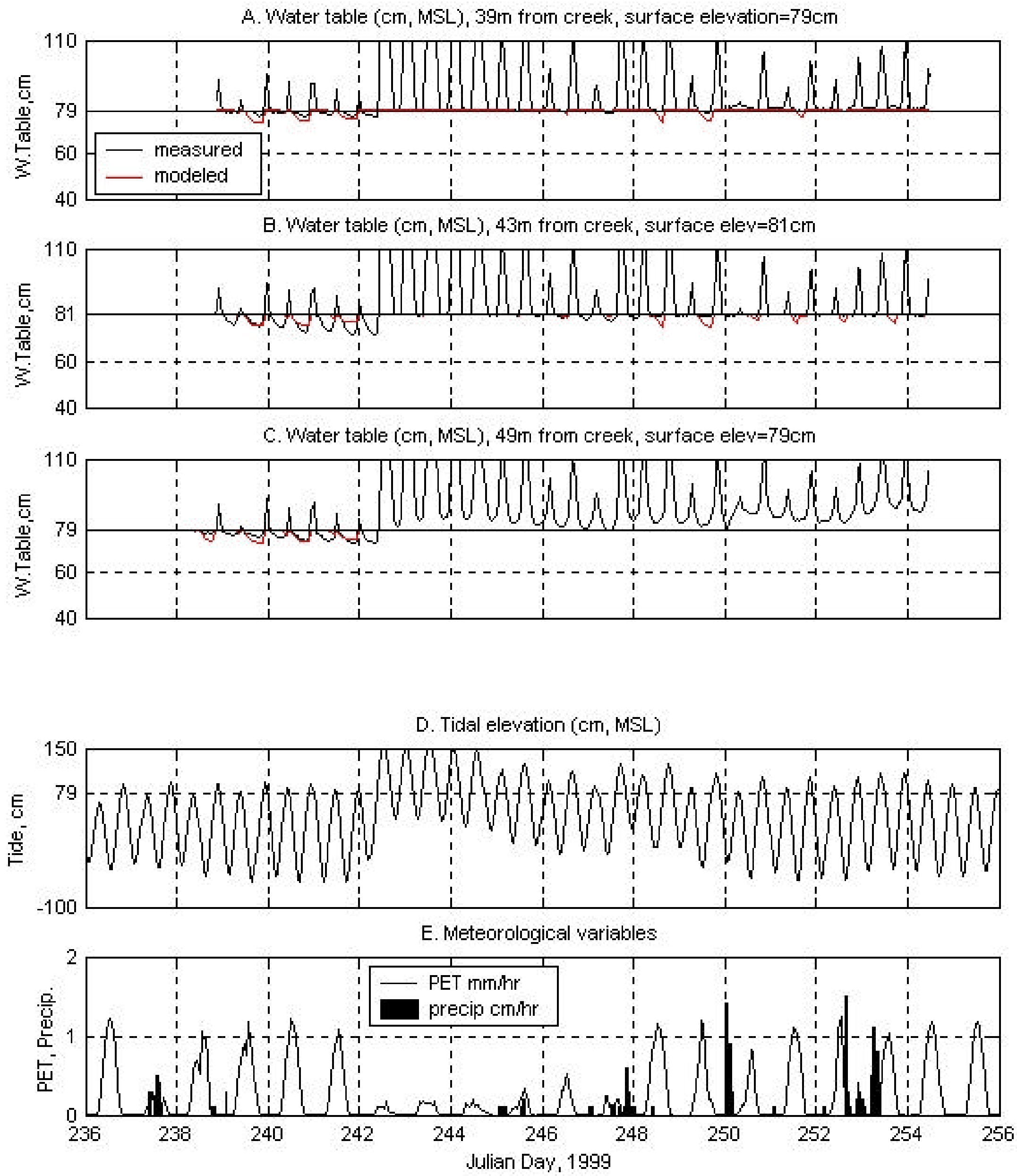
A. Water table (cm, MSL), 39m from creek, surface elevation=79cm
B. Water table (cm, MSL), 43m from creek, surface elev=81cm
C. Water table (cm, MSL), 49m from creek, surface elev=79cm
W.Table,cm
measured
modeled
110
79
81
60
40
D. Tidal elevation (cm, MSL)
Tide, cm
150
79
-100
E. Meteorological variables
PET, Precip.
PET mm/hr
precip cm/hr
2
1
0
236
238
240
242
244
246
248
250
252
254
256
Julian Day, 1999

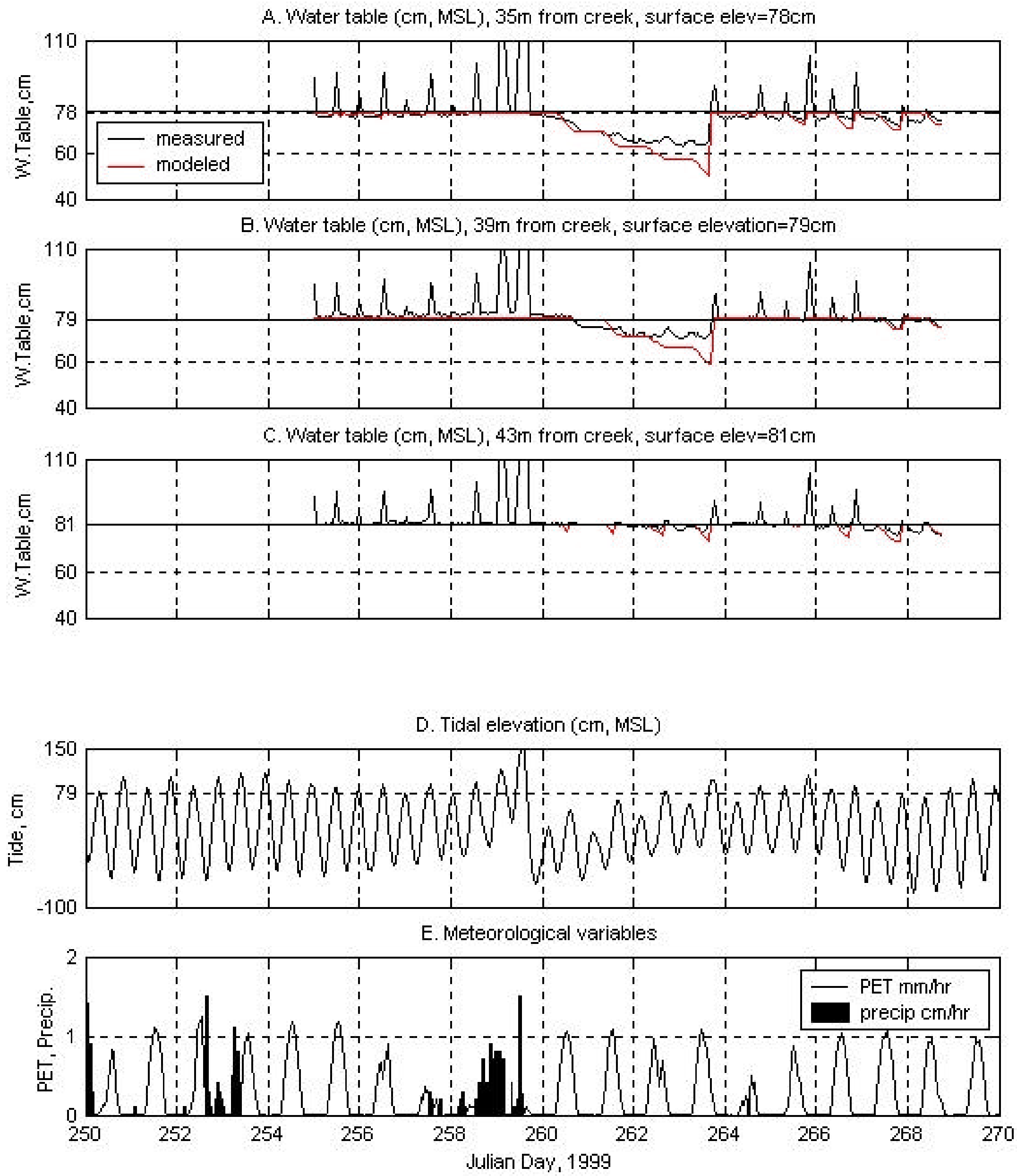

A. Water table (cm, MSL), 35m from creek, surface elev=78cm
W.Table,cm
110
78
60
40
measured
modeled
B. Water table (cm, MSL), 39m from creek, surface elevation=79cm
W.Table,cm
110
79
60
40
C. Water table (cm, MSL), 43m from creek, surface elev=81cm
W.Table,cm
110
81
60
40
D. Tidal elevation (cm, MSL)
Tide, cm
150
79
-100
E. Meteorological variables
PET, Precip.
2
1
0
PET mm/hr
precip cm/hr
250
252
254
256
258
260
262
264
266
268
270
Julian Day, 1999

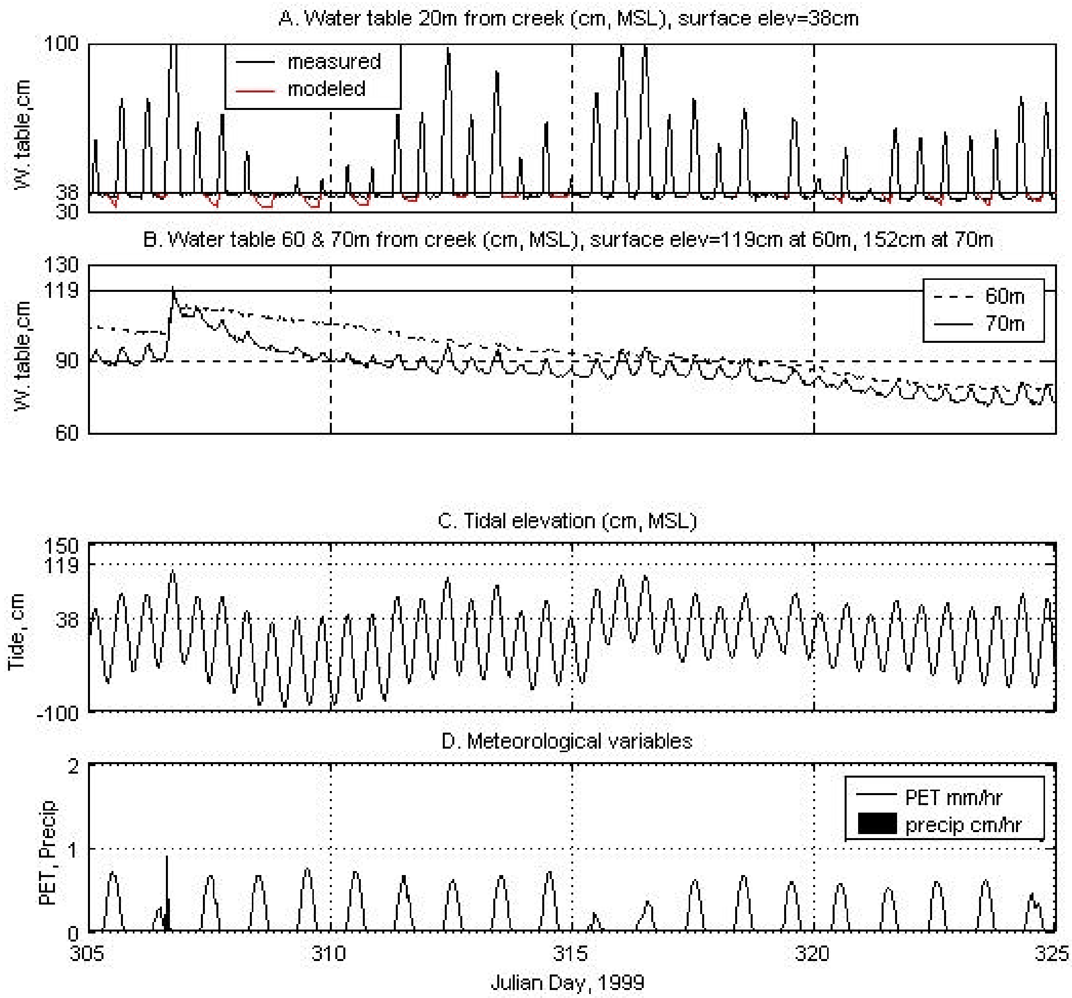
A. Water table 20m from creek (cm, MSL), surface elev=38cm
W. table,cm
100
38
30
measured
modeled
B. Water table 60 & 70m from creek (cm, MSL), surface elev=119cm at 60m, 152cm at 70m
W. table,cm
130
119
90
60
60m
70m
C. Tidal elevation (cm, MSL)
Tide, cm
150
119
38
-100
D. Meteorological variables
PET, Precip
2
1
0
PET mm/hr
precip cm/hr
305
310
315
320
325
Julian Day, 1999

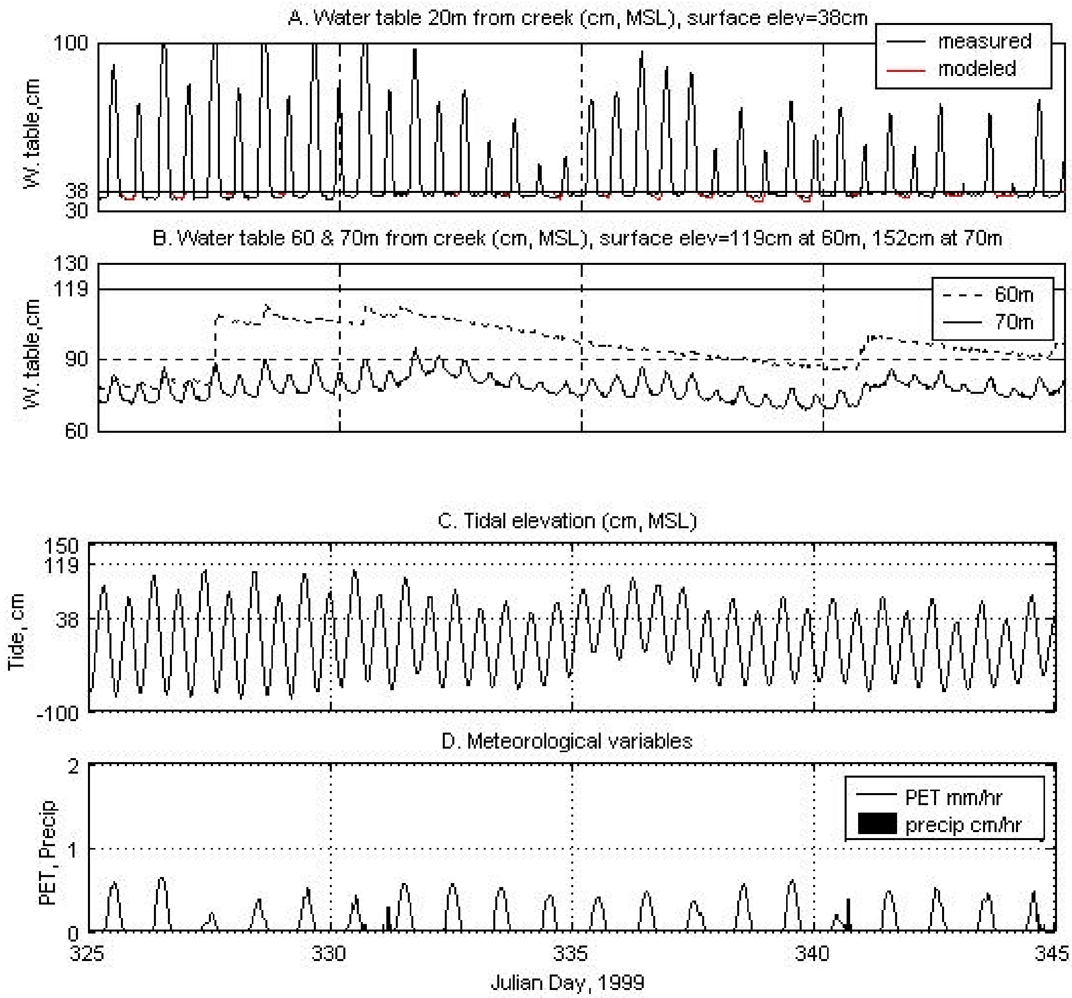
A. Water table 20m from creek (cm, MSL), surface elev=38cm
W. table,cm
100
38
30
measured
modeled
B. Water table 60 & 70m from creek (cm, MSL), surface elev=119cm at 60m, 152cm at 70m
W. table,cm
130
119
90
60
60m
70m
C. Tidal elevation (cm, MSL)
Tide, cm
150
119
38
-100
D. Meteorological variables
PET, Precip
2
1
0
PET mm/hr
precip cm/hr
325
330
335
340
345
Julian Day, 1999

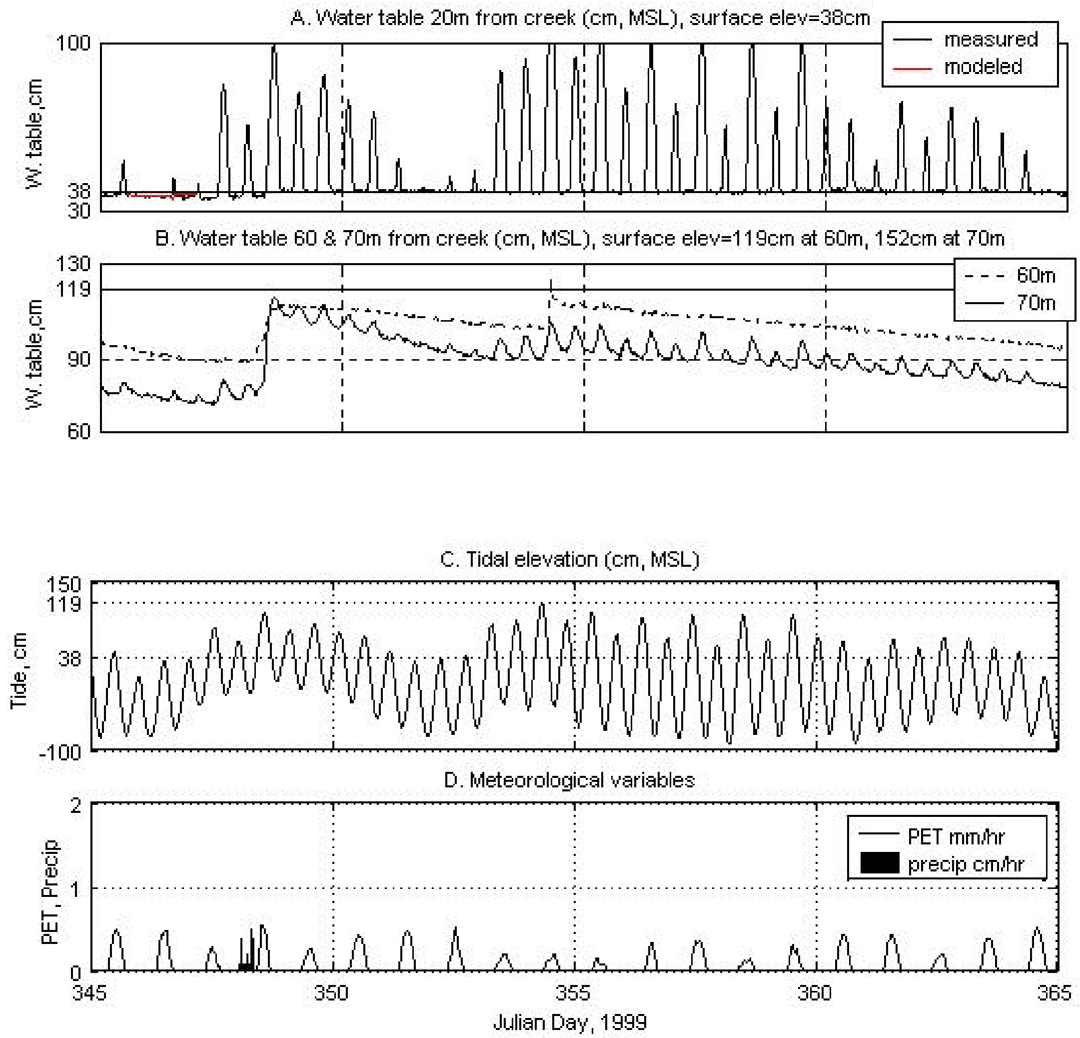

A. Water table 20m from creek (cm, MSL), surface elev=38cm
W. table,cm
100
38
30
measured
modeled
B. Water table 60 & 70m from creek (cm, MSL), surface elev=119cm at 60m, 152cm at 70m
W. table,cm
130
119
90
60
60m
70m
C. Tidal elevation (cm, MSL)
Tide, cm
150
119
38
-100
D. Meteorological variables
PET, Precip
2
1
0
PET mm/hr
precip cm/hr
345
350
355
360
365
Julian Day, 1999

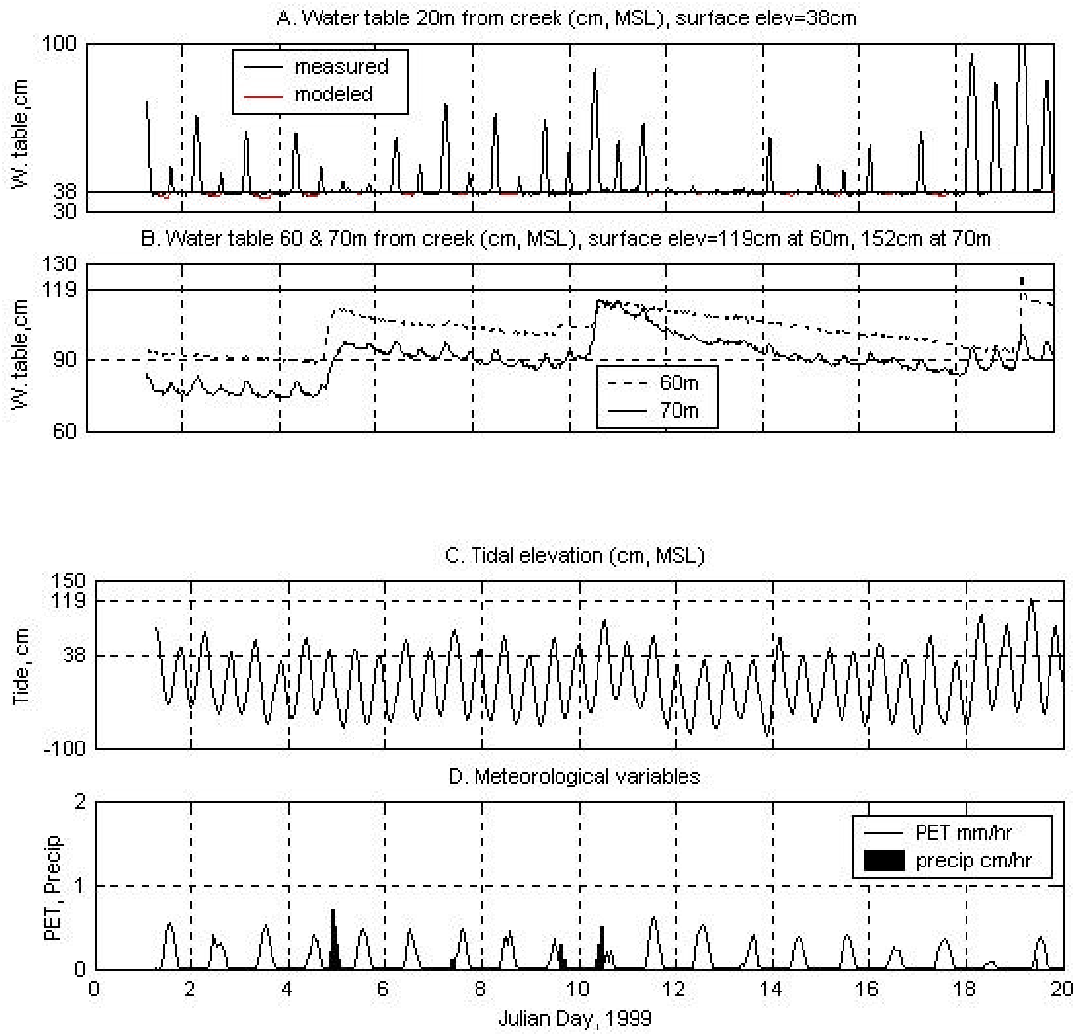
A. Water table 20m from creek (cm, MSL), surface elev=38cm
W. table,cm
100
38
30
measured
modeled
B. Water table 60 & 70m from creek (cm, MSL), surface elev=119cm at 60m, 152cm at 70m
W. table,cm
130
119
90
60
60m
70m
C. Tidal elevation (cm, MSL)
Tide, cm
150
119
38
-100
D. Meteorological variables
PET, Precip
2
1
0
PET mm/hr
precip cm/hr
0 2 4 6 8 10 12 14 16 18 20
Julian Day, 1999

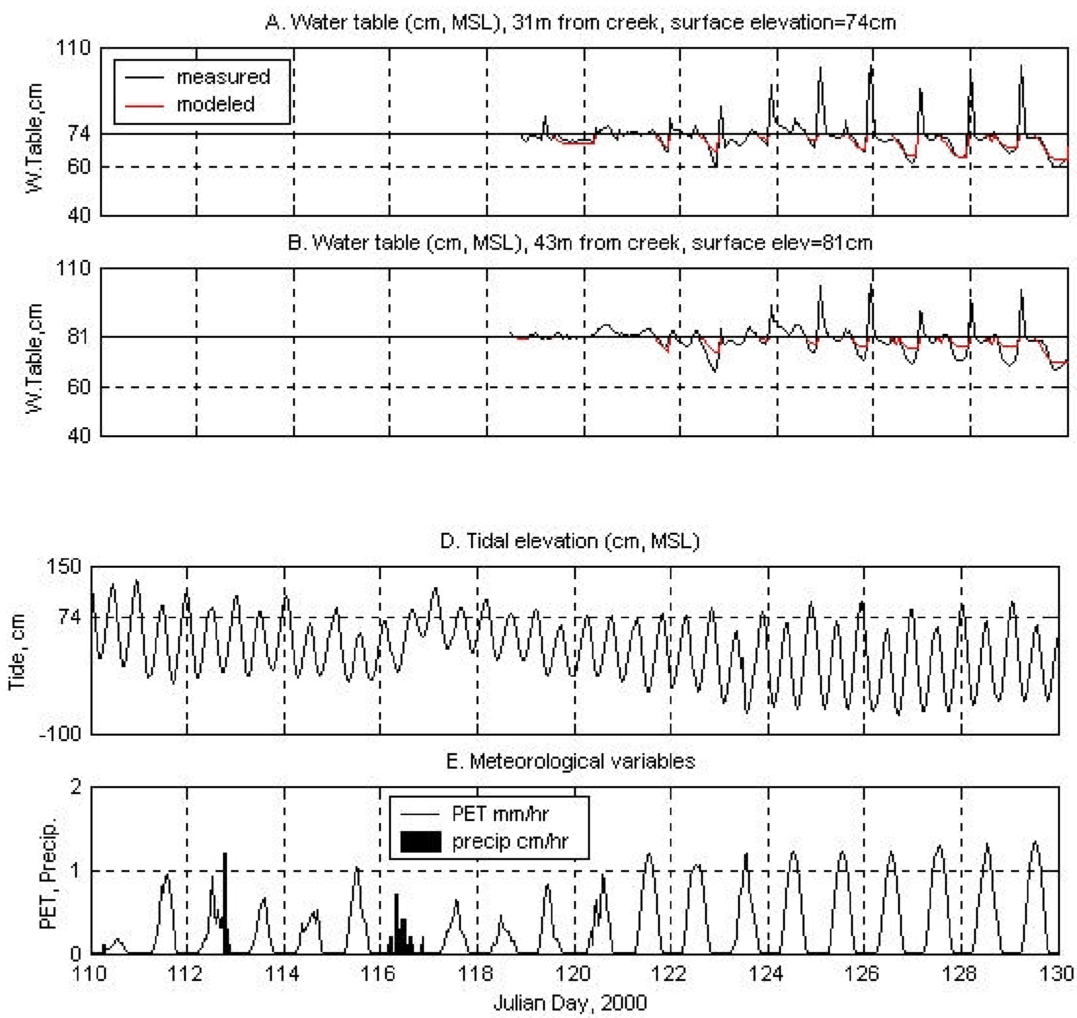
A. Water table (cm, MSL), 31m from creek, surface elevation=74cm
110
74
60
40
W.Table,cm
measured
modeled
B. Water table (cm, MSL), 43m from creek, surface elev=81cm
110
81
60
40
W.Table,cm
D. Tidal elevation (cm, MSL)
150
74
-100
Tide, cm
E. Meteorological variables
2
1
0
PET, Precip.
PET mm/hr
precip cm/hr
110
112
114
116
118
120
122
124
126
128
130
Julian Day, 2000

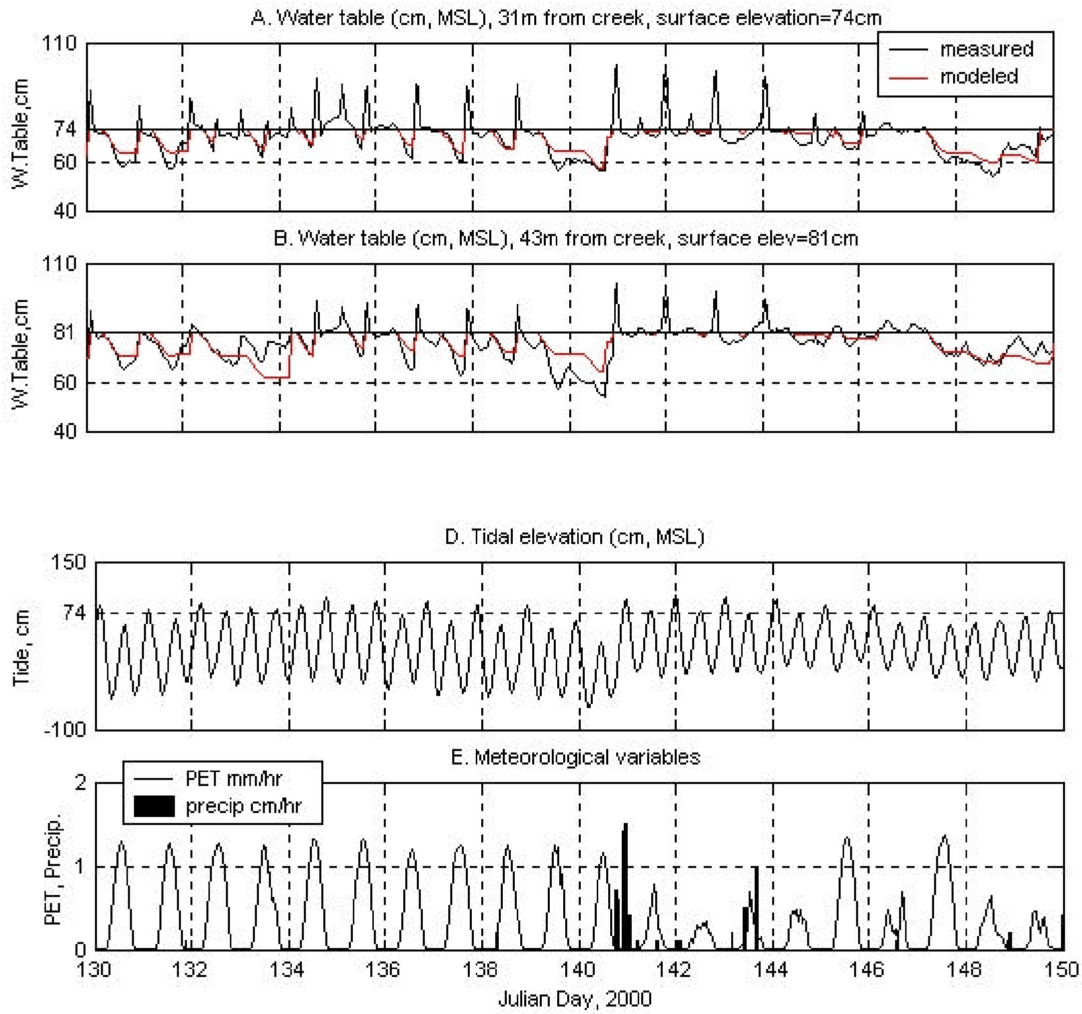
A. Water table (cm, MSL), 31m from creek, surface elevation=74cm
measured
modeled
W.Table,cm
110
74
60
40
B. Water table (cm, MSL), 43m from creek, surface elev=81cm
W.Table,cm
110
81
60
40
D. Tidal elevation (cm, MSL)
Tide, cm
150
74
-100
E. Meteorological variables
PET mm/hr
precip cm/hr
PET, Precip.
2
1
0
130
132
134
136
138
140
142
144
146
148
150
Julian Day, 2000

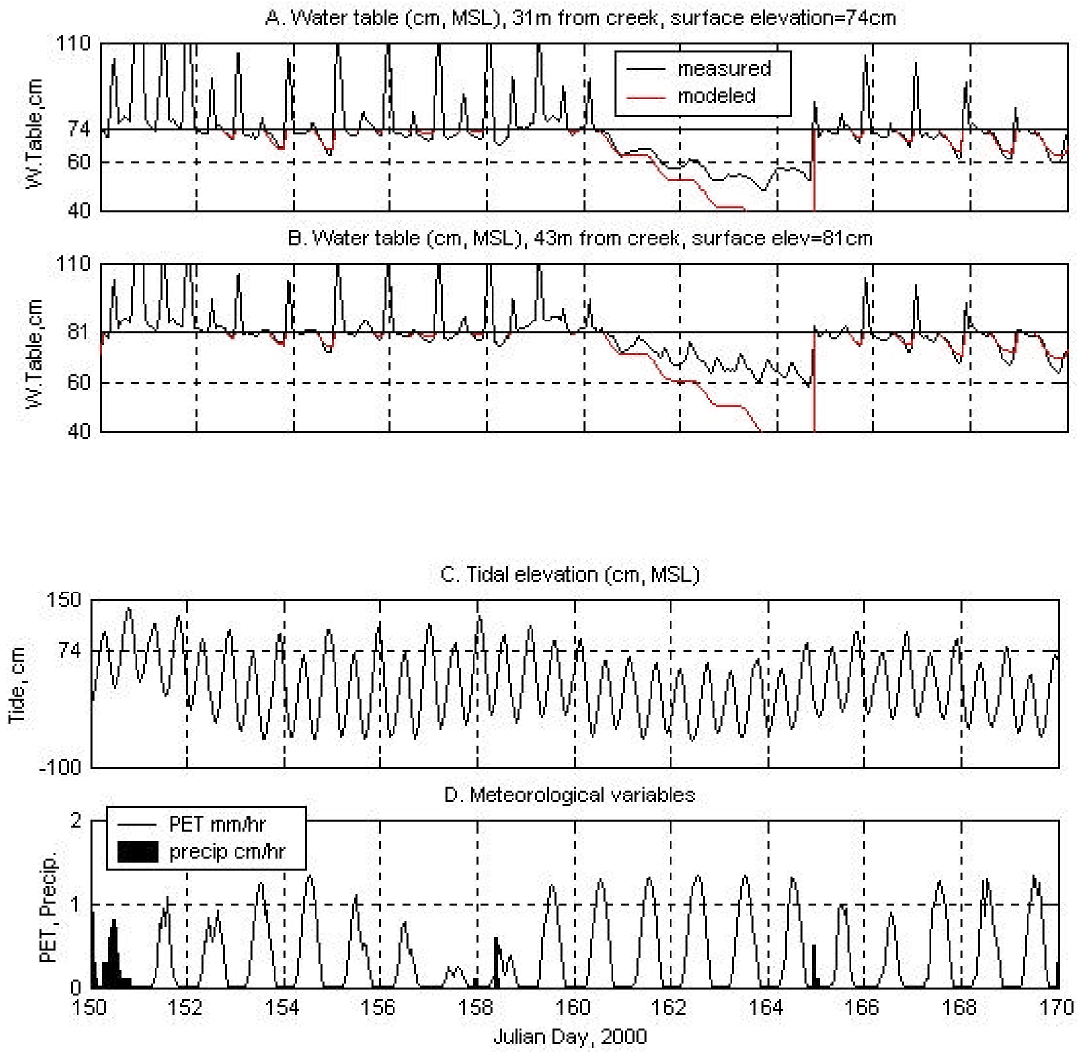
A. Water table (cm, MSL), 31m from creek, surface elevation=74cm
W.Table,cm
110
74
60
40
measured
modeled
B. Water table (cm, MSL), 43m from creek, surface elev=81cm
W.Table,cm
110
81
60
40
C. Tidal elevation (cm, MSL)
Tide, cm
150
74
-100
D. Meteorological variables
PET, Precip.
2
1
0
PET mm/hr
precip cm/hr
150
152
154
156
158
160
162
164
166
168
170
Julian Day, 2000

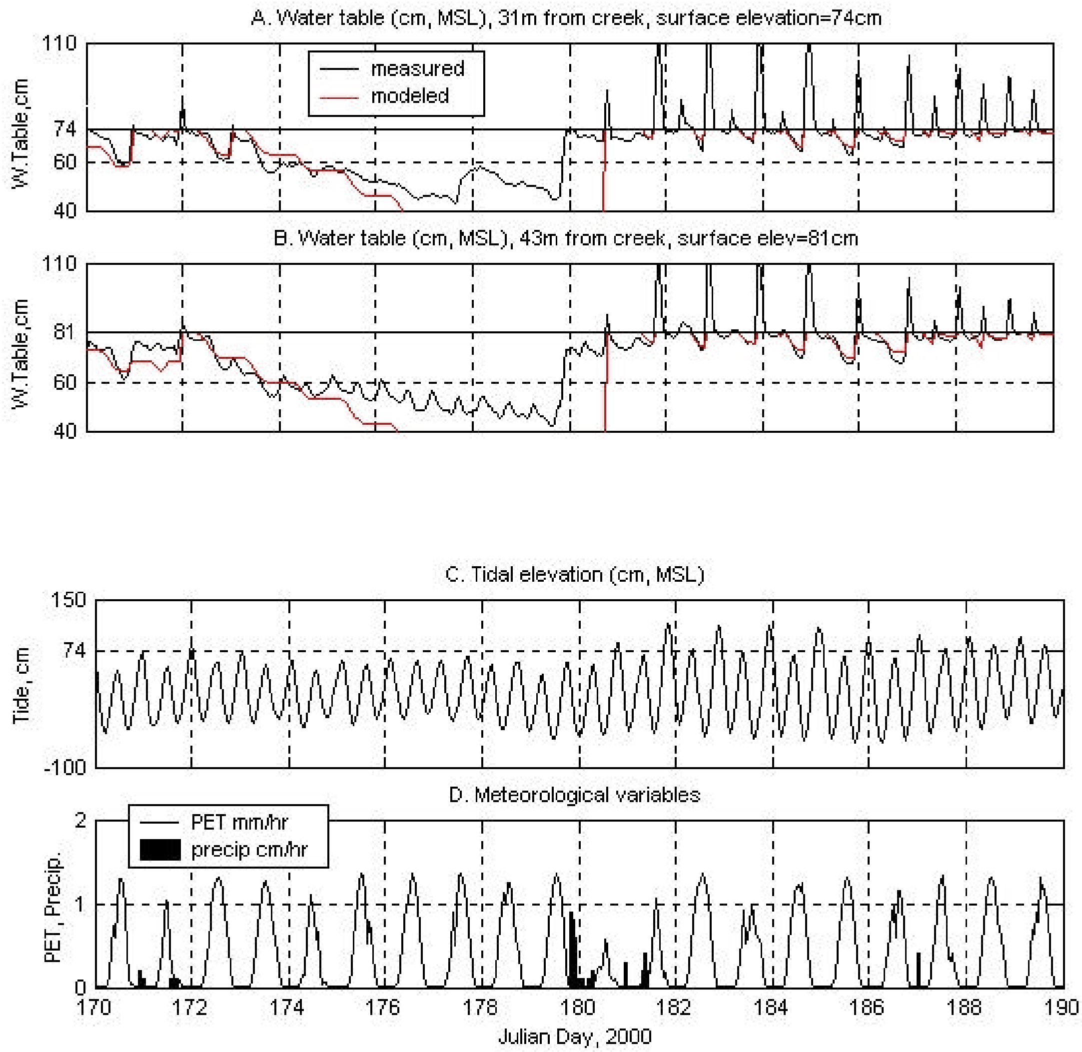
A. Water table (cm, MSL), 31m from creek, surface elevation=74cm
measured
modeled
W.Table,cm
110
74
60
40
B. Water table (cm, MSL), 43m from creek, surface elev=81cm
W.Table,cm
110
81
60
40
C. Tidal elevation (cm, MSL)
Tide, cm
150
74
-100
D. Meteorological variables
PET mm/hr
precip cm/hr
PET, Precip.
2
1
0
170
172
174
176
178
180
182
184
186
188
190
Julian Day, 2000

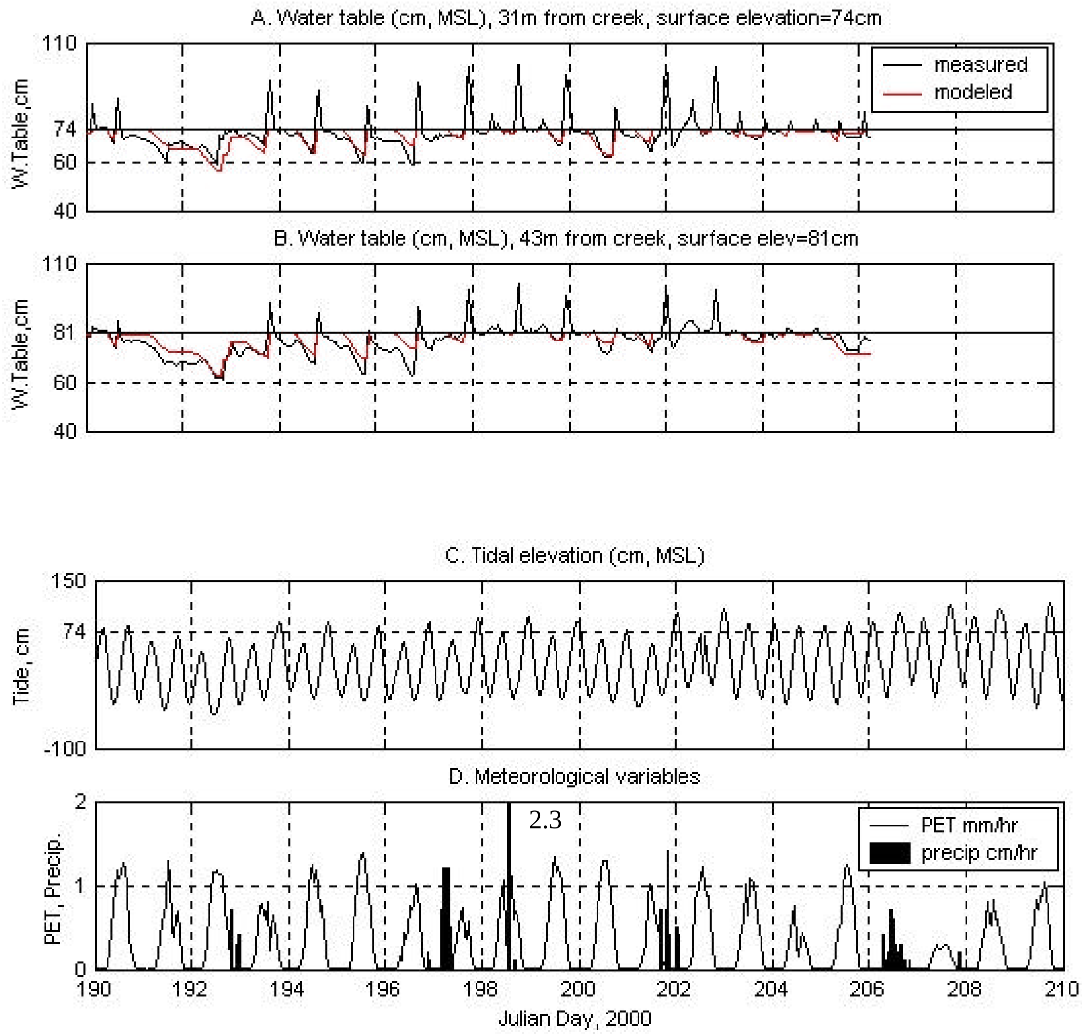
A. Water table (cm, MSL), 31m from creek, surface elevation=74cm
110
74
60
40
W.Table,cm
measured
modeled
B. Water table (cm, MSL), 43m from creek, surface elev=81cm
110
81
60
40
W.Table,cm
C. Tidal elevation (cm, MSL)
150
74
-100
Tide, cm
D. Meteorological variables
2
1
0
PET, Precip.
2.3
PET mm/hr
precip cm/hr
190
192
194
196
198
200
202
204
206
208
210
Julian Day, 2000

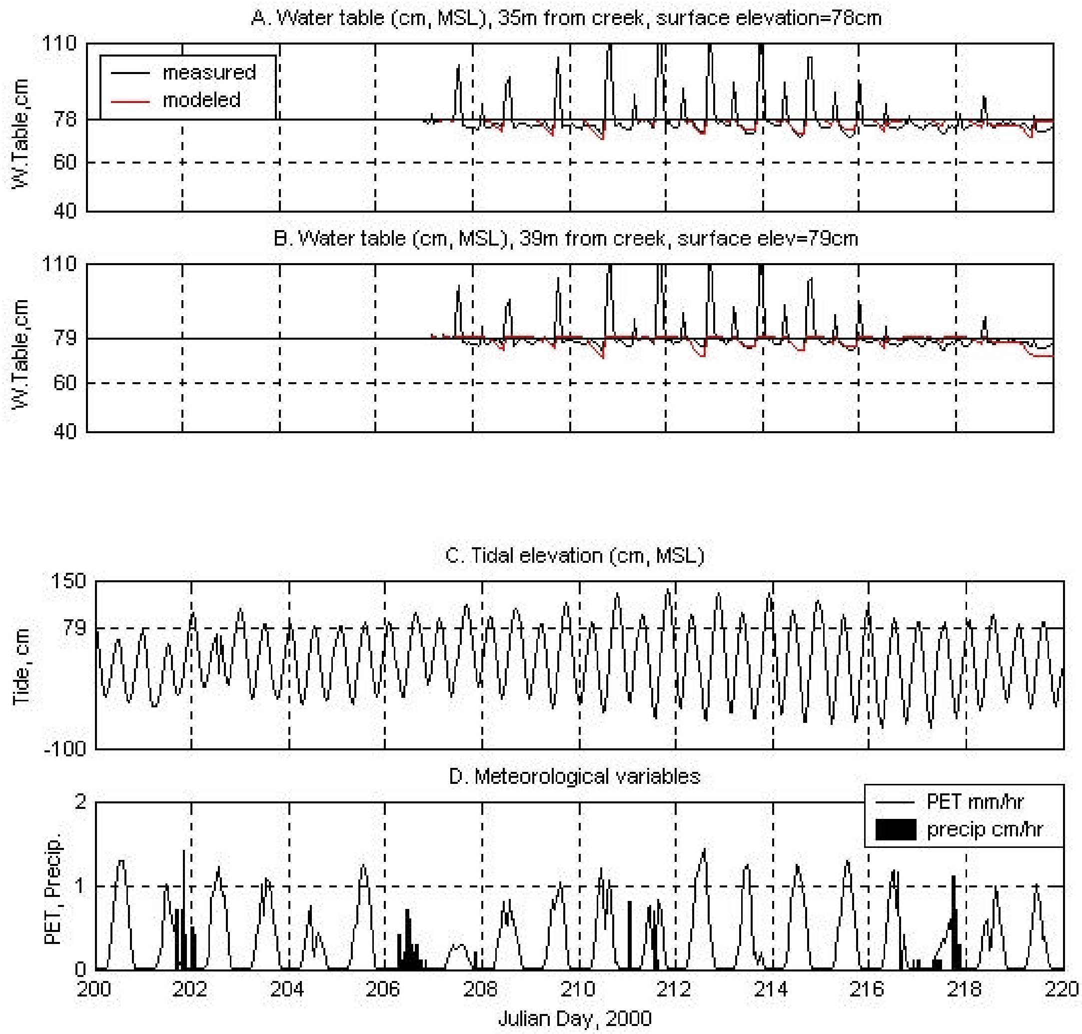
A. Water table (cm, MSL), 35m from creek, surface elevation=78cm
measured
modeled
W.Table,cm
110
78
60
40
B. Water table (cm, MSL), 39m from creek, surface elev=79cm
W.Table,cm
110
79
60
40
C. Tidal elevation (cm, MSL)
Tide, cm
150
79
-100
D. Meteorological variables
PET mm/hr
precip cm/hr
PET, Precip.
2
1
0
200 202 204 206 208 210 212 214 216 218 220
Julian Day, 2000

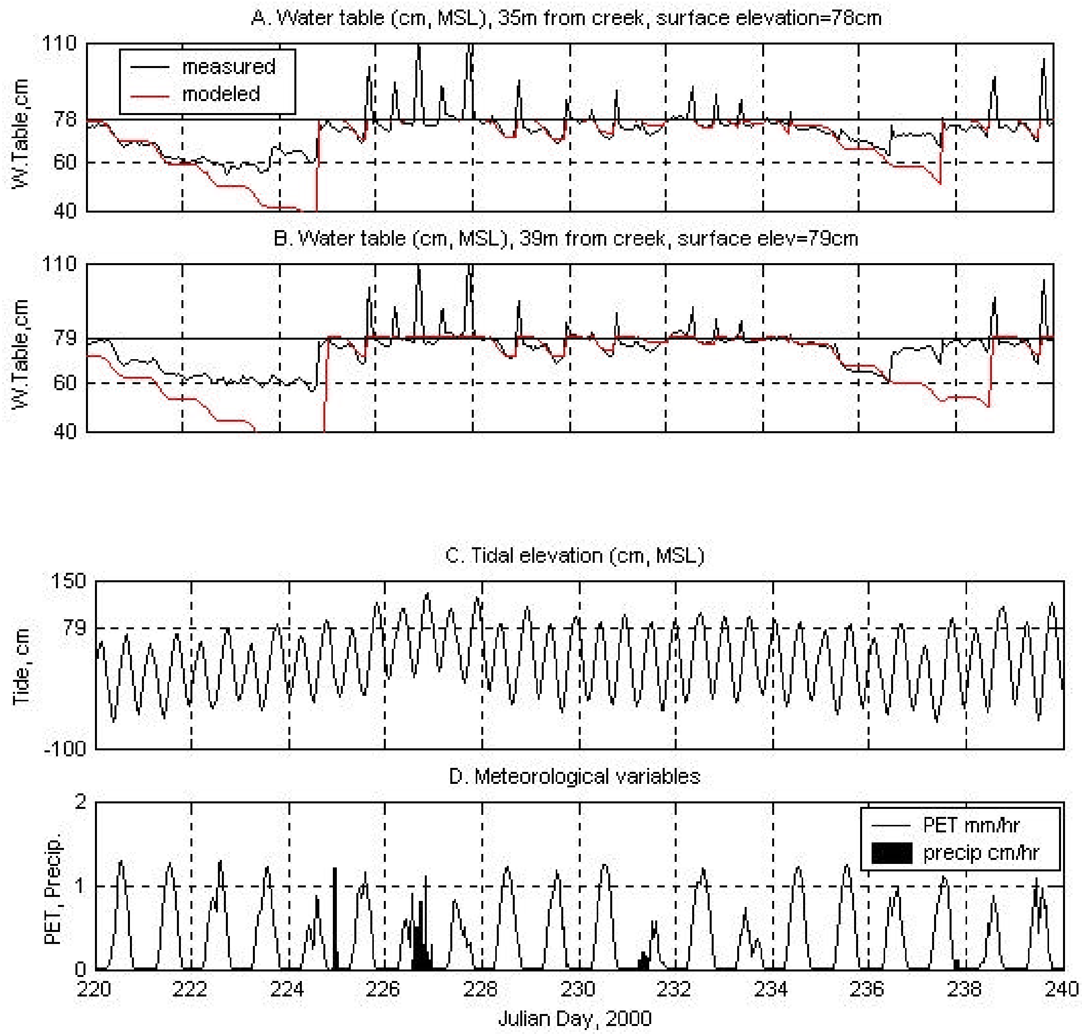
A. Water table (cm, MSL), 35m from creek, surface elevation=78cm
measured
modeled
W.Table,cm
110
78
60
40
B. Water table (cm, MSL), 39m from creek, surface elev=79cm
W.Table,cm
110
79
60
40
C. Tidal elevation (cm, MSL)
Tide, cm
150
79
-100
D. Meteorological variables
PET mm/hr
precip cm/hr
PET, Precip.
2
1
0
220
222
224
226
228
230
232
234
236
238
240
Julian Day, 2000

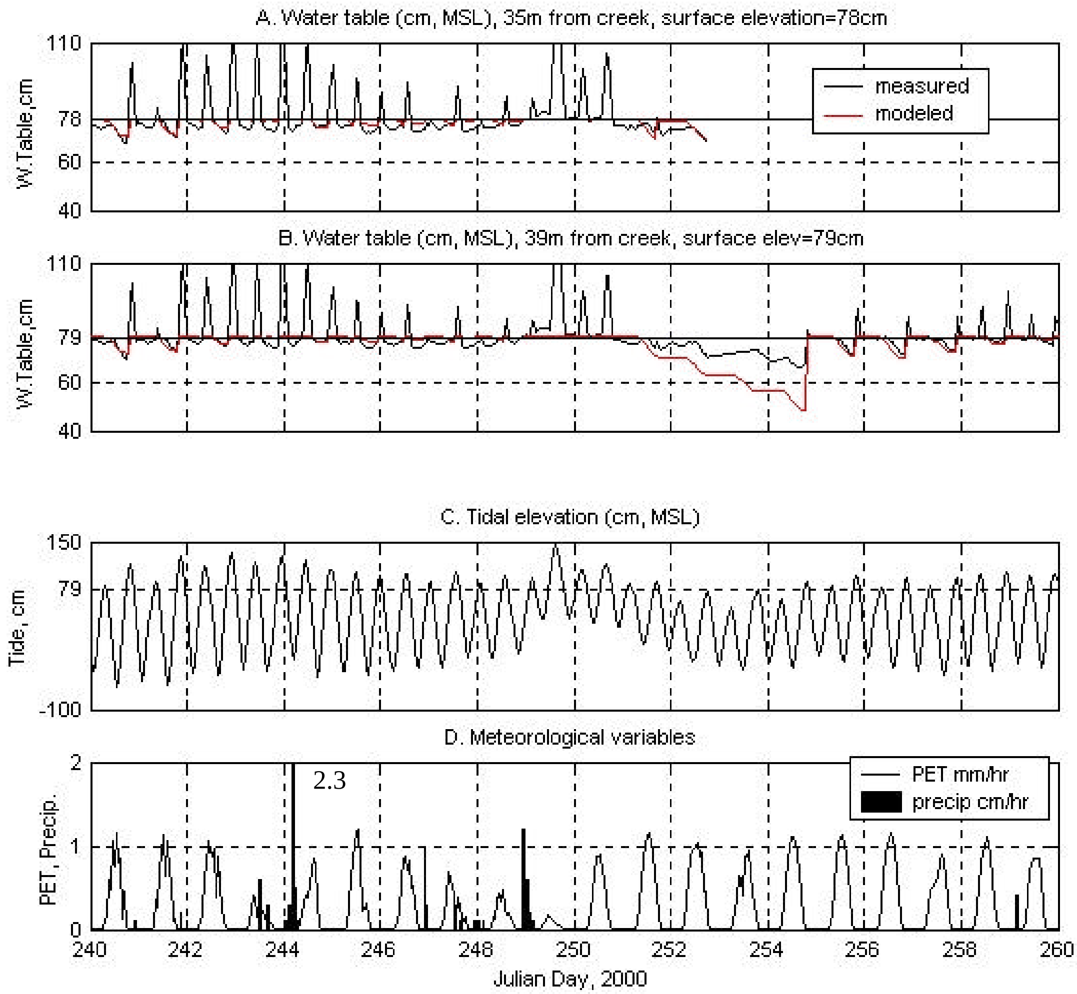
A. Water table (cm, MSL), 35m from creek, surface elevation=78cm
W.Table,cm
measured
modeled
B. Water table (cm, MSL), 39m from creek, surface elev=79cm
W.Table,cm
C. Tidal elevation (cm, MSL)
Tide, cm
D. Meteorological variables
PET, Precip.
2.3
PET mm/hr
precip cm/hr
Julian Day, 2000

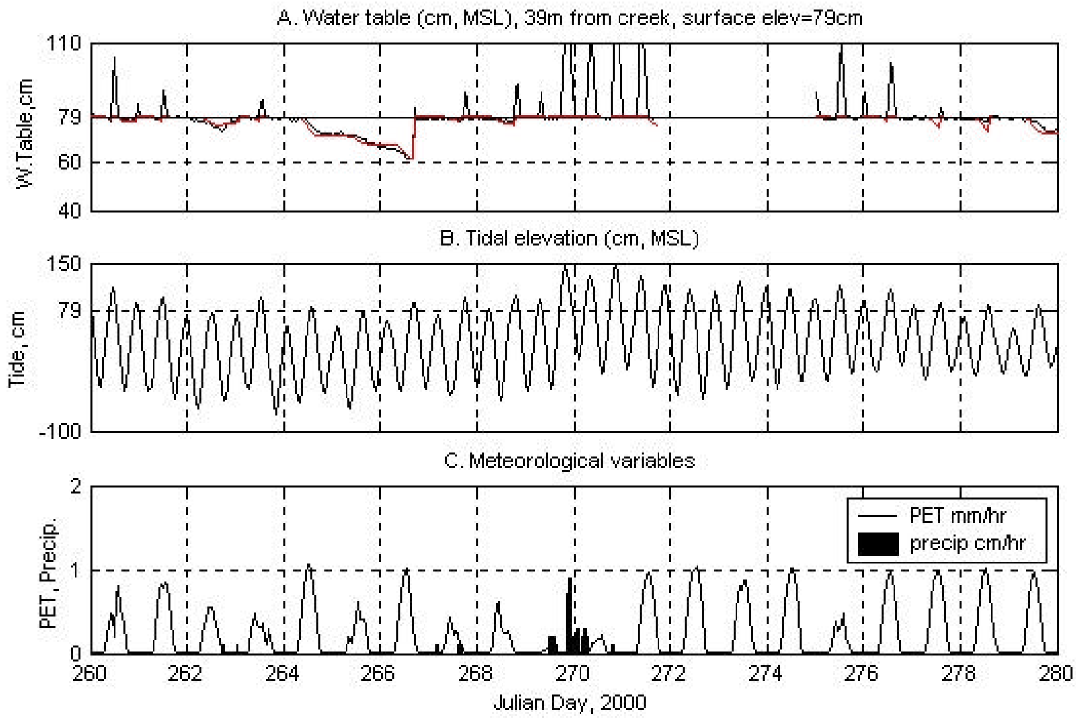
A. Water table (cm, MSL), 39m from creek, surface elev=79cm
W.Table,cm
110
79
60
40
B. Tidal elevation (cm, MSL)
Tide, cm
150
79
-100
C. Meteorological variables
PET, Precip.
2
1
0
PET mm/hr
precip cm/hr
260
262
264
266
268
270
272
274
276
278
280
Julian Day, 2000

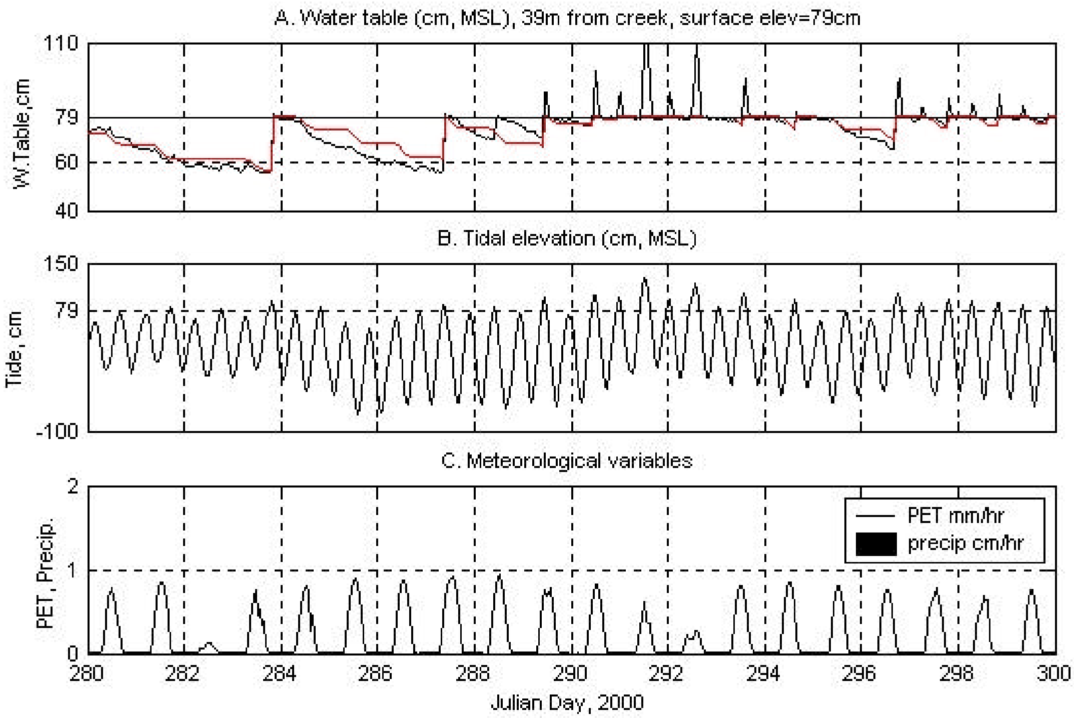
A. Water table (cm, MSL), 39m from creek, surface elev=79cm
W.Table,cm
110
79
60
40
B. Tidal elevation (cm, MSL)
Tide, cm
150
79
-100
C. Meteorological variables
PET, Precip.
2
1
0
PET mm/hr
precip cm/hr
280 282 284 286 288 290 292 294 296 298 300
Julian Day, 2000

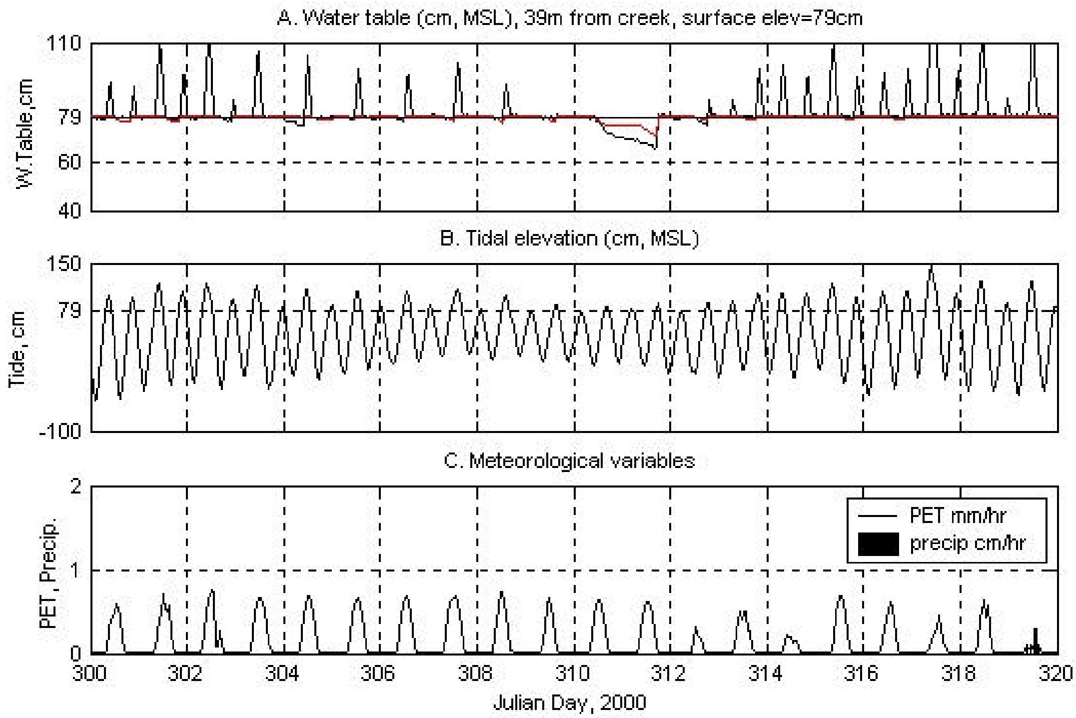
A. Water table (cm, MSL), 39m from creek, surface elev=79cm
W.Table,cm
110
79
60
40
B. Tidal elevation (cm, MSL)
Tide, cm
150
79
-100
C. Meteorological variables
PET, Precip.
2
1
0
PET mm/hr
precip cm/hr
300
302
304
306
308
310
312
314
316
318
320
Julian Day, 2000

Appendix 3. Modeled saturation excess at 80 cm elevation, with associated environmental factors.

Key:

Panel A. Hourly saturation deficit or excess from the water balance model, for 80 cm elevation (MSL) using converted Wachapreague tidal elevations for inundation. The sum of saturation excess in each event was also shown as bars placed at the start of the event. Saturation excess sums greater than 5 cm and hourly saturation deficit less than -5 cm were cut off. In these instances values were inserted as text.

Panel B. Tidal elevations (cm, MSL) at the study site, converted from Wachapreague tidal data.

Panel C. Tide deviations (cm) were the difference between measures and predicted tides. Deviation = (measured) - (predicted), such that a positive deviation indicated a measured tide greater than predicted.

Panel D. Wind speed (m s^{-1}) and direction (0-360 degrees) measured at Phillips Creek Marsh.

Panel E. Barometric pressure (mb) measured at Wachapreague.

Panel F. Precipitation (cm hr^{-1}) measured at Phillips Creek Marsh. Values greater than 2 were cut-off and inserted as text.

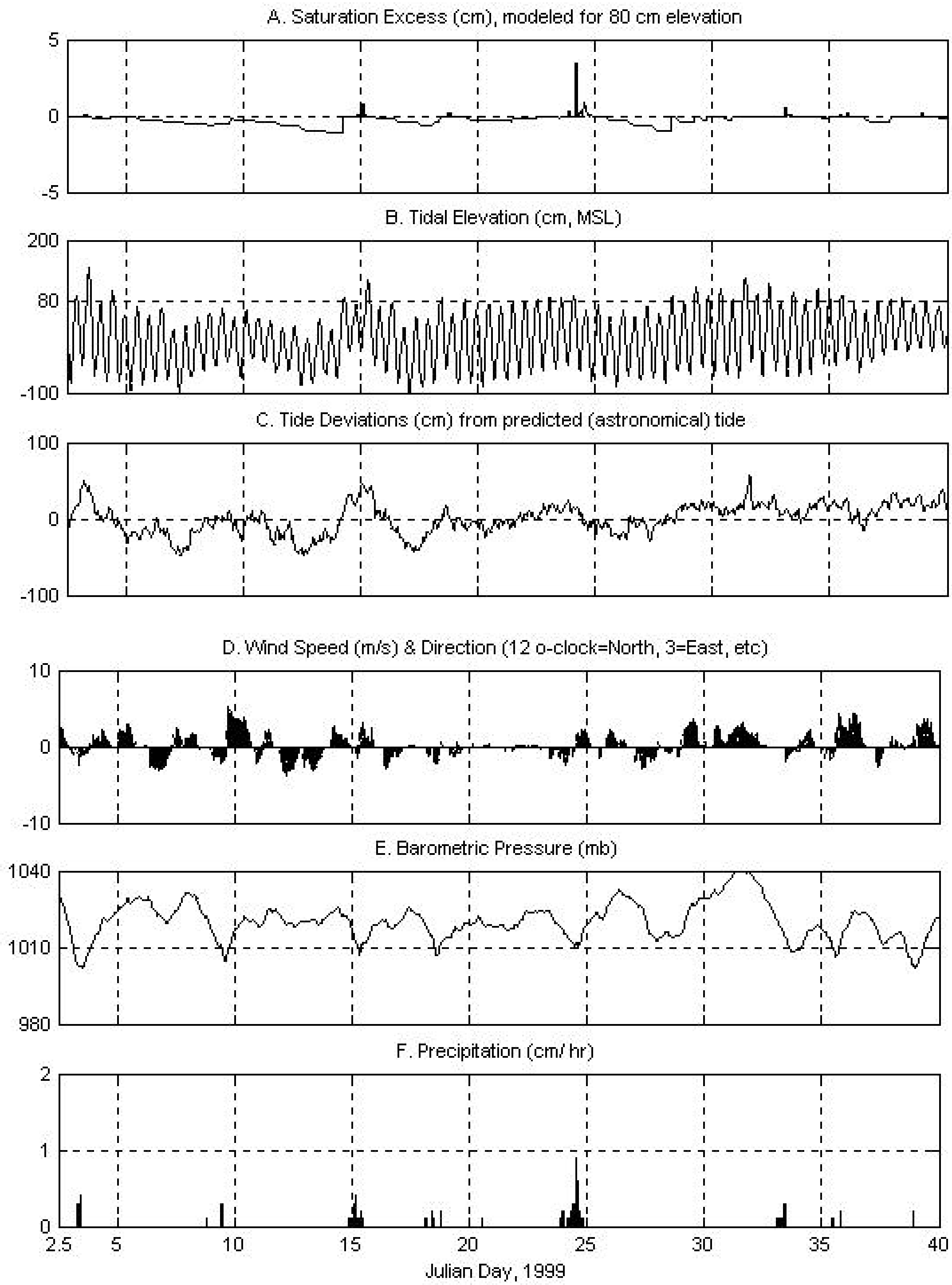
A. Saturation Excess (cm), modeled for 80 cm elevation
5
0
-5
B. Tidal Elevation (cm, MSL)
200
80
-100
C. Tide Deviations (cm) from predicted (astronomical) tide
100
0
-100
D. Wind Speed (m/s) & Direction (12 o-clock=North, 3=East, etc)
10
0
-10
E. Barometric Pressure (mb)
1040
1010
980
F. Precipitation (cm/ hr)
2
1
0
2.5 5 10 15 20 25 30 35 40
Julian Day, 1999

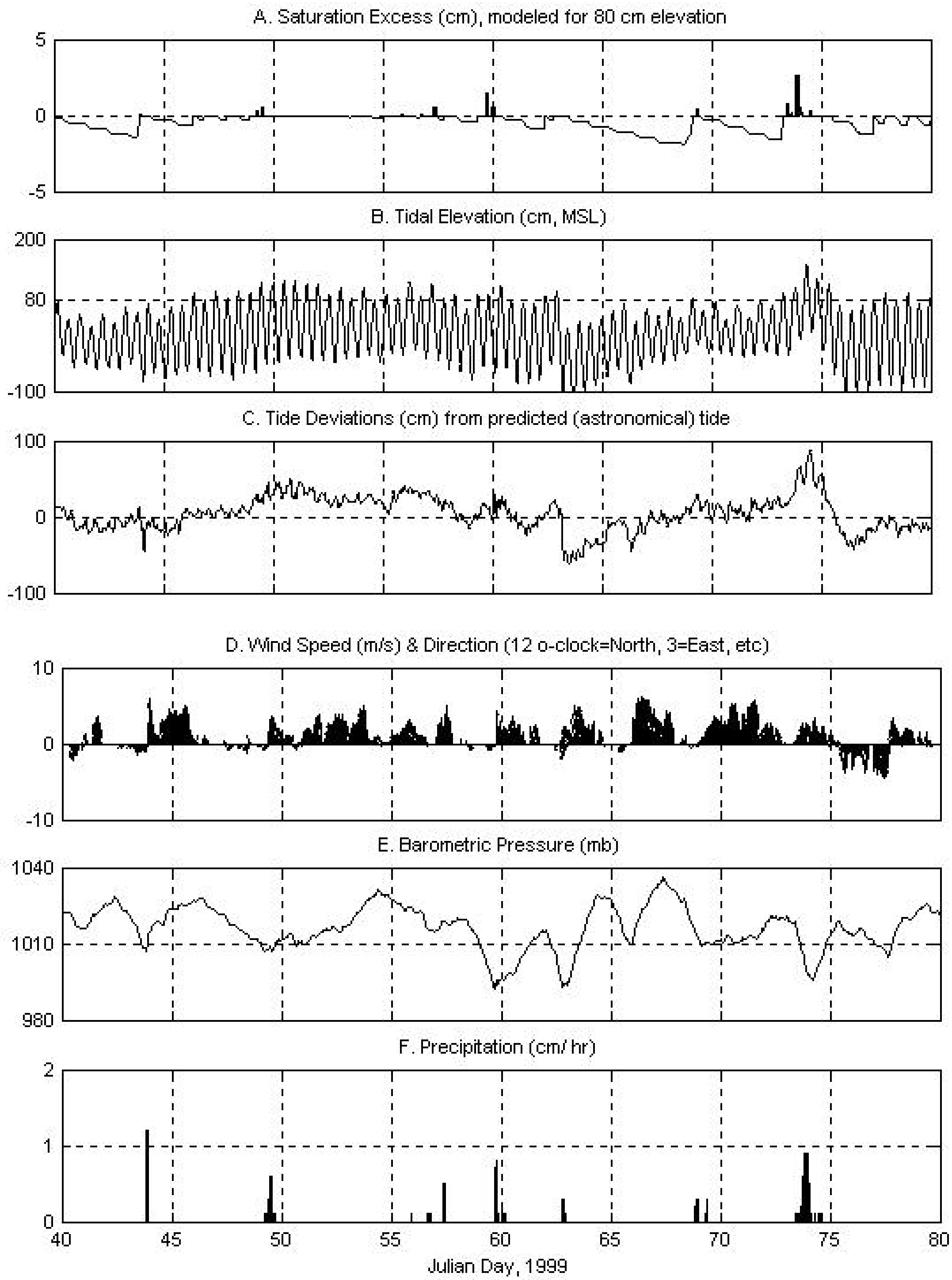
A. Saturation Excess (cm), modeled for 80 cm elevation
5
0
-5
B. Tidal Elevation (cm, MSL)
200
80
-100
C. Tide Deviations (cm) from predicted (astronomical) tide
100
0
-100
D. Wind Speed (m/s) & Direction (12 o-clock=North, 3=East, etc)
10
0
-10
E. Barometric Pressure (mb)
1040
1010
980
F. Precipitation (cm/ hr)
2
1
0
40
45
50
55
60
65
70
75
80
Julian Day, 1999

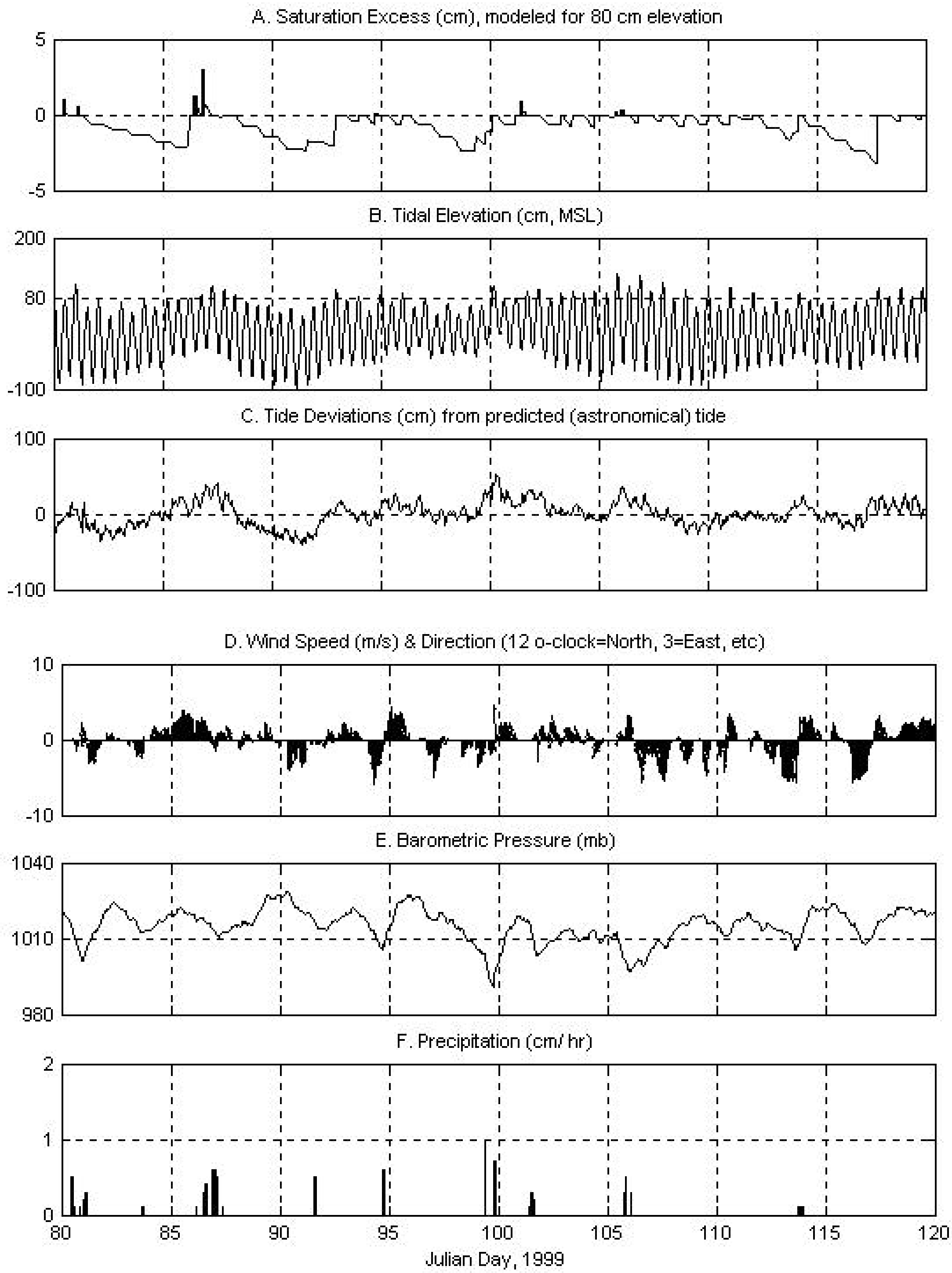
A. Saturation Excess (cm), modeled for 80 cm elevation
5
0
-5
B. Tidal Elevation (cm, MSL)
200
80
-100
C. Tide Deviations (cm) from predicted (astronomical) tide
100
0
-100
D. Wind Speed (m/s) & Direction (12 o-clock=North, 3=East, etc)
10
0
-10
E. Barometric Pressure (mb)
1040
1010
980
F. Precipitation (cm/ hr)
2
1
0
80
85
90
95
100
105
110
115
120
Julian Day, 1999

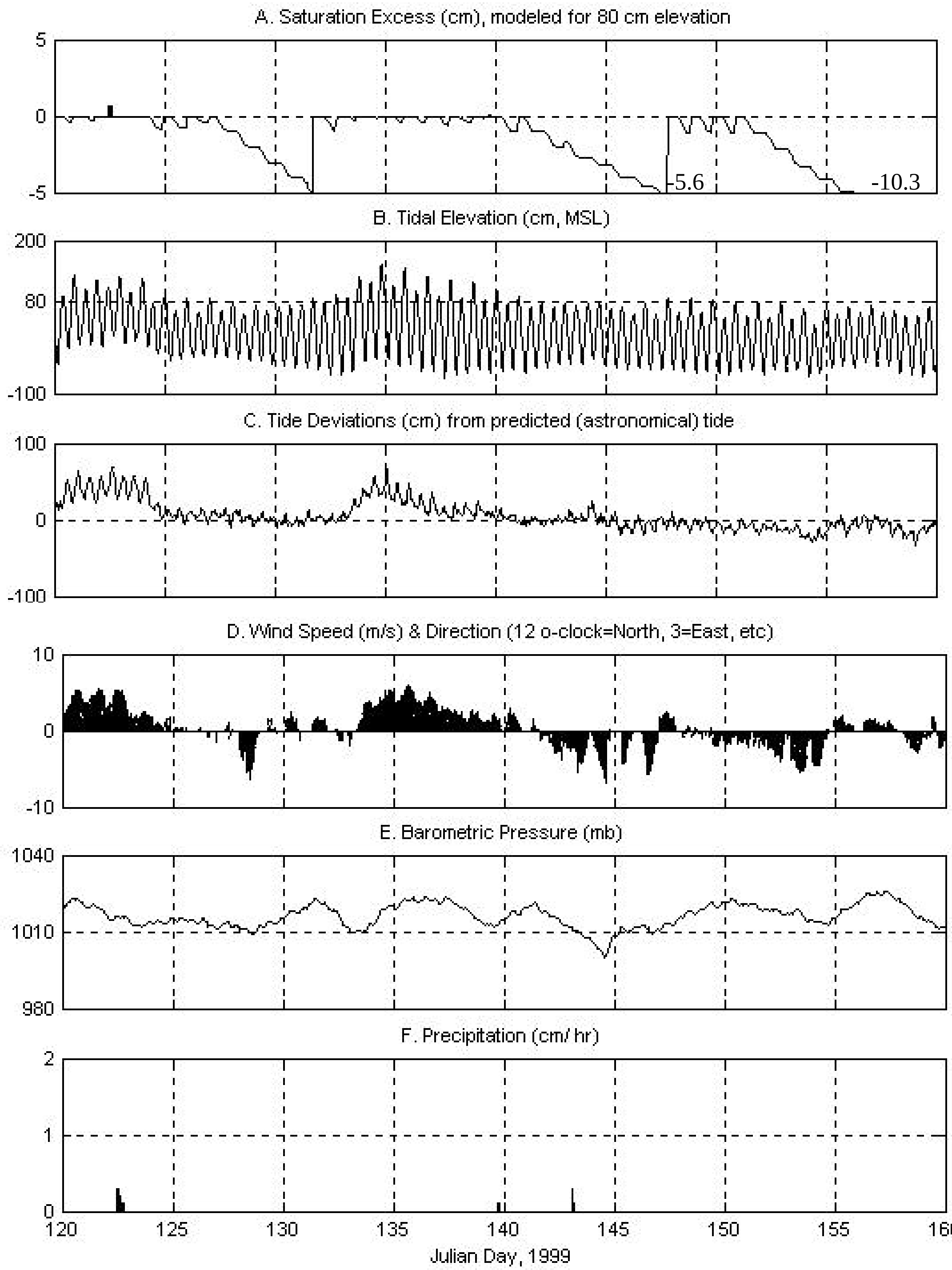
A. Saturation Excess (cm), modeled for 80 cm elevation
5
0
-5
-5.6
-10.3
B. Tidal Elevation (cm, MSL)
200
80
-100
C. Tide Deviations (cm) from predicted (astronomical) tide
100
0
-100
D. Wind Speed (m/s) & Direction (12 o-clock=North, 3=East, etc)
10
0
-10
E. Barometric Pressure (mb)
1040
1010
980
F. Precipitation (cm/ hr)
2
1
0
120 125 130 135 140 145 150 155 160
Julian Day, 1999

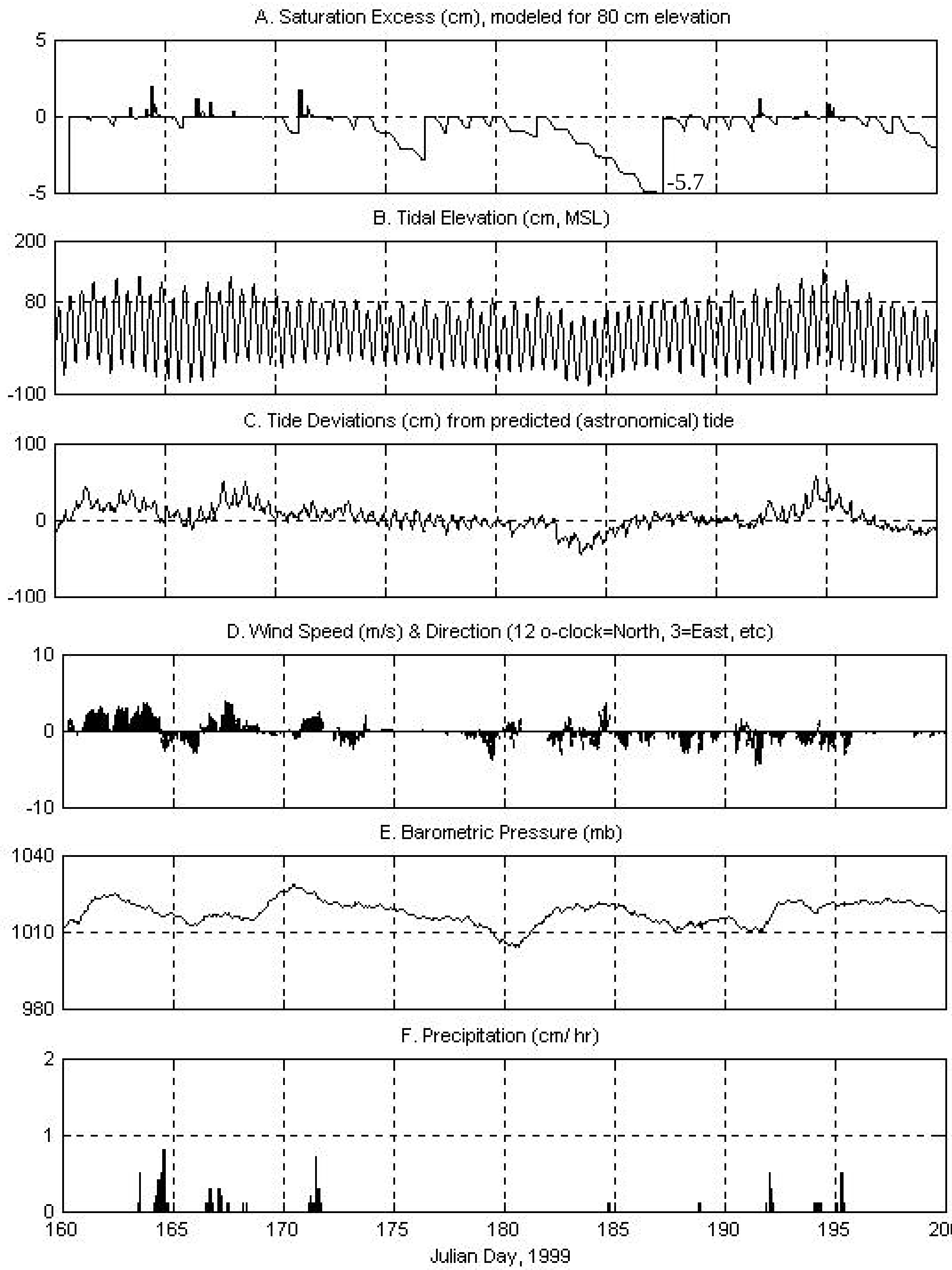
A. Saturation Excess (cm), modeled for 80 cm elevation
5
0
-5
-5.7
B. Tidal Elevation (cm, MSL)
200
80
-100
C. Tide Deviations (cm) from predicted (astronomical) tide
100
0
-100
D. Wind Speed (m/s) & Direction (12 o-clock=North, 3=East, etc)
10
0
-10
E. Barometric Pressure (mb)
1040
1010
980
F. Precipitation (cm/ hr)
2
1
0
160
165
170
175
180
185
190
195
200
Julian Day, 1999

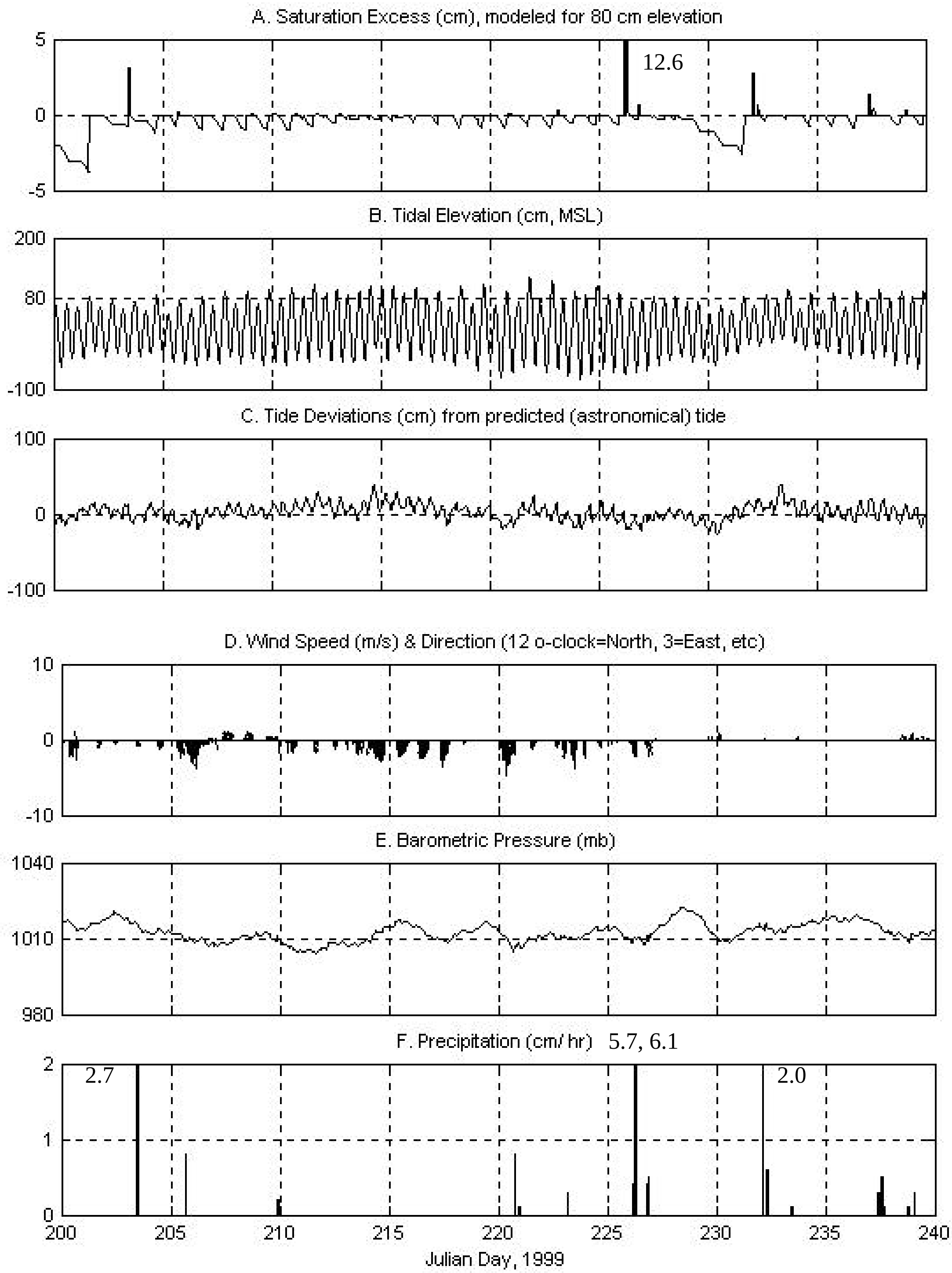
A. Saturation Excess (cm), modeled for 80 cm elevation
5
0
-5
12.6
B. Tidal Elevation (cm, MSL)
200
80
-100
C. Tide Deviations (cm) from predicted (astronomical) tide
100
0
-100
D. Wind Speed (m/s) & Direction (12 o-clock=North, 3=East, etc)
10
0
-10
E. Barometric Pressure (mb)
1040
1010
980
F. Precipitation (cm/ hr) 5.7, 6.1
2
1
0
2.7
2.0
200
205
210
215
220
225
230
235
240
Julian Day, 1999

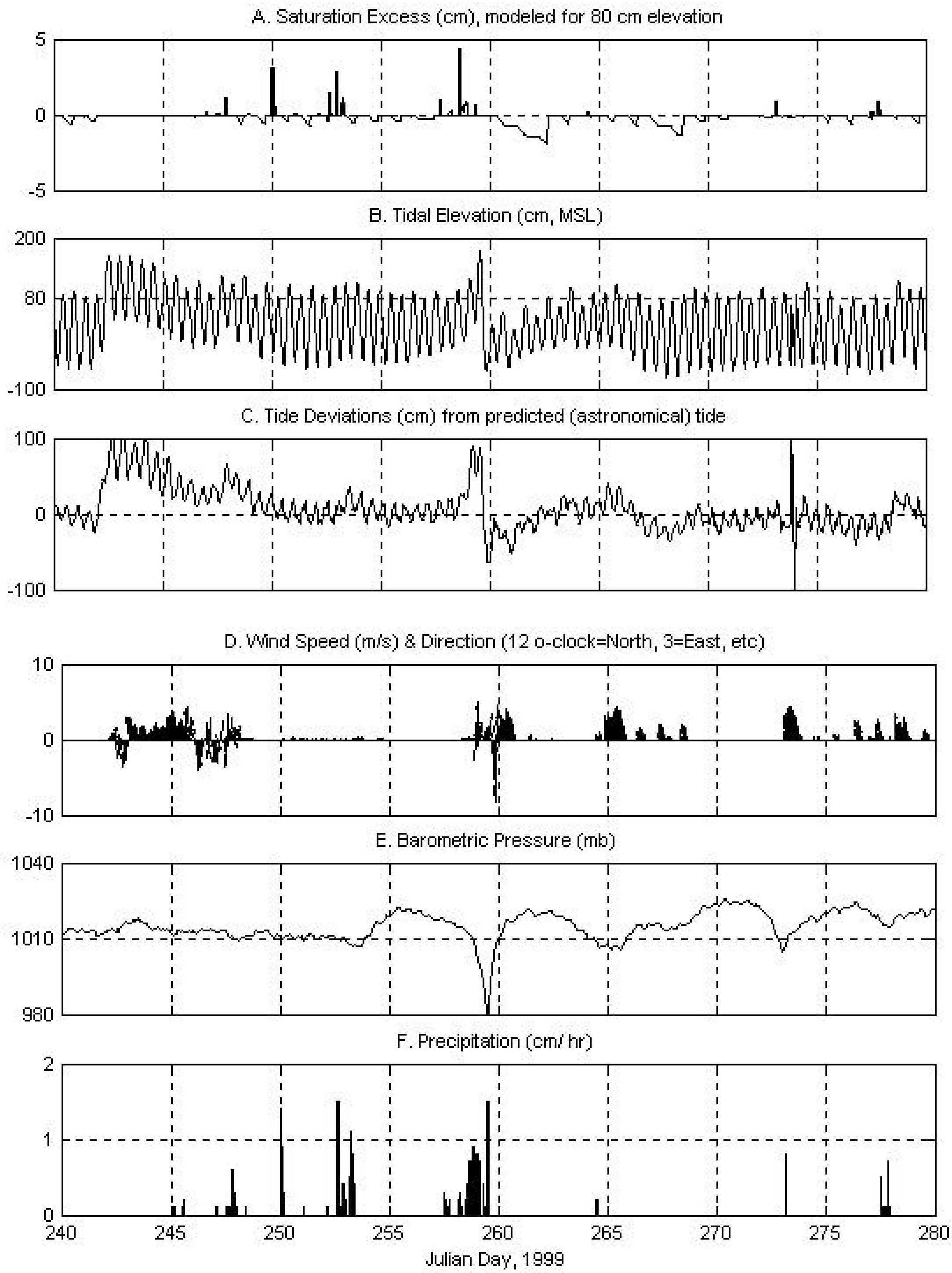

A. Saturation Excess (cm), modeled for 80 cm elevation
5
0
-5
B. Tidal Elevation (cm, MSL)
200
80
-100
C. Tide Deviations (cm) from predicted (astronomical) tide
100
0
-100
D. Wind Speed (m/s) & Direction (12 o-clock=North, 3=East, etc)
10
0
-10
E. Barometric Pressure (mb)
1040
1010
980
F. Precipitation (cm/ hr)
2
1
0
240
245
250
255
260
265
270
275
280
Julian Day, 1999

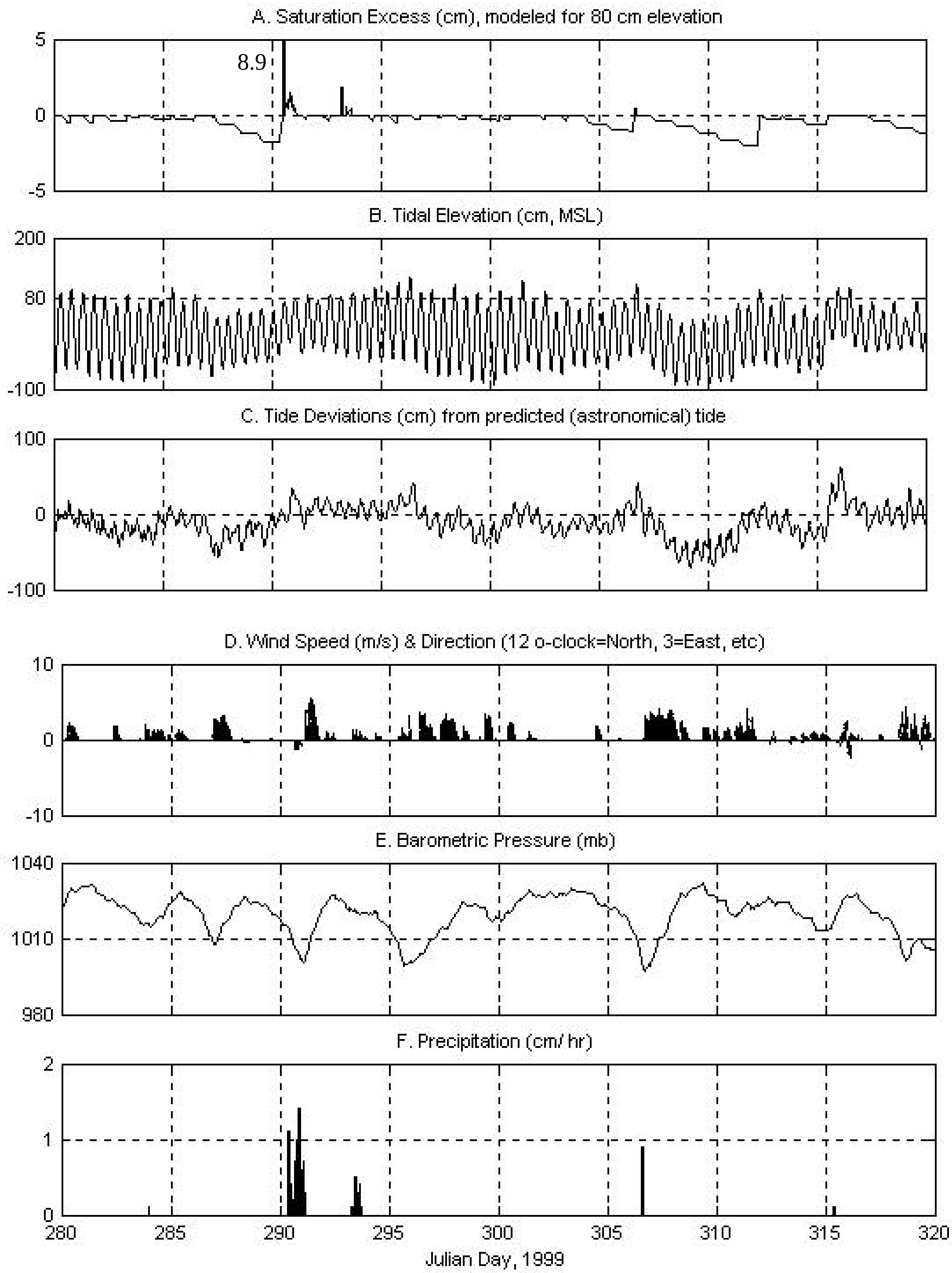
A. Saturation Excess (cm), modeled for 80 cm elevation
8.9
5
0
-5
B. Tidal Elevation (cm, MSL)
200
80
-100
C. Tide Deviations (cm) from predicted (astronomical) tide
100
0
-100
D. Wind Speed (m/s) & Direction (12 o-clock=North, 3=East, etc)
10
0
-10
E. Barometric Pressure (mb)
1040
1010
980
F. Precipitation (cm/ hr)
2
1
0
280
285
290
295
300
305
310
315
320
Julian Day, 1999

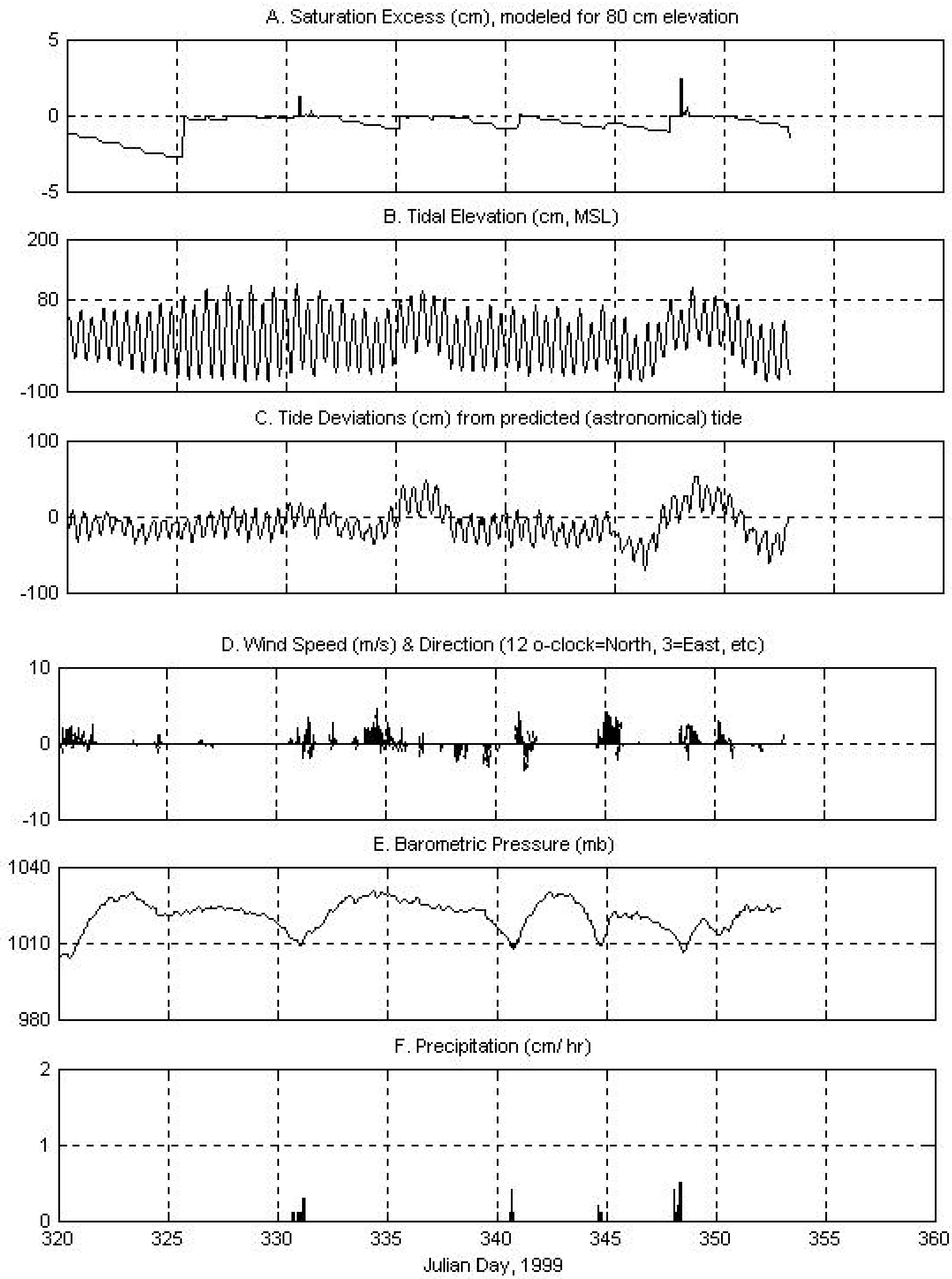
A. Saturation Excess (cm), modeled for 80 cm elevation
5
0
-5
B. Tidal Elevation (cm, MSL)
200
80
-100
C. Tide Deviations (cm) from predicted (astronomical) tide
100
0
-100
D. Wind Speed (m/s) & Direction (12 o-clock=North, 3=East, etc)
10
0
-10
E. Barometric Pressure (mb)
1040
1010
980
F. Precipitation (cm/ hr)
2
1
0
320
325
330
335
340
345
350
355
360
Julian Day, 1999

Appendix 4. Julian Days Calendar. (Add 1 to unshaded values during leap years; 2000 was a leap year).

	JAN	FEB	MAR	APR	MAY	JUN	JUL	AUG	SEP	OCT	NOV	DEC
1	1	32	60	91	121	152	182	213	244	274	305	335
2	2	33	61	92	122	153	183	214	245	275	306	336
3	3	34	62	93	123	154	184	215	246	276	307	337
4	4	35	63	94	124	155	185	216	247	277	308	338
5	5	36	64	95	125	156	186	217	248	278	309	339
6	6	37	65	96	126	157	187	218	249	279	310	340
7	7	38	66	97	127	158	188	219	250	280	311	341
8	8	39	67	98	128	159	189	220	251	281	312	342
9	9	40	68	99	129	160	190	221	252	282	313	343
10	10	41	69	100	130	161	191	222	253	283	314	344
11	11	42	70	101	131	162	192	223	254	284	315	345
12	12	43	71	102	132	163	193	224	255	285	316	346
13	13	44	72	103	133	164	194	225	256	286	317	347
14	14	45	73	104	134	165	195	226	257	287	318	348
15	15	46	74	105	135	166	196	227	258	288	319	349
16	16	47	75	106	136	167	197	228	259	289	320	350
17	17	48	76	107	137	168	198	229	260	290	321	351
18	18	49	77	108	138	169	199	230	261	291	322	352
19	19	50	78	109	139	170	200	231	262	292	323	353
20	20	51	79	110	140	171	201	232	263	293	324	354
21	21	52	80	111	141	172	202	233	264	294	325	355
22	22	53	81	112	142	173	203	234	265	295	326	356
23	23	54	82	113	143	174	204	235	266	296	327	357
24	24	55	83	114	144	175	205	236	267	297	328	358
25	25	56	84	115	145	176	206	237	268	298	329	359
26	26	57	85	116	146	177	207	238	269	299	330	360
27	27	58	86	117	147	178	208	239	270	300	331	361
28	28	59	87	118	148	179	209	240	271	301	332	362
29	29	60	88	119	149	180	210	241	272	302	333	363
30	30		89	120	150	181	211	242	273	303	334	364
31	31		90		151		212	243		304		365

Appendix 4. Julian Days Calendar. (Add 1 to unshaded values during leap years; 2000 was a leap year).

	JAN	FEB	MAR	APR	MAY	JUN	JUL	AUG	SEP	OCT	NOV	DEC
1	1	32	60	91	121	152	182	213	244	274	305	335
2	2	33	61	92	122	153	183	214	245	275	306	336
3	3	34	62	93	123	154	184	215	246	276	307	337
4	4	35	63	94	124	155	185	216	247	277	308	338
5	5	36	64	95	125	156	186	217	248	278	309	339
6	6	37	65	96	126	157	187	218	249	279	310	340
7	7	38	66	97	127	158	188	219	250	280	311	341
8	8	39	67	98	128	159	189	220	251	281	312	342
9	9	40	68	99	129	160	190	221	252	282	313	343
10	10	41	69	100	130	161	191	222	253	283	314	344
11	11	42	70	101	131	162	192	223	254	284	315	345
12	12	43	71	102	132	163	193	224	255	285	316	346
13	13	44	72	103	133	164	194	225	256	286	317	347
14	14	45	73	104	134	165	195	226	257	287	318	348
15	15	46	74	105	135	166	196	227	258	288	319	349
16	16	47	75	106	136	167	197	228	259	289	320	350
17	17	48	76	107	137	168	198	229	260	290	321	351
18	18	49	77	108	138	169	199	230	261	291	322	352
19	19	50	78	109	139	170	200	231	262	292	323	353
20	20	51	79	110	140	171	201	232	263	293	324	354
21	21	52	80	111	141	172	202	233	264	294	325	355
22	22	53	81	112	142	173	203	234	265	295	326	356
23	23	54	82	113	143	174	204	235	266	296	327	357
24	24	55	83	114	144	175	205	236	267	297	328	358
25	25	56	84	115	145	176	206	237	268	298	329	359
26	26	57	85	116	146	177	207	238	269	299	330	360
27	27	58	86	117	147	178	208	239	270	300	331	361
28	28	59	87	118	148	179	209	240	271	301	332	362
29	29	60	88	119	149	180	210	241	272	302	333	363
30	30		89	120	150	181	211	242	273	303	334	364
31	31		90		151		212	243		304		365

Appendix 5. Discussion of incorrect calculation of potential evapotranspiration.

Incoming short-wave solar radiation (SWin) was used to calculate PET in the Priestly-Taylor equation. Field measurements of SWin were used for the "Q" term described in the Methods section. The proper method is to use net heat flux (Q). The following calculations and discussion show that use of SWin resulted in overestimating PET.

Net radiation (Rn) is the sum of incoming short and long wave radiation, minus outgoing short and long waves. Some of this energy goes to the absorbing body (heat flux, G). Net heat flux, then, is the net radiation minus this heat flux (Q = Rn – G).

To assess the error introduced by using SWin, net radiation measurements from an agricultural field in the region can be compared to measurements of SWin. (Data from John Albertson, personal communication. The data were originally collected by Laura Murray in 1998 in an upland field across the street from the LTER research facility ("Shirley House") in Oyster.) These data will be correlated with SWin measurements in Phillips Creek Marsh. Correlation of SWin from Phillips Creek and Hog Island (figure 13) shows solar radiation data are regionally representive. Measurements of Rn in the upland field roughly approximate the region, without accounting for differences in soil type, wetness, and vegetation. Rn was approximately 60% of SWin for Days 183-201, 1998 (figure below).

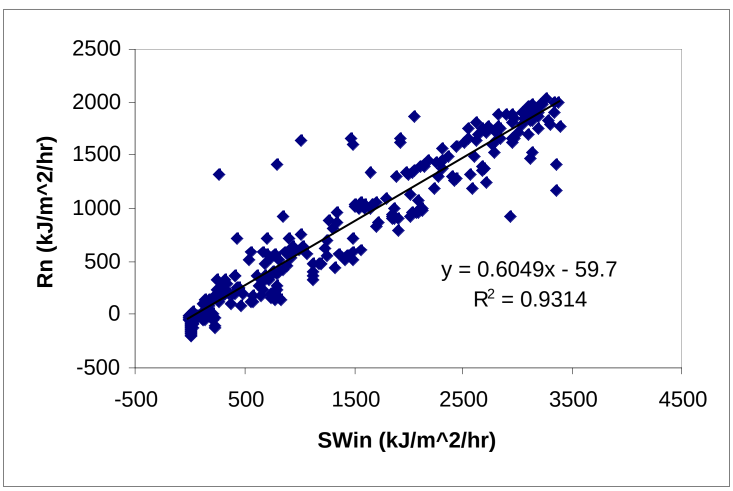

With this correlation of Rn and SWin, we need an estimate of G. Let Fv be the fraction of the surface area that is vegetated. Then 1-Fv is the fractional area of bare soil. Rn is “split” into what hits the plants and the bare soil: Rn = Fv Rn + (1-Fv) Rn, where (1-Fv) Rn is the portion of Rn to the bare soil.

Similarly, G, the absorbed energy, is “split”: G = Gv + (1-Gv), where 1-Gv is the Gs, the portion of energy absorbed by the ground, also called soil heat flux. Because Gv is negligible, G = Gs. For a wet soil, G is approximately 0.3 of the Rn to the soil (Brutsaert, 1982). Therefore, G = 0.3 (1-Fv) Rn.

Say Fv = 0.7. Then G = 0.3 (1-0.7) Rn, or G = 0.09 Rn. This crude estimate can be compared to Murray’s data for the upland field, which show the ratio of G to Rn is approximately 10% (figure below).

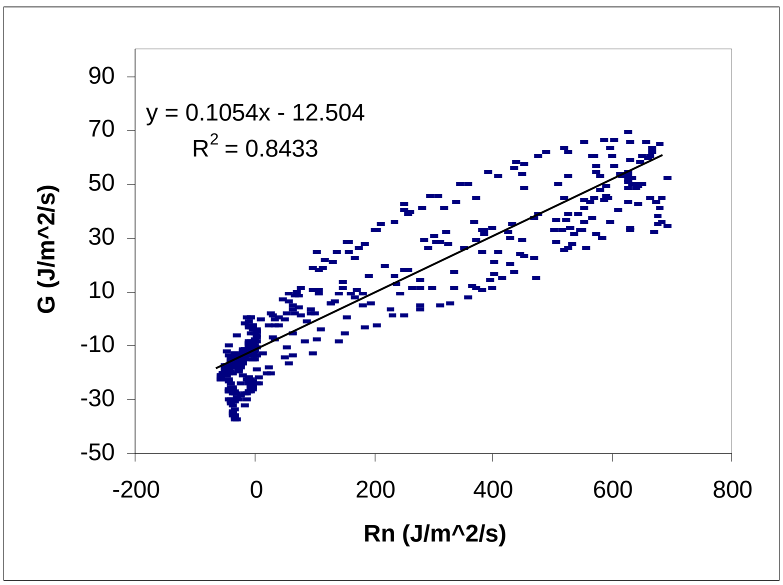

In addition to our measured SWin, we now have approximations for Rn (Rn ~ 0.60 SWin) and G (G ~ 0.09 Rn). We can use these to compare SWin to Q at the study area for this thesis. This comparison was made for Days 170-210, 1999; a period similar to that used to correlate Rn and SWin in 1998. Q was approximately 55% of SWin (figure below, note that the R^2 was 1.0 because Q uses Rn, which was calculated from SWin).

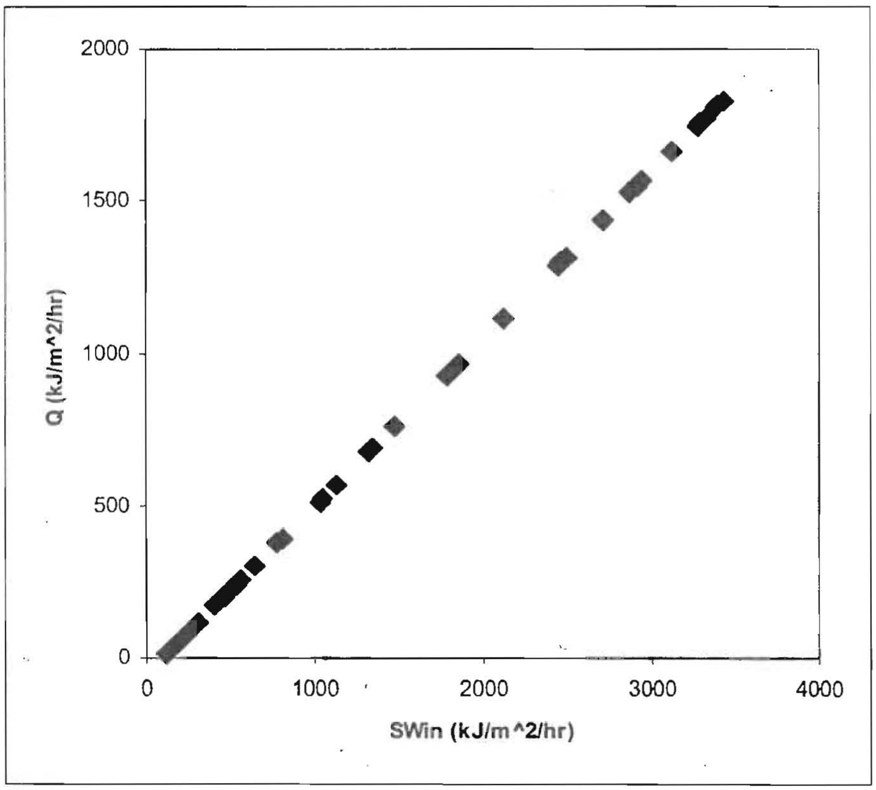

If Q is 55% of SWin, then PET calculated with Q is 55% of PET calculated with SWin, because Q is in the numerator of the PET equation: PET = $\alpha \dfrac{\Delta}{\Delta + \gamma} Q$.

However, the water balance model was still validated with Sy = 0.10 by comparison to field measurements of water table position at 39 m from the creek (79 cm elevation, MSL) for Days 206-252, 2000 (figure and table next page, compare to figure 41 and table 13).

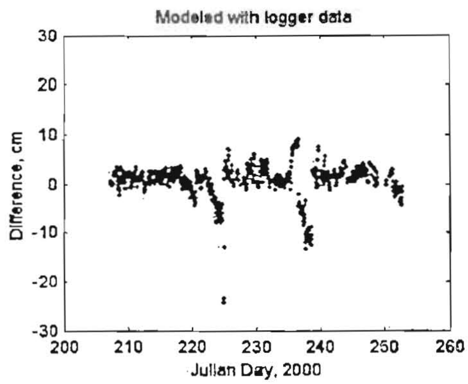

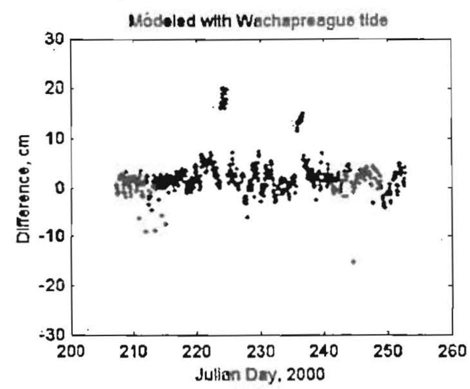

Model result statistics for Days 206-252, 2000, with Q in PET instead of SWin.

Tide data source	Mean difference (cm)	Standard deviation (cm)	% within ± 5 cm	% within ± 10 cm	% within ± 20 cm	% within ± 30 cm
Logger	0.6	3.7	88	97	100	100
Wacha-preague	2.5	4.0	87	94	99	100

Decreasing PET in this way would result in less water removal from the soil, lowering saturation deficit model-results. Probability curves for saturation deficit or excess will be "shifted right", with less frequent occurrence of saturation deficit and more frequent occurrence of saturation excess, although the magnitude of the shift is small (figure below, compare to figure 43). The broader implication is that less frequent tidal inundation will be required to give an area a low average saturation deficit and a high frequency of occurrence for saturation excess. This means the portion of a marsh prone to rainfall-runoff and erosion will extend to higher elevations and include a greater proportion of the entire marsh area.